

University of Mississippi

eGrove

Electronic Theses and Dissertations

Graduate School

2012

Admicellar Polymerization to Compatibilize Calcium Carbonate With Oil-Based Drilling Mud

Olugbenga Samuel Ojo

Follow this and additional works at: <https://egrove.olemiss.edu/etd>



Part of the [Chemical Engineering Commons](#)

Recommended Citation

Ojo, Olugbenga Samuel, "Admicellar Polymerization to Compatibilize Calcium Carbonate With Oil-Based Drilling Mud" (2012). *Electronic Theses and Dissertations*. 214.

<https://egrove.olemiss.edu/etd/214>

This Thesis is brought to you for free and open access by the Graduate School at eGrove. It has been accepted for inclusion in Electronic Theses and Dissertations by an authorized administrator of eGrove. For more information, please contact egrove@olemiss.edu.

ADMICELLAR POLYMERIZATION TO COMPATIBILIZE CALCIUM CARBONATE
WITH OIL-BASED DRILLING MUD

A Thesis
presented in partial fulfillment of requirements for the degree of

Master of Science

Department of Chemical Engineering
The University of Mississippi

OLUGBENGA S. OJO

December 2012

Copyright© by Olugbenga S. Ojo 2012

ALL RIGHTS RESERVED

ABSTRACT

Weighting agents like calcium carbonate (CC) are added to drilling mud to improve mud properties and performance during oil and gas drilling operations. Oil-based mud (OBM), a more preferred drilling mud, being hydrophobic is particularly non-compatible with hydrophilic CC. This work explored an economically viable admicellar polymerization technique to surface-modify the high energy hydrophilic CC surface to a low energy hydrophobic surface by polymerizing organic styrene monomer within an admicelle of nonionic surfactant Triton X-100 adsorbed on the CC surface. BET N₂ particle size analysis, Soxhlet extraction of the coated polymer, Fourier transform infrared-attenuated total reflectance (FTIR-ATR) spectra analysis, and thermogravimetric analysis (TGA) of the treated CC and polymer extract confirmed the production of a successful thin film polystyrene-coated CC. The coarse CC size grade had the most polymer. Consequently, OBM formulated with the treated CC is expected to; be more homogeneous, achieve higher wellbore pressure, remove drill cuttings better, have a more stable thin film low-permeability filter cake, and exhibit an enhanced overall performance. Pilot mud testing of a surface-modified CC formulated OBM is under way.

Dedicated to my parents,
Mr. Olurotimi Rufus Ojo and Mrs. Aina Florence Ojo,
whose prayers, love, care, encouragement and concern for my future has been my greatest
inspiration.

LIST OF ABBREVIATIONS AND SYMBOLS

CC	Calcium carbonate (CaCO_3)
XFCC	Extrafine calcium carbonate (Extrafine CC)
TX-100	Triton X-100 (4-octylphenol polyethoxylate)
PS	Polystyrene standard
AIBN	2,2'-azobisisobutyronitrile
THF	Tetrahydrofuran
FTIR	Fourier transform infrared spectroscopy
ATR	Attenuated total reflectance
K_{AS}	Partition coefficient
TGA	Thermo gravimetric analyzer/analysis
UV-VIS	Ultraviolet-visible spectrophotometer
CMC	Critical micelle concentration
CAC	Critical admicellar concentration
CHC	Critical hemimicelle concentration

ACKNOWLEDGMENTS

I deeply acknowledge the efforts of my advisor, Dr. John H. O'Haver, for his unrelenting guidance and encouragement all through the period of this work. I very much appreciate his support, words of advice and fatherly gestures. I am also highly grateful to the other members of my committee, Dr. Paul Scovazzo and Dr. Adam Smith, thank you for your time and numerous inputs, especially in the laboratory. I would like to thank the entire faculty of the chemical engineering department, particularly the department chair, Dr. Clint W. Williford and my advisor for providing the funds for my studies and research.

I would also like to thank the chemistry, pharmaceuticals, and civil engineering department for helping out with some of their instruments. Finally, my heartfelt gratitude also goes to my fellow graduate colleagues and my research partners, especially Eneruvie Okinedo, Poh Lee Cheah and Samuel Apetuje, your friendship and timely support were very helpful in the completion of this work.

TABLE OF CONTENTS

TITLE PAGE	i
ABSTRACT	ii
DEDICATION	iii
LIST OF ABBREVIATIONS AND SYMBOLS.....	iv
ACKNOWLEDGMENTS	v
TABLE OF CONTENTS	vi
LIST OF TABLES	ix
LIST OF FIGURES	x
 CHAPTER ONE.....	 1
1.1 INTRODUCTION.....	1
1.2 REFERENCES.....	6
CHAPTER TWO.....	8
LITERATURE REVIEW.....	8
2.1 NATURE AND STRUCTURE OF SURFACTANTS.....	8
2.2 MICELLE FORMATION BY SURFACTANTS.....	11
2.3 SURFACTANT ADSORPTION.....	12
2.3.1 Adsorption Mechanism.....	13
2.4 SURFACTANT SOLUBILIZATION AND ADSOLUBILIZATION OF SOLUTES....	14
2.5 POLYMER THIN FILM FORMATION VIA ADMICELLAR POLYMERIZATION...	15

2.6	REFERENCES.....	18
CHAPTER THREE.....		22
ADMICELLAR POLYMERIZATION AND SURFACE MODIFICATION.....		22
3.1	INTRODUCTION.....	22
3.2	REVIEWS ON SURFACE MODIFICATION.....	22
3.2.1	Alumina and Aluminum.....	22
3.2.2	Silica (rubber fillers).....	24
3.2.3	Composite fillers.....	26
3.2.4	Cotton fibers.....	27
3.2.5	Calcium Carbonate.....	29
3.2.6	Other mineral surfaces.....	32
3.3	COMMENTARY.....	33
3.4	REFERENCES.....	36
CHAPTER FOUR.....		41
ADMICELLAR POLYMERIZATION OF POLYSTYRENE TO COMPATIBILIZE CALCIUM CARBONATE WITH OIL-BASED DRILLING MUD (OBM): FOR IMPROVED MUD PERFORMANCE.....		41
4.1	INTRODUCTION.....	42
4.2	EXPERIMENTAL.....	44
4.2.1	Materials.....	44
4.2.2	Qualitative analysis of the calcium carbonates.....	44
4.2.3	Specific Surface Area Analysis of the calcium carbonates.....	45
4.2.4	Surfactant adsorption.....	45

4.2.5	Monomer adsolubilization.....	46
4.2.6	Admicellar polymerization.....	47
4.2.7	Characterization of the treated calcium carbonate.....	47
4.2.8	Characterization of the polystyrene coated on calcium carbonate surface.....	48
4.3	RESULTS AND DISCUSSION.....	48
4.3.1	Surface area of the calcium carbonates.....	48
4.3.2	Surfactant adsorption.....	49
4.3.3	Monomer adsolubilization and polymerization.....	55
4.3.4	Characterization of the treated calcium carbonate.....	58
4.3.5	Characterization of the extracted polymer.....	67
4.4	CONCLUSIONS.....	74
4.5	REFERENCES.....	76
	CHAPTER FIVE.....	80
	CONCLUSIONS AND RECOMMENDATIONS.....	80
5.1	CONCLUSIONS.....	80
5.2	RECOMMENDATIONS AND FUTURE WORK.....	81
5.3	REFERENCES.....	84
	LIST OF APPENDICES.....	85
	VITA.....	125

LIST OF TABLES

<u>TABLE</u>	<u>PAGE</u>
3.1 Approximate values of adsorbed surfactant molecules to adsolubilized monomer molecules from some authors.....	34
4.1 Particle size properties of the four industrial CC size grades.....	49
4.2 Comparison of TX-100 CMC (approximate) before and after adsorption.....	50
4.3 Hydrodynamic radius of TX-100 micelles at various surfactant concentrations.....	54
4.4 Comparing BET N ₂ specific surface areas of the untreated and treated industrial CC.....	63
4.5 Comparison of % extraction and % weight loss of treated CC samples.....	68
4.6 Mass balance of the polymer extract.....	74

LIST OF FIRURES

<u>FIGURE</u>	<u>PAGE</u>
1.1 Schematic of the surface modification process.....	3
2.1 Hydrophilic and hydrophobic groups of some surfactant molecules.....	10
2.2 Surfactant orientation at various interfaces.....	12
2.3 Admicelle, Hemimicelle, Micelle and Inverse Micelle.....	13
4.1 Tensiometer display during determination of TX-100 CMC before adsorption.....	51
4.2 Tensiometer display during determination of TX-100 CMC after adsorption.....	52
4.3 Adsorption isotherms of TX-100 on XFCC.....	53
4.4 Adsolubilization isotherms of styrene in TX-100 admicelle on XFCC.....	57
4.5 FTIR-ATR spectra of neat XFCC before treatment.....	59
4.6 FTIR-ATR spectra of polystyrene standard, extracted polymer, treated XFCC before extraction, and treated XFCC after extraction.....	60
4.7 FTIR-ATR spectra of treated and untreated XFCC.....	62
4.8 Thermal decomposition plots of untreated (b), treated (c), and after extraction treated (a) industrial Coarse CC.....	64
4.9 Thermal decomposition plots of untreated (b), treated (c), and after extraction treated (a) industrial Fine CC.....	65
4.10 Thermal decomposition plots of untreated (b), treated (c), and after extraction	

	treated (a) industrial XFCC.....	66
4.11	Picture of dried polystyrene extract from treated Coarse CC.....	67
4.12	Comparison of the IR spectra of (a) extracted material and (b) polystyrene standard.....	69
4.13	Thermal decomposition plots of polystyrene standard (a), XFCC extract (b), Fine CC extract (c), Coarse CC extract (d), and TX-100 (e).....	72
4.14	% Weight loss of extracted material: Extract from XFCC (a), Fine CC (b), and Coarse CC (c).....	73
5.1	Suggested explanation for the high polymer conversion.....	81

CHAPTER ONE

1.1 INTRODUCTION

The three fundamental equations (*Young-Laplace, Gibbs, and Kelvin equations*) of surface chemistry as well as an understanding of the nature and structure of water give us insight into what happens at interfaces. This knowledge enables us to fully utilize the amphipathic nature of surfactants for various applications. This amphipathic nature of surfactants results from their characteristic molecular structure which enables them to form aggregates, to be surface active causing reduction of interfacial free energy or interfacial tension, and to adsorb at interfaces changing surface properties. Consequently, they are vastly utilized in everyday living, in various industrial processes and in environmental remediation, among other things. Invariably, a basic understanding of the fundamentals of how surfactants work is key to improving current applications and for the formulation of new ones, particularly in the area of surface modification.

The word, surfactant, has a somewhat unusual origin, it was first created and registered as a trademark by the General Aniline and Film Corp. for their surface-active products. The company later, about 1950, released the term to the public domain for others to use.¹ A surfactant (a contraction of the term *surface-active agent*) is a substance that, when present at low concentration in a system, has the property of adsorbing onto the surfaces or interfaces of the system and of altering to a marked degree the surface or interfacial free energies of those surfaces (or interfaces).² This particular property makes surfactants fit into a wide variety of applications. Surfactants appear in such diverse products as the motor oils used in automobiles,

the pharmaceuticals we take when we are ill, the detergents we use in cleaning our laundry and homes, the drilling muds used in obtaining petroleum, the floatation agents used in purifying ores, electronics printing, magnetic recording, biotechnology, micro-electronics and viral research. Many surfactant applications utilize the process of micellization, which is the property of surface active solutes has of forming colloidal-sized clusters (*micelles*) in solution. Another important property of surfactants is their ability to adsorb at interfaces. This phenomenon is important in applications such as the stabilization of dispersions and enhanced oil recovery.²

Wu, et al. were the first to observe that adsorbed surfactant aggregates called admicelles or surface micelles have the ability to preferentially adsorb organic solutes from solution, a process called adsolubilization.³ Interestingly, surfactants exhibit this solubilizing property at interfaces, just as they do in solution. This ability of adsorbed surfactant aggregates at the solid/liquid interface to solubilize nonpolar solutes has been described as adsolubilization,³ surface solubilization⁴ and coadsorption,⁵ a phenomenon involving the formation of ordered aggregates capable of acting as two-dimensional solvents for sparingly soluble compounds. Adsolubilization is the surface analog to solubilization, with adsorbed surfactant bilayers playing the role of micelles.⁴ The concept of adsolubilization forms the basis for surface modification.

Over two decades ago, Wu et al.³ developed a novel surface modification technique that utilizes adsorbed surfactant aggregates (admicelles) as a template to synthesis polymer thin films with thicknesses less than 10 nm and in some cases less than 1 nm. This technique, called admicellar polymerization, consists of four major steps (Figure 1.1), (I) surfactant adsorption / admicelle formation, (II) adsolubilization of monomer(s), (III) polymerization (polymer formation) and (IV) surfactant removal.⁵⁻⁷

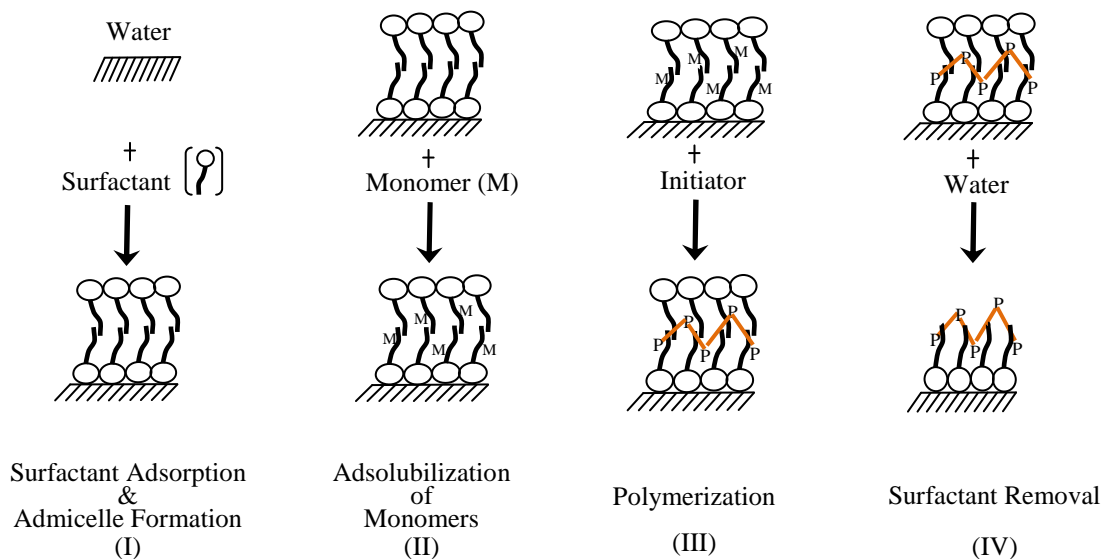


Figure 1.1: Schematic of the surface modification process.

The polymer matrixes formed by admicellar polymerization have varying morphologies, depending on the substrate. On an amorphous silica substrate, O'Haver found bands of styrene-butadiene copolymer formed within the "valleys" of the silica.⁹ On flat surfaces, a non-uniform coating of polystyrene was observed by Sakhalkar on glass fibers.¹⁰ Lai, on the other hand, found a uniform layer of poly(tetrafluoroethylene) on alumina plate.¹¹ However, Genetti observed a thin layer of polypyrrole covering nickel flakes.¹²

Weighting materials are often added to drilling fluids as densifiers to support and stabilize the wellbore during drilling operations. Calcium carbonate is often used in preference to barite because it is acid soluble and can therefore be easily dissolved as part of the process of cleaning up the production zone. Moreover, it is readily available in usable form and at low cost.

But, a major problem is the incompatibility of its high-energy, hydrophilic surface with the low-energy, hydrophobic phase of oil-based drilling fluid.

This thesis examines the admicellar polymerization of styrene in nonionic surfactant admicelles at the water-calcium carbonate interface by investigating each step in the process: adsorption, adsolubilization, polymerization, washing, and drying in order to obtain a thin polymer film coated on the surface of the substrate. A short introduction, summary of the investigations and the structure of this thesis are presented in this first chapter. Chapters two and three present a thorough literature review of various findings that are relevant to this research. Chapter four is written as a paper to be submitted for publication, it reports the results and conclusions of the work. Lastly, a proposal for the future work that can be done to aid our understanding of the interactions between nonionic surfactants and industrial grade calcium carbonate is presented in chapter five. Detailed results and instrumental stepwise procedures are given in the Appendices.

LIST OF REFERENCES

1.2 REFERENCES

1. Stevens, C.E. In *Kirk-Othmer Encyclopedia of Chemical Technology*, 2nd ed.; Wiley: New York. **1969**, Vol. 19, 507-593.
2. Rosen, M.J. *Surfactants and Interfacial Phenomena*, 3rd ed.; John Wiley & Sons Inc., Hoboken, New Jersey. **2004**.
3. Wu, J.J.; Harwell, J.H.; O'Rear, E.A. Two-Dimensional Reaction Solvents: Surfactant Bilayers in the Formation of Ultrathin Films. *Langmuir*. **1987**, 3(4), 531-537.
4. O'Haver, J.H.; Harwell, J.H. Adsolubilization: Some Expected and Unexpected Results. American Chemical Society Symposium. **1995**, Series No. 615, Chapter 4, 49-66.
5. Newman, P.D.; Newman G.K.; Harwell, J.H. *Mat. Res. Soc. Symp. Proc.* **1987**, 447 127.
6. Wu, J.; Harwell, J.H.; O'Rear, E.A. Two-Dimensional Solvents: Kinetics of Styrene Polymerization in Admicelles at or near Saturation. *Journal of Physical Chemistry*. **1987**, 91(3), 623-34.
7. Rungruang, P.; Grady, B.P.; Supaphol, P. Surface-Modified Calcium Carbonate Particles by Admicellar Polymerization to be used as Filler for Isotactic Polypropylene. *Colloids and Surfaces A: Physicochem. Eng. Aspects*. **2006**, 275, 114-125.
8. See, C.H. Understanding and Controlling the Process of Admicellar Polymerization. Ph.D. Dissertation. The University of Mississippi. **2004**.
9. O'Haver, J.H.; Harwell, J.H.; O'Rear, E.A.; Snodgrass, L. J.; Waddell, W. H. In situ Formation of Polystyrene in Adsorbed Surfactant Bilayers on Precipitated Silica. *Langmuir*. **1994**, 10(8), 2588-93.
10. Sakhalkar, S.S.; Hirt, D.E. Admicellar Polymerization of Polystyrene on Glass Fibers. *Langmuir*. **1995**, 3369-73.

11. Lai, C.L.; Harwell, J.H.; O'Rear, E.A.; Komatsuzaki, S; Arai, J.; Nakakawaji, T.; Ito, Y.
Formation of Poly(tetrafluoroethylene) Thin Films on Alumina by Admicellar
Polymerization. *Langmuir*. **1995**, 11(3), 905-11.
12. Genetti, W.B.; Yuan, W.L.; Grady, B.P.; O'Rear E.A.; Lai, C.L.; Glatzhofer, D.T.
Polymer Matrix Composites: Conductivity Enhancement through Polypyrrole Coating of
Nickel Flake. *Journal of Materials Science*. **1998**, 33(12), 3085-3093.

CHAPTER TWO

LITERATURE REVIEW

The origins of surfactants can be traced back to the discovery that early soap, formed by mixing and heating animal fat with wood ash (which acts as the base), with both of them being heated (heat + time), exhibited a cleansing property. This process was later termed saponification. The root word *sapo* first appeared in the *Natural History* encyclopedia published by Pliny the Elder.¹ This was the background against which it was discovered that surfactants were the active agents in soaps, responsible for their cleansing property. Consequently, their dual nature engendered them to be widely utilized for many applications.

2.1 NATURE AND STRUCTURE OF SURFACTANTS

Surfactants, short for surface-active agents, are molecules that tend to adsorb at interfaces. The reason for this is that most surfactants have both hydrophilic and hydrophobic groups present in their molecules. The hydrophilic group, also called the head group, is (in aqueous systems) water-loving and either polar or ionic. Conversely, the hydrophobic group, also called the tail group, is water-hating or oil-loving and usually nonpolar hydrocarbon chains. The hydrophilic and hydrophobic groups of two widely used surfactants are shown in Figure 2.1.

Surfactants have an *amphipathic* characteristic molecular structure,² consisting of a structural group that has very little attraction for the solvent, the hydrophobic or lyophobic group, together with a group that has a strong attraction for the solvent, the hydrophilic or lyophilic group. The chemical structures of groupings suitable as the lyophobic and lyophilic

portions of the surfactant molecule vary with the nature of the solvent and the conditions of use. In a highly polar solvent such as water, the lyophobic group may be a hydrocarbon or fluorocarbon or siloxane chain of proper length, whereas in a less polar solvent only some of these may be suitable. As use conditions like temperature, presence of electrolyte or organic additives changes, it may become necessary to modify the structure of the lyophobic and lyophilic groups in order to maintain surface activity at a suitable level. Surfactants are generically classified according to the nature of their hydrophilic group into:²

Anionic – When the surface-active portion of the molecule carries a negative charge, for instance, $\text{RCOO}^- \text{Na}^+$ (soap), $\text{RC}_6\text{H}_4\text{SO}_3^- \text{Na}^+$ (alkylbenzene sulfonate).

Cationic – When the surface-active portion bears a positive charge, for instance, $\text{RNH}_3^+ \text{Cl}^-$ (salt of a long-chain amine), $\text{RN}(\text{NH}_3)^+ \text{Cl}^-$ (quaternary ammonium chloride).

Zwitterionic – When both positive and negative charges may be present in the surface-active portion, for instance, $\text{RN}^+\text{H}_2\text{CH}_2\text{COO}^-$ (long-chain amino acid), $\text{RN}^+ (\text{CH}_3)_2\text{CH}_2\text{CH}_2\text{SO}_3^-$ (sulfobetaine)

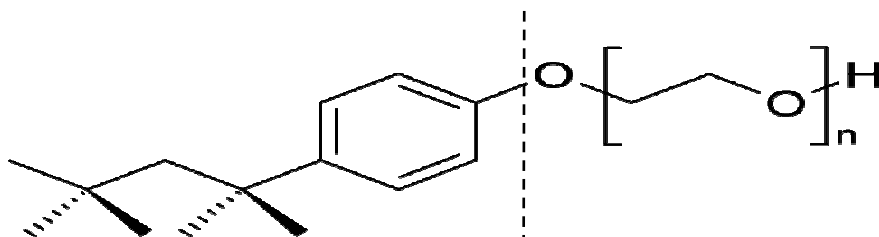
Nonionic – When the surface-active portion carries no apparent ionic charge, for instance, $\text{RCOOCH}_2\text{CHOHCH}_2\text{OH}$ (monoglyceride of long-chain fatty acid), $\text{RC}_6\text{H}_4(\text{OC}_2\text{H}_4)_x\text{OH}$ (polyoxyethylenated alkylphenol), $\text{R}(\text{OC}_2\text{H}_4)_x\text{OH}$ (polyoxyethylenated alcohol).

*Dimeric (gemini) surfactants*³ – are made up of two amphiphilic moieties connected at the level of, or very close to, the head groups by a spacer group of varying nature: hydrophilic or hydrophobic, rigid or flexible. These surfactants represent a new class of surfactants that is finding its way into surfactant-based formulations. Dimeric surfactants represent a new class of

surfactants. They are made up of two amphiphilic moieties connected at the level of the head groups or very close to the head groups by a spacer group.

4-octylphenol polyethoxylate (Triton X-100, $\text{C}_8\text{H}_{17}\text{-C}_6\text{H}_4\text{-(OC}_2\text{H}_4)_n\text{OH}$, $\text{C}_{14}\text{H}_{22}\text{O(C}_2\text{H}_4\text{O)}_n$)

($n = 9\text{-}10$)



Hexadecyltrimethylammonium bromide (C_{16}TAB , $\text{C}_{19}\text{H}_{42}\text{BrN}$)

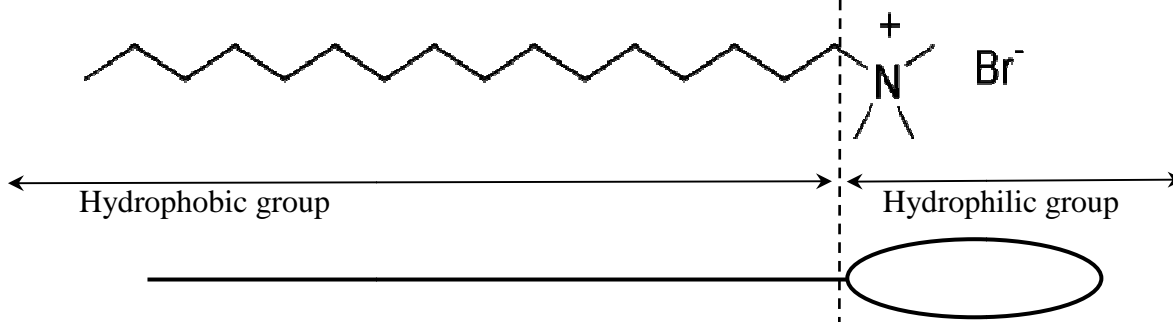


Figure 2.1: Hydrophilic and hydrophobic groups of some surfactant molecules.

2.2 MICELLE FORMATION BY SURFACTANTS

In a phenomenon termed the “hydrophobic effect”,⁴ surfactants act the way they do in aqueous systems due to their nature/structure and the nature/structure of water. Once a surfactant monomer is added to water, water forms a “cage” around the hydrophobic carbon chain. This enclosure is driven by the strength of the hydrogen bonds between the water molecules, leading to loss of entropy of the water molecules. It is this entropy loss rather than bond energy that leads to an unfavorable free energy change for the process. Once added to a system, before equilibrium is reached between the surfactant monomers at the interface and those in the bulk, surfactants concentrate at the interfaces, where they gradually decrease the overall free energy or surface tension of the system. Their orientation at the interface varies, depending on the components of the system. At a water/ air interface, the head group is buried in the solution while the tail group extends out of the solution. At oil/air interface, the tail group is buried in the oil while the head group stays on the interface. A diagrammatic representation is given in Figure 2.2. These orientations are due to the amphipathic nature of surfactant molecules, and the fact that like dissolves like. The hydrophilic head group interacts strongly with water while the hydrophobic tail interacts strongly with oil. These dual properties of surfactants are the basis of their wide applications.

The formation of micelles in aqueous solution is generally viewed as a compromise between the tendency for alkyl chains to avoid energetically (and enthalpically) unfavorable contact with water, and the desire for the polar parts to maintain contact with the aqueous environment. Micelles are formed as a result of the interactions between the aqueous phase and the lipophobic portions of the molecules.⁵ Many physical properties of surfactants including

conductivity and surface tension have sharp discontinuities in the region of the CMC. Surfactant adsorption and micelle formation properties are both utilized in detergency.^{6, 7}

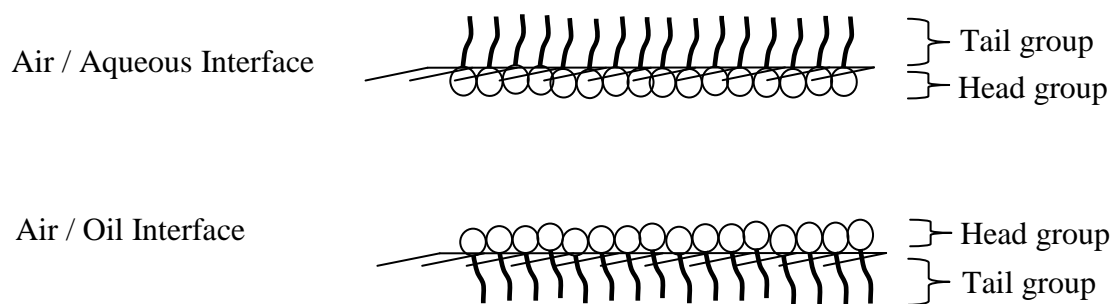


Figure 2.2: Surfactant orientation at various interfaces.

2.3 SURFACTANT ADSORPTION

Surfactants adsorb onto the solid particles when added to a liquid-substrate system. They first (not always) form local monolayers (hemimicelles) and then local bilayers (admicelles) or something in between.⁶ Some mechanisms that induce adsorption include ion exchange, ion pairing, acid-base, polarization of π electrons, dispersion forces, and hydrophobic effect. The hydrophobic effect⁴ describes the entropic advantage achieved during adsorption, as water forms a “cage” around the surfactant tail in solution. The concentration at which hemimicelles and admicelle begin to form are called critical hemimicelle concentration (CHC) and critical admicelle concentration (CAC) respectively, both are analogous to the critical micelle concentration (CMC), the concentration at which micelles begin to form. The structure of these

aggregates differs depending on the medium and the surfactant. Generally, micelles are represented as shown in Figure 2.3. But in a non-polar system, the structure is reversed forming an inverse or reverse micelle, also shown in Figure 2.3.

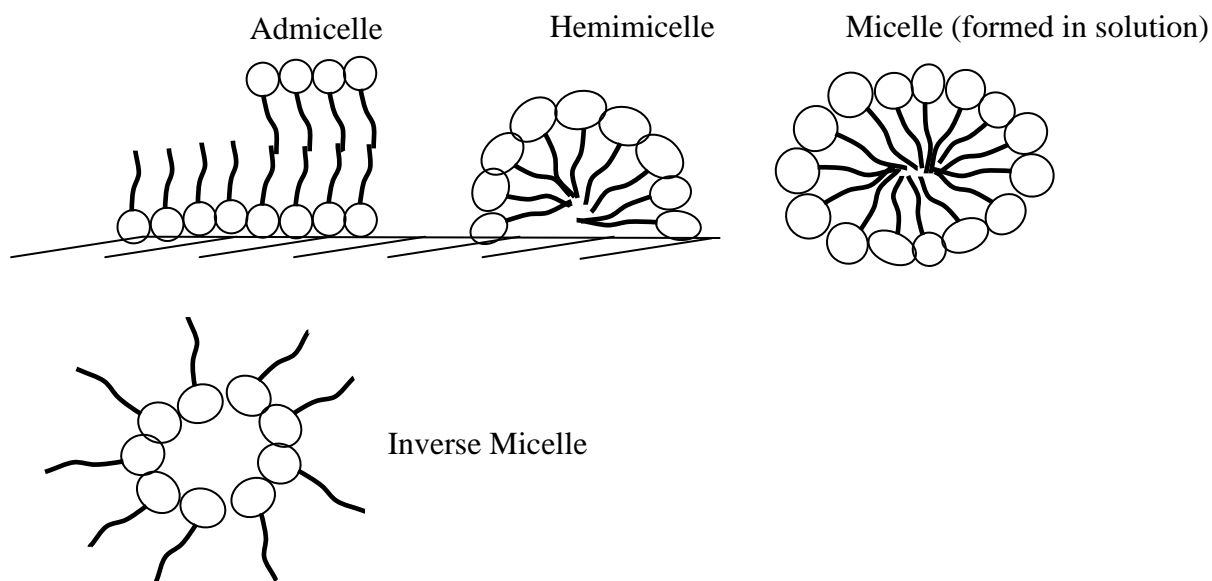


Figure 2.3: Admicelle, Hemimicelle, Micelle and Inverse Micelle.

2.3.1 Adsorption Mechanism

The adsorption mechanism of ionic surfactants differs from that of nonionic surfactants. The schematic of a typical surfactant adsorption isotherm frequently seen for the adsorption of ionic surfactants on oppositely charged surfaces is commonly divided into four regions,^{9, 10} the shape of a typical adsorption isotherm of a nonionic surfactant follows Langmuir equation. Unlike ionic surfactants, the adsorption isotherms of nonionic surfactants do not have clear transition points. At very low concentration, nonionic surfactant monomers adsorb via

hydrogen bonding between the substrate and the hydrophilic groups. The amount of adsorbed surfactant increases slowly with increasing equilibrium concentration in the bulk phase. After the CHC or CAC, the slope of the isotherm increases until the CMC and then flattens out.⁸

2.4 SURFACTANT SOLUBILIZATION AND ADSOLUBILIZATION OF SOLUTES

One distinctive property of a micelle is its capacity for solute solubilization within the interior of the micelle. When micelles absorb organic solutes from solution, we say that the solute is solubilized. Likewise, when admicelles absorb organic solutes from solution, we say that the solute is adsolubilized. Solubilization is the spontaneous dissolving of a substance (solid, liquid or gas) by reversible interaction with the micelles of a surfactant in a solvent to form a thermodynamically stable isotropic solution with reduced thermodynamic activity of the solubilized material.² The hydrophilic groups create a hydrophilic/polar region within the micelle while the hydrophobic tail groups form a nonpolar region. Consequently, solutes preferentially partition into regions of similar nature.⁸

Admicelles have the ability to preferentially absorb organic solutes from solution, a process called adsolubilization. Adsolubilization is the surface analog to solubilization, with adsorbed surfactant bilayers playing the role of micelles. The organic solutes, with limited solubilities in water, preferentially partition into the interior of the admicelle.⁶ Partitioning of solutes has been studied not only at the solid/liquid interface but also at the air/liquid interface.¹⁴ The formation of surfactant aggregates at interfaces, usually by self-assembly, can be by ion exchange¹⁵ or chemical bonding.¹⁶ Substrates such as layered silicates,¹⁷ surgical grafts¹⁸ and Maghmite^{19, 20} have been examined. Surfactant bilayer structure can change after adsolubilization of different solutes.^{21, 22}

Ultimately, adsolubilization depends on adsorption (which varies from substrate to substrate), surfactant chain length and chain number. The adsolubilization of naphthol could be as high as 5.5 times that of the adsorbed surfactant itself.⁸ When the surfactant concentration is above the CMC, adsolubilization decreases for a given amount of solute due to competition between solubilization and adsolubilization.²³⁻²⁵

2.5 POLYMER THIN FILM FORMATION VIA ADMICELLAR

POLYMERIZATION

Admicellar polymerization, the formation of ultrathin polymer films within the two-dimensional solvents of surfactant bilayers in a surfactant, monomer, and substrate system, was first studied by Wu et al.²⁶ The nanoscopic polymer morphology observed from Scanning Electron Microscope (SEM), Scanning Tunneling Microscope (STM) and AFM shows patchy and irregular films on substrates with wrinkles and adsorbed latex particles on flat and particulate surfaces.²⁷⁻³² The four major steps of the thin film synthesis via admicellar polymerization are shown in Figure 1.1.

Surfactant Adsorption – A prepared surfactant solution is added to the substrate, giving rise to surfactant adsorption on the substrate and subsequent formation of admicelles. Adsorption isotherm is generated at this step. The surfactant concentration should be above the CAC but below the CMC, in order to avoid emulsion polymerization. The admicelle acts as the template for the polymer film.

Adsolubilization of Monomers – Once the organic solute is added to the system, this nonpolar compound, partitions into the admicelle region. Thus, monomer adsolubilization occurs. The adsolubilization isotherm is obtained at this step.

Initiator Addition – Azo-initiators are preferred in place of the commonly used potassium persulfate, which does not give a consistent result because it decomposes to HSO_4^- , affecting the system's pH and surfactant adsorption.³³ The adsolubilized monomers are polymerized once the initiator is added to the system. Consequently, admicellar polymerization is achieved.

Surfactant Removal – This is achieved by washing with DI or distilled water at room temperature and then drying at a temperature below the glass transition temperature of the polymer. See observed that the stability of the polymer film is affected by the washing process, that after most the surfactant is removed, the non-polar polymer surface will be exposed to the water and this may lead to the coalescence of the polymer film in order to reduce the surface energy, leading to patches having greater thickness than the admicelle they formed from.³³ This might lead to a non-uniform distribution of the polymer film on the substrate. Therefore, another method for removing the outer head group of the admicelle will be preferable, especially for surface modification.

LIST OF REFERENCES

2.6 REFERENCES

1. Pliny the Elder, "Volume 1 of the *Natural History* of Gaius Plinius Secundus" `1669 Edition.
2. Rosen, M.J. *Surfactants and Interfacial Phenomena*, 3rd ed.; John Wiley & Sons Inc., Hoboken, New Jersey. **2004**.
3. Raoul, Z. Dimeric (Gemini) Surfactants: Effect of the Spacer Group on the Association Behavior in Aqueous Solution. *Journal of Colloid and Interface Science*. **248**, 203-220 (2002).
4. Tanford, C. *The Hydrophobic Effect: Formation of Micelles And Biological Membranes*, John Wiley & Sons, Inc. **1973**.
5. Schramm, L.L.; Marangoni, D.G. *Surfactants and Their Solutions: Basic Principles. Surfactants: Fundamental and Applications in the Petroleum Industry*. Schramm, L.L. Cambridge University Press. **2000**.
6. O'Haver, J.H.; Harwell, J.H. Adsolubilization: Some Expected and Unexpected Results. *American Chemical Society Symposium*. **1995**, Series No. 615, Chapter 4, 49-66.
7. Newman, P.D.; Newman G.K.; Harwell, J.H. *Mat. Res. Soc. Symp. Proc.* **1987**, 447 127.
8. Tan, Y. Experimental and Modeling of Investigations of Styrene Adsolubilization in Nonionic Surfactant Admicelles, Ph.D. Dissertation, The University of Mississippi. **2004**.
9. Somasundaran, P.; Fuerstenau, D.W. *Journal of Physical Chemistry*. **1982**, 79:90.
10. Scamehorn, J.F.; Schechter, R.S.; Wade, W.H. *Journal of Colloid Interface Science*. **1982**, 85:463.

11. O'Haver, J.H.; Harwell, J.H.; Lobban, L.L.; O'Rear, E.A. "Adsolubilization", in *Solubilization in Surfactants Solutions*, Christian, S.D. and Scamehorn, J.F. Eds; Surfactant Science Series. **1995**, Vol. 55; Marcel Dekker, Newyork.
12. Austad, T.; Lovreide, T.; Olsvik, K.; Rolfsvag, T.A.; Staurland, G. Competition Static Adsorption of Mixtures of Ethoxylated Surfactants onto Kaolinite and Quartz. *Journal of Petroleum Science & Engineering*. **1991**, 6(2), 107-124.
13. Wesson, L.L.; Harwell, J.H. Surfactant Adsorption in Porous Media. *Surfactants*. **2000**, 121-158.
14. Aveyard, R.; Binks, B.P.; Fletcher, P.D.I.; MacNab, J.R. Interaction of Alkanes with Monolayers of Nonionic Surfactants. *Langmuir*. **1995**, 11(7), 2515-2524.
15. Vaia, R.A.; Giannelis, E.P. Polymer Melt Intercalation in Organically-Modified Layered Silicates: Model Predictions and Experiment. *Macromolecules*. **1997**, 30(25), 8000-8009.
16. Thakulsukanant, C.; Lobban, L.L.; Osuwan, S.; Waritswat, A. Adsolubilization and Stability Characteristics of Hydrocarbon Aggregates Chemically Bonded to Porous Silica. *Langmuir*. **1997**, 13(17), 4595-4599.
17. Dekany, I.; Szanto, F.; Weiss, A.; Lagaly, G. Interlamellar Liquid Sorption on Hydrophobic Silicates. *Berichte der Bunsen-Gesellschaft*. **1985**, 89(1), 62-67.
18. Yao, J.; Strauss, G. Adsorption of Cationic Surfactants on Medical Polymers: Effects of Surfactant and Substrate Structures. *Langmuir*. **1992**, 8(9), 2274-2278.
19. Ma, C.; Li, C. Interaction between Polyvinylpyrrolidone and Sodium Dodecyl Sulfate at Solid/Liquid Interface. *Journal of Colloid and Interface Science*. **1989**, 131(2), 485-492.

20. Dao, K.; Bee, A.; Treiner, C. Adsorption Isotherm of Sodium Octylbenzenesulfonate on Iron Oxide Particles in Aqueous Solutions. *Journal of Colloid and Interface Science*. **1998**, 204(1), 61-65.
21. Venkataraman, N.V.; Mohanambe, L.; Vasudevan, S. Functionalization of the Inner Surfaces of Layered Cadmium Thiophosphate with Cationic Surfactants: Adsolubilization of Uncharged Organic Molecules. *Journal of Materials Chemistry*. **2003**, 13(2), 170-171.
22. Venkataraman, N.V.; Vasudevan, S. Solubilization of Phenol in an Intercalated Surfactant Bilayer. *Journal of Physical Chemistry*. **2003**, 107(22), 5371-5381.
23. Schieder, D.; Dobias, B.; Klumpp, E.; Schwuger, M.J. Adsorption and Solubilization of Phenols in the Hexadecyltrimethylammonium Chloride Adsorbed Layer on Quartz and Corundum. *Colloids and Surfaces A: Physicochemical and Engineering Aspects*. **1994**, 88(1), 103-111.
24. Klumpp, E.; Heitmann, H.; Schwuger, M.J. Synergistic Effects between Cationic Surfactants and Organic Pollutants on Clay Minerals. *Colloids and Surfaces A: Physicochemical and Engineering Aspects*. **1993**, 78(1-3), 93-98.
25. Klumpp, E.; Heitmann, H.; Lewandowski, H.; Schwuger, M.J. Enhancing Effects during the Interaction of Cationic Surfactants and Organic Pollutants with Clay Minerals. *Progress in Colloid & Polymer Science* 89 (Trends Colloid Interface Sci. VI). **1992**, 181-185.
26. Wu, J.J.; Harwell, J.H.; O'Rear, E.A. Two-Dimensional Reaction Solvents: Surfactant Bilayers in the Formation of Ultrathin Films. *Langmuir*. **1987**, 3(4), 531-537.

27. Wu, J.; Harwell, J.H.; O'Rear, E.A.; Christian, S.D. Application of Thin Films to Porous Mineral Oxides using Two-Dimensional Solvents. *AIChE Journal*. **1988**, 34(9), 1511-18.
28. Genetti, W.B.; Yuan, W.L.; Grady, B.P.; O'Rear, E.A.; Lai, C.L.; Glatzhofer, D.T. Polymer Matrix Composites: Conductivity Enhancement through Polypyrrole Coating of Nickel Flake. *Journal of Materials Science*. **1998**, 33(12), 3085-3093.
29. Yuan, W.L.; Lin, D.Y.; Chiang, S.C. Conductivity Characterization using STM of Polypyrrole Ultrathin Films Prepared from Admicellar Polymerization. *International Journal of Nanoscience*. **2003**, 2(4 & 5), 245-255.
30. See, C.H.; O'Haver, J.H. Atomic Force Microscopy Studies of Admicellar Polymerization Polystyrene-Modified Amorphous Silica. *Journal of Applied Polymer Science*. **2003**, 87(2), 290-299.
31. See, C.H.; O'Haver, J.H. Atomic Force Microscopy Characterization of Ultrathin Polystyrene Films formed by Admicellar Polymerization on Silica Disks. *Journal of Applied Polymer Science*. **2003**, 89(1), 36-46.
32. Yuan, W.L.; O'Rear, E.A.; Cho, G.; Funkhouser, G.P.; Glatzhofer, D.T. Thin Polypyrrole Films Formed on Mica and Alumina with and without Surfactant Present: Characterization by Scanning Probe and Optical Microscopy. *Thin Solid Films*. **2001**, 385(1, 2), 96-108.
33. See, C.H. Understanding and Controlling the Process of Admicellar Polymerization. Ph.D. Dissertation. The University of Mississippi. **2004**.

CHAPTER THREE

ADMICELLAR POLYMERIZATION AND SURFACE MODIFICATION

3.1 INTRODUCTION

In a process now known as admicellar polymerization, Wu et al.^{1, 2} proposed that ultrathin films were formed within adsorbed surfactant bilayers acting as two-dimensional solvents in a surfactant, monomer, and substrate system; showing for the first time that the admicelles (adsorbed micelles), just like micelles in solution, have the capacity to solubilize organics within their core (a process known as adsolubilization). They found that polymerization took place within the surfactant admicelles, and polystyrene was formed within the admicelles of the sodium dodecyl sulfate (SDS) surfactant adsorbed on the surface of the alumina. The technique was extended to alumina powder in 1988;³ the calculated film thickness was comparable to the SDS admicelle thickness, and washing after admicellar polymerization affected the substrate's final surface property, setting the stage for a novel process for surface modification.

3.2 REVIEWS ON SURFACE MODIFICATION

3.2.1 Alumina and Aluminum

In a corrosion control study on aluminum alloys, Le et al.,⁴ deposited thin films of poly(2,2,2-trifluoroethyl acrylate) (PTFEA) and poly(methyl methacrylate) (PMMA) via admicellar polymerization, on aluminum alloy coupons. The PTFEA film reduced the

percent of corroded area to 20%, and because it has a higher hydrophobicity than a PMMA-modified surface, it exhibits a better corrosion protection over PMMA film.

As an alternative to carbon black application in rubber reinforcement, white mineral particulates (alumina particles), was coated with an ultra thin film of polystyrene cross-linked with divinylbenzene, poly(styrene-co-divinylbenzene), or P(S-co-DVB), by Wang (2006),⁵ using SDS surfactant. Direct observation of the polymer film was found to be insensitive in attenuated total reflectance (ATR) and diffuse reflectance infrared Fourier Transform (DRIFT), but extraction with tetrahydrofuran (THF) showed positive results, even though extraction of the polymer was difficult, since a more tightly bound P(S-co-DVB) cannot be extracted. After polymerization, scanning electron microscopy (SEM) showed changes in topography but failed to differentiate among different coatings. However, thermogravimetric analysis (TGA) provided strong evidence of the presence for residual SDS and P(S-co-DVB). Hydrophobic properties were achieved to resist water for up to 90 minutes.

Karlsson et al.,⁶ examined the protection of aluminum pigments by means of an encapsulating polymer layer by admicellar polymerization. Good results were obtained in terms of protection from an alkaline solution, an indication that the polymer coating (PMMA and polystyrene (PS)) was an efficient inhibitor. Hydrophobic initiator was preferred because of the hydrophobicity of the tail region in the admicelle for polymerization. Inhibition tests on the susceptibility of the aluminum pigments to alkaline water for PMMA-modified aluminum pigment powder were stable up to 110 days with no visible changes.

Adsorption and adsolubilization of polymerizable surfactants on aluminum oxide was investigated by Attaphong et al.⁷ Styrene and ethylcyclohexane adsolubilization were

independent of the number of ethylene oxide (EO) groups in the surfactant. The admicelle layer as well as the adsolubilization capacity of that layer remained stable after washing, thus, the polymerization of polymerizable surfactants increased the stability of surfactants adsorbed onto the alumina surface and reduced surfactant desorption from the alumina surface.

3.2.2 Silica (rubber fillers)

Admicellar polymerization on amorphous precipitated silica substrates was first studied by O'Haver et al.⁸ using different types of surfactants, water soluble cationic cetyltrimethyl ammonium bromide (CTAB), water insoluble cationic surfactant methyltri(C8-C10) ammonium chloride (ADOGEN 464) and nonionic surfactant octylphenoxy poly(ethoxy) ethanol (MACOL OP10SP). It was explained that the nonionic surfactant had the lowest adsorption on silica because of its larger hydrophobic group. Consequently, ADOGEN gave the highest surfactant adsorption on silica, followed by CTAB and MACOL. The ratio of adsorbed CTAB to adsolubilized styrene was 2:1. Different initiation schemes for polymerization were used, thermal initiation with a water-insoluble initiator 2,2' -azobis(2-methylpropionitrile) (AIBN) and redox initiation using ferrous sulfate. A slower rate of conversion was observed in redox polymerization due to the small amount of ferrous sulfate. According to the paper, high initiator to monomer concentration was necessary when using AIBN because the ethanol used to dissolve AIBN participated in adsolubilization and may consume free radicals that were formed (but it is likely that the free radicals were consumed by the oxygen present in the system since the styrene monomer was not purified). The formation of an integral polymer-silica composite was achieved. Polymer extracts were obtained by refluxing tetrahydrofuran (THF). Only a small amount of polymer, presumably those on or near the silica surface were recoverable. Those formed within the silica pores were most likely difficult to extract.

Properties of rubber after reinforcement by two surface-modified silicas, silane-coupled and admicellar polymerized, were compared by Thammathadanukul et al.⁹ Admicelles were formed using cetyltrimethyl ammonium bromide (CTAB), with styrene–isoprene or styrene–butadiene being used as co-monomers for thin film formation. They observed that higher surface areas of the polymerized silica resulted in better rubber physical properties. Both techniques improved overall rubber properties after reinforcement with the modified silicas, with the admicellar polymerized silica providing better flex cracking resistance.

Nontasorn et al.¹⁰ produced surface-modified silicas by admicellar polymerization in a continuous stirred tank reactor. Rubber testing results were consistent with those obtained from batch systems and reinforcement into rubber compounds improved the physical properties.

Rangsunvigit et al.¹¹ produced a surface-modified silica using CTAB, and polyoxyethylene octylphenol ether (OPEO₁₀) with co-monomers of styrene and isoprene to form the polymer coating. Increase in the OPEO₁₀: CTAB ratio decreased surfactant maximum adsorption because of weaker interactions and steric effect of the bulky head group of nonionic surfactant on silica. The total amount of CTAB required to form a monolayer was reduced using OPEO₁₀. After modification, the specific surface area was reduced while mean agglomerate particle size increased. Coated polymer was further characterized using thermogravimetric analysis (TGA) and scanning electron microscopy (SEM). It was found that of all those tested in this study, the best mechanical properties of rubber compound with modified silica were obtained when CTAB: OPEO₁₀ ratio of 1:3 was used.

Yooprasert et al.¹² observed the effects of surfactant chain length in a study of radiation-induced admicellar polymerization of isoprene on silica. Modification of silica with

CTAB via radiation-induced admicellar polymerization had the best performance among the systems tested. This correlates with a later work by Pongprayoon et al.¹³ who compared different methods of admicellar polymerization to modify silica surface for the rubber reinforcement application, thermal or radiation-induced admicellar polymerization. Cationic surfactants C₁₂-, C₁₄-, C₁₆- trimethyl ammonium bromide (DTAB, TTAB, CTAB) were used to obtain an admicelle layer and isoprene was used as the monomer. Reports show that 40 phr (phr = parts per hundred rubber) of silica was the optimum ratio for the reinforcement of a model rubber compound. Rubber compound with modified silica showed improved mechanical properties. CTAB adsolubilized the highest amount of monomers, since it has the longest hydrophobic chain length with closer packing, hence had the best film formation. SEM images further confirmed the better dispersion in rubber compound with modified silica.

3.2.3 Composite fillers

Graphene was surface modified with nylon 6, 10 and nylon 6, 6 coatings by Das et al.¹⁴ This modification prevented aggregation and showed better dispersibility in a bulk nylon matrix. The organic solvent carbon tetrachloride (CCl₄) was used to swell the sodium dodecyl benzene sulfate (SDBS) surfactant admicelle, providing a better environment for polymerization at the interface. The SEM, atomic force microscope (AFM) and transmission electron microscope (TEM) images showed that nylon film can be non-covalently bonded onto a graphene surface and remained stable in low pH (1.7-2.5) conditions and after freeze-drying.

Likewise, Zhao et al.¹⁵ formed poly(methyl methacrylate) (PMMA) nano film on the surface of rice straw fiber (RSF). PMMA-modified RSF showed good miscibility with poly(lactic acid) (PLA), and stably dispersed in PLA with less agglomeration. Consequently,

reinforcement of PLA composite with modified RSF showed improved tensile strength, increased thermal stability and increased elongation.

3.2.4 Cotton fibers

In 2008, Ren et al.¹⁶ obtained antimicrobial *N*-halamine polymeric coatings on cotton fibers. FTIR and SEM confirmed the presence of *N*-halamines polymer. The coated polymer was stable and rechargeable even after 50 machine washing cycles. After chlorination, the polymeric-coated cotton showed high efficiency in inactivating *Staphylococcus aureus* and *Escherichia coli*.

In a 2008 paper, Tragoonwichian et al.¹⁷ produced a UV-protective cotton by grafting (covalently bonding) a UV-absorbing agent, 2,4-dihydroxybenzophenone, with the monomer, acryloyl chloride, and polymerizing the product, 2-hydroxy-4-acryloyloxybenzophenone (HAB) on the cotton surface by admicellar polymerization using dodecylbenzenesulfonic acid, sodium salt (DBSA) surfactant. Increase in temperature increased surfactant adsorption rate but slightly decreased amount of adsorbed surfactant. Closer packing of adsorbed surfactant was observed in the presence of sodium chloride (NaCl) electrolytes. The reported molar ratio of HAB to DSAB was about 1:2. FTIR and SEM images demonstrated the presence of poly(HAB). After treatment with HAB at concentrations greater than 1.2 mM, the Ultraviolet Protection Factor (UPF) of the cotton fabric was greatly improved from a value of 4 for plain fabric to greater than 40 (excellent protection) after treatment and is effective even under continuous UV exposure up to 24 h.

As a complement to the earlier work, Tragoonwichian et al.¹⁸ in 2009 performed double coating via repeat admicellar polymerization using DBSA as surfactant to recoat an HAB-coated cotton surface with methacryloxymethyltrimethylsilane (MSi). The presence of poly(HAB) and poly(MSi) films were confirmed using SEM and FTIR. The coating of poly(MSi) on poly(HAB)

coated fabric resulted in a fabric with slight decrease in its UV-protection property, but with significant improvement in its water repellency.

Siriviriyanun et al.¹⁹ using the cationic surfactants, CTAB dodecyltrimethylammonium bromide (DTAB), coated a flame retardant cotton fabric with phosphorus-containing thin film poly(acryloyloxyethyl diethyl phosphate) (PADEP). CTAB, having a larger hydrophobic core, showed higher adsorption than DTAB and PADEP-coated cotton using HTAB had a self-extinguishing characteristics. PADEP-coated cotton prepared with DTAB showed a slow flame spread burning the entire fabric without char formation, whereas, untreated cotton had a fast flame spread burning the entire fabric without char formation.

Maity et al.²⁰ compared two surface modification methods, direct fluorination and admicellar polymerization. Both methods resulted in greater hydrophobicity of the cotton fabric. Merits and demerits of both methods were discussed, and based on their results, admicellar polymerization was found to be better compatible with existing textile processing techniques.

In 2011, Tragoonwichian et al.²¹ extended their work on water repellent cotton fabric by admicellar polymerization to include a nonionic surfactant methacryloxypropylpentamethyldisiloxane (MDSi). Analyses from wetting, SEM, Fourier transform infrared spectroscopy, energy dispersive spectroscopy (EDS) and contact angle, confirmed the formation of polymer films. The cationic surfactant, MSi, had a higher adsorption leading to more hydrophobicity and better water repellency of the treated cotton than the nonionic surfactant.

3.2.5 Calcium Carbonate

Chibowski²² examined the adsorption of SDS on a CC surface in the presence of polyacrylamide (PAA) using radiotracer techniques for SDS. The presence of PAA on the surface of CaCO_3 increased SDS adsorption especially when the pH is greater than the point of zero charge (pzc) (the pH at which the electrical charge density on a surface is zero). It was observed that PAA-SDS complexes formed in the bulk when premixing high concentration SDS and PAA solutions which contributed to the decrease in SDS adsorption.

In a rheological study of oil dispersion properties of silanated CaCO_3 , Kurkarni, et al.²³ found that silanes reduced particle-particle interaction and decreased dissipation energy under shear. They discovered that significant modifications in the dispersion properties, and hence rheology, can be affected by the appropriate choice of treating silane.

Wettability as a test for surface modification has been examined by various writers this past decade. In 2003, Standnes and Austad,²⁴ investigated ion-pair interaction between a cationic surfactant, DTAB, and the carboxylates present in crude oil and model oil systems. Dynamic experiments, using model oil systems, containing different types of fatty acids and C_{12}TAB dissolved in brine, showed that the surfactant solution imbibed spontaneously into the oil-wet material in a counter-current flow regime governed by mainly capillary forces, indicating that a wettability alteration process had taken place.

The effects of the structure of fatty acids, water composition and pH on wettability of calcite surface were studied via contact angle measurement by Rezaei, Gomari and Hamouda.²⁵ They showed that fatty acids in the presence of a water film alter the calcite surface to oil-wet, presence of magnesium and sulfate ions increased the water-wetness of the calcite, and wetting was dependent on the pH. Increasing pH from 5 to 7, in the presence of both ions, increased the

water wettability of the calcite. While further increase in pH (above 7) in the presence of the magnesium ions continue to increase water wettability, there was decreased water wettability in the presence of sulfate ions (at pH above 7), resulting in a slightly oil-wet calcite surface.

In 2006, Strand et al.²⁶ obtained information about the chemical mechanism behind wettability alteration of carbonates by sulfate ions. It was shown that at high temperatures, an injection fluid containing sulfate ions changed the wetting state of chalk from preferential oil-wet to preferential water-wet. Adsorption of sulfate onto chalk was studied at different concentration of calcium ions. It was observed that the adsorption of sulfate onto chalk increased as the temperature and concentration of calcium ions increased.

Jarrahian, et al.²⁷, altered the wettability of carbonate rocks using three types of surfactants. Cationic surfactant C₁₂TAB irreversibly desorbed stearic acid from the dolomite surface via ionic interaction. Triton-X 100 adsorbed on the surface by the polarization of π electrons and ion exchange, releasing more stearic acid from the solid surface, which is then adsorbed as a new layer on the surface through hydrophobic interaction between the tail of adsorbed surfactants and the non-polar part of the stearic acid. The anionic surfactant SDS adsorbed on the surface via hydrophobic interaction between the tail of surfactant and the adsorbed acid, thereby changing the wettability of the surface to neutral wet condition.

Admicellar polymerization was recently employed in the surface modification of calcium carbonate particles for use as filler by Rungruang et al.²⁸ The point of zero charge (pzc) for CaCO₃ used was reported to be 11.4. Sodium dodecylsulfate (SDS) was used as the surfactant. Equilibration time for SDS adsorption on CaCO₃ was achieved after 18 hours. The effect of increasing sodium ions provided shielding to surfactant head group repulsion and increased the amount of adsorbed SDS. An SDS adsorption isotherm was obtained and admicellar

polymerization was run using gaseous propylene monomer. FTIR characterization analysis, gravimetric weight loss analysis, increased diameter of particles showed the presence of thin film of polypropylene on CaCO_3 . The isopropylene (iPP) treated CaCO_3 composite was tested for non-isothermal crystallization studies. Crystallization temperature and the melting endotherm of iPP filled with modified CaCO_3 was lower than those for untreated CaCO_3 composite samples, which indicated reduced nucleation of filler particles. Decreases in Wide Angle X-ray Diffraction (WAXD) crystallinity were also observed. Mechanical properties testing on iPP filled with modified CaCO_3 showed reduced yield stress, increased yield strain, reduced flexural strength and increased impact resistance because the thin film acted as a lubricant between particles and the polymer matrix. Better dispersion and distribution of modified CaCO_3 was confirmed in Scanning Electron Microscopy (SEM) study.

H. Ding ²⁹ modified CaCO_3 by grinding CaCO_3 with SDS in an ultrafine stirred mill and used this as filler in polyethylene (PE). Analysis with Infrared (IR) and X-ray photoelectron energy spectroscopy (XPS) was performed. Decreases in particle size or increases in specific surface area of the particles improved modification effect which means a more hydrophobic surface. Optimum experimental conditions were studied such as concentration of SDS, mass ratio of grinding media to feeding, and grinding forces and duration. Modified CaCO_3 incorporated into PE as filler showed improved mechanical and physico-chemical properties. IR and XPS show SDS adsorption on the surface of CaCO_3 .

J. Zhang et al.³⁰ synthesized maleic anhydride grafted polyethylene wax (MA-g- PEW) by mixing melted polyethylene wax, maleic anhydride and free radical initiator di-tertbutyl peroxide (DTBP). Purified MA-g-PEW was dissolved in toluene and mixed with CaCO_3 by mechanical stirring. Fourier transform infrared spectroscopy (FTIR) characterization showed the

presence of MA-g-PEW in modified CaCO_3 . Transmission emission microscopy (TEM) showed less agglomeration and increases in CaCO_3 thickness after the modification. 100% active ratio (ratio of floated product over overall dispersed sample used to check for hydrophobicity) was able to be achieved at 2.5% MA-g-PEW or above. Decrease in shear forces and viscosity (less agglomeration) with increase weight ratio of MA-g-PEW to modified CaCO_3 indicated reduction in resistance forces. Overall, the optimum weight ratio of MA-g-PEW to modified CaCO_3 in order to change the CaCO_3 surface from hydrophilic to hydrophobic was reported as 2.5%.

3.2.6 Other mineral surfaces

Wei et al.³¹ inspected the ability of different washing steps on removal of materials from admicellar polymerized titanium dioxide and alumina. X-ray photoelectron spectroscopy (XPS) measurements indicated that after admicellar polymerization, organic material and surfactant are present on the surface of the solids. The study showed that polymer formed on both the outside surface and the inside surface of a rough, porous solid. Only about half of the material could be removed on the outside surface after solvent washes (water washing followed by Soxhlet extraction with toluene). Ratio of surfactant to polymer on the outside surface after admicellar polymerization and solvent wash was approximately 1:1, whereas the ratio on the interior surface is approximately 3:1.

Lastly, Marquez et al.³² compared three different methods of attaching polymers to sand. In-situ graft polymerization of vinyl monomers (acrylamide or acrylic acid with vinyl acetate) onto an organosilane sub layer chemically bonded to the sand surface (γ -methacryloxypropyl-trimethoxysilane (MPS) was used as the silane-coupling agent for the silanation reactions). Chemical grafting of preformed water-soluble polymers onto an organosilane sub layer chemically bonded to the sand surface, and admicellar polymerization using

cetyltrimethylammonium bromide (CTAB) surfactant and various monomers (acrylic acid, vinyl acetate and acrylamide). Presence of polymer on the surface was confirmed in all three cases. The highest amounts of polymer coating were achieved by grafting of preformed water-soluble polymers compared to all of the other techniques.

3.3 COMMENTARY

The same surfactant on different substrates gives different ratio of adsolubilized monomer to adsorbed surfactant (Table 3.1, comparing O'Haver⁸ and Kitiyanan³⁴). Likewise, different surfactants on the same substrate give different adsolubilized monomer to surfactant ratios (Table 3.1, comparing O'Haver⁸ and Tan³³). Though adsolubilization is generally agreed to increase with increased adsorption, addition of lipophilic linkers (for nonionic surfactant)³³ and the effect of the structure of the monomer,¹⁹ (see Table 3.1) showed that adsolubilization depends on other factors, especially the surface properties (like surface area and surface energy) of the substrate. This observation was evident in the present work, where the ratio of adsolubilized monomer molecules to adsorbed surfactant molecules was 50:1 with extra-fine CC (XFCC).

These varying results are indications that every system is unique and apparently unpredictable, thus, the success of admicellar polymerization on any system should be predicated on sound experimental testing of that particular system.

Table 3.1: Approximate values of adsorbed surfactant molecules to adsolubilized monomer molecules from some authors

	Adsolubilized monomer molecules	Adsorbed surfactant molecules
Wu et al. ^{1,1} (Styrene and SDS on alumina)	1	2
O'Haver et al. ⁸ (Styrene and CTAB on Hi-Sil 233)	1	2
Kitiyanan ³⁴ (Styrene and CTAB on Hi-Sil 255) (Isoprene and CTAB on Hi-Sil 255)	1.7 3.69	1 1
Tan et al. ³³ (Styrene and Triton X on Hi-Sil 233)	2.7	1
Tragoonwichian et al. ¹⁹ (HAB and DBSA on cotton fabric)	1	2

¹Indicates one mole of styrene was adsolubilized by two molecules of SDS, indirectly supporting the existence of a bilayer.

LIST OF REFERENCES

3.4 REFERENCES

1. Wu, J.; Harwell, J. H.; O'Rear, E. A. Two-Dimensional Reaction Solvents: Surfactant Bilayers in the Formation of Ultrathin Films. *Langmuir*. **1987**, 3, p531-37.
2. Wu, J.; Harwell, J. H.; O'Rear, E. A. Two-Dimensional Solvents: Kinetics of Styrene Polymerization in Admicelles at or near Saturation. *J. Phys. Chem.* **1987**, p623-34.
3. Wu, J.; Harwell, J. H.; O'Rear, E. A. Application of Thin Films to Porous Mineral Oxides Using Two-Dimensional Solvents. *AIChE Journal*. **1988**, 34, 9, p1511-18.
4. Le, D.V.; Kendrick, M.M.; O'Rear, E.A. Admicellar Polymerization and Characterization of Thin Poly (2,2,2-trifluoroethyl acrylate) Film on Aluminum Alloys for In-Cervice Corrosion Control. *Langmuir*. **2004**, 20 (18), p7802-10.
5. Wang, S.; Russo, T.; Qiao, G.G.; Solomon, D.H.; Shanks, R.A. Admicellar Polymerization of Styrene with Divinyl Benzene on Alumina Particles: The Synthesis of White Reinforcing Fillers. *J. Mater. Sci.* **2006**, 41, p7474-82.
6. Karlsson, P.M.; Esbjornsson, N.B.; Holmberg, K. Admicellar Polymerization of Methyl Methacrylate on Aluminum Pigments. *J. Colloid and Interface Science*. **2009**, 337, p364-68.
7. Attaphong, C.; Asnachinda, E.; Charoensaeng, A.; Sabatini, D.A.; Khaodhiar, S. Adsorption and Adsolubilization of Polymerizable Surfactants on Aluminum Oxide. *J. Colloid and Interface Science*. **2010**, 344, p126-131.
8. O'Haver, J.H.; Harwell, J.H.; Snodgrass, L.J.; Waddell, W.H. In Situ Formation of Polystyrene in Adsorbed Surfactant Bilayers on Precipitated Silica. *Langmuir*. **1994**, 10, p2588-93.

9. Thammathadanukul, V.; O'Haver, J.H.; Harwell, J.H.; Osuwan, S.; NaRanong, N.; Waddell, W.H. Comparison of Rubber Reinforcement Using Various Surface-Modified Precipitated Silicas. *J. Applied Polymer Science*. **1996**, 59, p1741-50.
10. Nontasorn, P.; Chavadej, S.; O'Haver, J.H.; Chaisirimahamorakot, S.; Na-Ranong, N. Admicellar Polymerization Modified Silica Via a Continuous Stirred-Tank Reactor System: Comparative Properties of Rubber Compounding. *Chemical Engineering Journal*. **2005**, 108, p213-18.
11. Rangsunvigit, P.; Imsawatgul, P.; Na-ranong, N.; O'Haver, J. H.; Chavadej, S. Mixed Surfactants for Silica Surface Modification by Admicellar Polymerization Using a Continuous Stirred Tank Reactor. *Chemical Engineering Journal*. **2008**, 136, p288-94.
12. Yooprasert, N.; Pongprayoon, T.; Suwanmala, P.; Hemvichian, K.; Tumcharern, G. Radiation-induced Admicellar Polymerization of Isoprene on Silica: Effects of Surfactant's Chain Length. *Chemical Engineering Journal*. **2010**, 156, p193-99.
13. Pongprayoon, T.; Yooprasert, N.; Suwanmala, P.; Hemvichian, K. Rubber Products Prepared from Silica Modified by Radiation-induced Admicellar Polymerization. *Radiation Physics and Chemistry*. **2012**, 81, p541-46.
14. Das, S.; Wajid, A.S.; Shelburne, J.L. Liao, Y., Green, M.J. Localized In Situ Polymerization on Graphene Surfaces for Stabilized Graphene Dispersions. *ACS Applied Materials and Interfaces*. **2011**, 3, p1844-51.
15. Zhao, Y.; Qui, J.; Feng, H.; Zhang, M.; Lei, L.; Wu, X. Improvement of Tensile and Thermal Properties of Poly(lactic acid) Composites with Admicellar Polymerization. *Chemical Engineering Journal*. **2011**, 173, p659-66.

16. Ren, X.; Kou, L.; Kocer, H.B.; Zhu, C.; Worley, S.D.; Broughton, R.M.; Huang, T.S. Antimicrobial Coating of an *N*-halamine Biocidal Monomer on Cotton Fibers via Admicellar Polymerization. *Colloids and Surfaces A: Physicochem. Eng. Aspects.* **2008**, 317, p711-16.
17. Tragoonwichian, S.; O'Rear, E. A.; Yanumet, N. Admicellar Polymerization of 2-hydroxy-4- acryloyloxybenzophenone: The Production of UV-Protective Cotton. *Colloids and Surfaces A: Physicochem. Eng. Aspects.* **2008**, 329, p87-94.
18. Tragoonwichian, S.; O'Rear, E. A.; Yanumet, N. Double Coating via Repeat Admicellar Polymerization for Preparation of Bifunctional Cotton Fabric: Ultraviolet Protection and Water Repellence. *Colloids and Surfaces A: Physicochem. Eng. Aspects.* **2009**, 349, p170-75.
19. Siriviriyannun, A.; O'Rear, E.A.; Yanumet, N. The Effect of Phosphorous Content on the Thermal and the Burning Properties of Cotton Fiber Coated with an Ultrathin Film of a Phosphorous- Containing Polymer. *Polymer Degradation and Stability.* **2009**, 94, 4, p558-65.
20. Maity, J.; Kothary, P.; O'Rear, E. A.; Jacob, C. Preparation and Comparison of Hydrophobic Cotton Fabric, Obtained by Direct Fluorination and Admicellar Polymerization of Fluoromonomers. *Ind. Eng. Chem.* **2010**, 49, p6075-79.
21. Tragoonwichian, S.; Kothary, P.; Siriviriyannun, A.; O'Rear, E. A.; Yanumet, N. Silicon-Compound Coating for Preparation of Water Repellent Cotton Fabric by Admicellar Polymerization. *Colloid and Surfaces A: Physicochem. Eng. Aspects.* **2011**, 384, p381-87.

22. Chibowski, S. Investigation on Interactions of Sodium Dodecyl Sulfate and Polyacrylamide Molecules on Calcium Carbonate Surface Using Radiotracer Technique. J. Colloid and Interface Science. **1980**, 76, 2, p371-74.
23. Kurkarni, R.D.; Leung, P.S.; Goddard, E.D. Oil Dispersion properties of Silanated Calcium Carbonate: A Rheological Study. Colloid and Surfaces. **1982**, 5, p321-32.
24. Standnes, D.C.; Austad, T. Wettability alteration in carbonates: Interaction between cationic surfactants and carboxylates as a key factor in wettability alteration from oil-wet to water-wet conditions. Colloids and Surfaces A: Physicochemical and Engineering Aspects. **2003**, 216, 1-3, p243-259.
25. Rezaei Gomari, K.A.; Hamouda, A.A. Effect of fatty acids, water composition and pH on the wettability alteration of calcite surface. J. Petroleum Science and Engineering. **2006**, 50, 2, p140-50.
26. Strand, S.; Hognesen, E.J.; Austad, T. Wettability alteration of carbonates – Effects of potential determining ions (Ca^{2+} and SO_4^{2-}) and temperature. Colloids and Surfaces A: Physicochemical and Engineering Aspects. **2006**, 275, 1-3, p1-10.
27. Jarrahan, Kh.; Seiedi, O.; Sheykhan, M.; Vafaie Sefti, M.; Ayatollahi, Sh. Wettability alteration of carbonate rocks by surfactants: A mechanistic study. Colloids and Surfaces A: Physicochemical and Engineering Aspects. **2012**, 410, p1-10.
28. Rungruang, P.; Grady, B.P.; Supaphol, P. Surface-modified calcium carbonate particles by admicellar polymerization to be used as filler for isotactic polypropylene. Colloids and Surfaces A: Physicochem Eng. Aspects. **2006**, 275, p114-25.

29. Ding, H.; Lu, S.; Deng, Y.; Du, G. Mechano-activated surface modification of calcium carbonate in wet stirred mill and its properties. *Trans. Nonferrous Met. Soc. China* **2007**, *17*, p1100-04.
30. Zhang, J.; Guo, J.; Li, T.; Li, X. Chemical Surface Modification of Calcium Carbonate Particles by Maleic Anhydride Grafting Polyethylene Wax. *International Journal Green Nanotechnology: Physics and Chemistry* **2010**, *1*, p65-71.
31. Wei, X.; Carswell, A. D. W.; Alvarez, W.; Grady, B. P. X-ray Photoelectron Spectroscopic Studies of Hydrophilic Surfaces Modified via Admicellar Polymerization. *J. Colloid and Interface Science*. **2003**, *264*, 1, p296-300.
32. Marquez, M.; Grady, B. P.; Robb, I. Different Methods for Surface Modification of Hydrophilic Particulates with Polymers. *Colloids and Surfaces A: Physicochem. Eng. Aspects*. **2005**, *266*, 1-3, p18-31.
33. Tan, Y. and O'Haver, J.H. Lipophilic Linker Impact on Adsorption of and Styrene Adsolubilization in Polyethoxylated Octylphenols. *Colloids and Surfaces A: Physicochem. Eng. Aspects*. **2004**, *232*, p101-11.
34. Kitiyanan, B.; O'Haver, J.H.; Harwell, J.H.; Somchai, O. Adsolubilization of Styrene and Isoprene in Cetyltrimethylammonium Bromide Admicelle on Precipitated Silica. *Langmuir*. **1996**, *12*, p1262-68.

CHAPTER FOUR

ADMICELLAR POLYMERIZATION OF POLYSTYRENE TO COMPATIBILIZE CALCIUM CARBONATE WITH OIL-BASED DRILLING MUD (OBM): FOR IMPROVED MUD PERFORMANCE

To improve the performance of oil-based drilling mud (OBM) by enhancing the mud compatibility with its weighting agent, calcium carbonate (CC), the surface of industrial CC was modified *in situ* by admicellar polymerization. An organic monomer, styrene, was polymerized on the surface of three different grades of industrial CC using (4-octylphenol polyethoxylate), Triton™ X-100 (TX-100), as surfactant and 2,2'-azobisisobutyronitrile (AIBN) as initiator. An adsorbed surfactant bilayer (admicelle) on the CC surface was used as the reaction site for the synthesis of the polymer film from adsolubilized monomer. The coated polymer was recovered by refluxing tetrahydrofuran (THF) in a Soxhlet extractor and was characterized with FTIR-ATR (Fourier transform infrared-attenuated total reflectance) and thermogravimetric analysis (TGA). Surface characterization and thermal analysis of the treated CC and the extracted material confirmed the existence of the polystyrene thin film on the CC surface. Extractable polymer of up to 2.6 weight % of the treated CC was obtained. The process presents an inexpensive technique to modify calcium carbonate's high energy hydrophilic surface into a low energy hydrophobic surface, increasing its compatibility with OBM used in oil and gas drilling operations. Better compatibility will allow higher filler loadings, enhance drilling fluid homogeneity leading to a more uniform viscosity thereby improving removal of drill cuttings,

increasing wellbore pressure, increased mud reuse, and overall improvement of the mud performance.

4.1 INTRODUCTION

Surface modification processes have been extensively explored to produce materials with improved performance for a wide range of applications. In admicellar polymerization, surfactants adsorbed on the surface of a substrate are utilized as a reaction template for *in situ* polymerization to modify the substrate surface and create materials with new surface properties. Admicellar polymerization is based on using adsorbed surfactant aggregates (admicelles) as a reaction medium. Numerous studies have shown that admicelles adhere well to the substrate.¹⁻⁶ Admicellar polymerization has been used to produce fillers with better compatibility.^{5,6} Since the film represents the interface between the two phases that are heterogeneous in nature,⁷ the resulting structure and properties of the formed ultrathin film will have a major impact on the final interfacial properties of the modified substrate. Through admicellar polymerization, different types of polymeric thin films have been formed on various substrates such as polystyrene on silica,¹ cotton,⁸⁻¹⁰ alumina,¹¹ styrene-isoprene copolymer on glass fiber,¹² and polypyrrole on mica.¹³

Weighting materials are often added to drilling fluids as densifiers to support and stabilize the wellbore during drilling operations. A good weighting agent should increase mud density to achieve wellbore pressure, seal permeable formations with thin low permeability filter cake minimizing formation damage, and be affordable. Calcium carbonate (CC) is often used in preference to barite because it is acid soluble and can therefore be easily dissolved as part of the

process of cleaning up the production zone. Moreover, it is readily available in usable form and at low cost. A major problem, however, is the incompatibility of its high-energy hydrophilic surface with the low-energy hydrophobic oil-based drilling fluid (oil-based mud) (OBM). The high energy hydrophilic surface of CC is a major limitation in the many applications (such as mineral filler for polymers, adhesives, paper, paints, and oil and gas drilling fluids) where it is used, creating a problem of weak compatibility. Consequently, much research has been performed on the surface modification of CC to enhance its compatibility with the host material.¹⁴⁻²² Applications of surfactant in drilling mud formulations abound,²³ but scarcely is there any attempt to surface modify the weighting agent used in these formulations, even though there is poor compatibility of the weighting agent and the widely used OBM. Thus, admicellar polymerization, for this particular application, is a novel approach.

The four-step film-forming process includes (1) adsorption of surfactant, e.g. TX-100, (2) adsolubilization of an organic monomer, styrene, (3) initiation of *in situ* polymerization of the monomer in the surfactant adsorbed layer, by addition of 2,2'-Azobisisobutyronitrile (AIBN) initiator, and (4) partial surfactant removal, by washing the treated CC, in order to remove accessible surfactant and expose the synthesized polymer film coated on the surface.

In this work, admicellar polymerization was used to produce ultrathin polystyrene films on the surface of four different size grades of industrial CC, Coarse CC, Medium CC, Fine CC, and Extrafine CC (XFCC) particles. The films were synthesized within the admicelles of TX-100 surfactant adsorbed on the CC surfaces. The adsolubilized polymer was exposed by washing with DI water. The polymer and remaining surfactant was successfully extracted, analyzed and characterized. Results confirm the formation of polystyrene.

It is expected that the polymer coated particles would contribute to the increased compatibility between the oil-based drilling fluid and the treated CC particles as opposed to untreated ones.

4.2 EXPERIMENTAL

4.2.1 Materials

Four different grades of industrial calcium carbonates, Adi™ CARB 5 (XF) (Extra-fine CC), Adi™ CARB 25 (F) (Fine CC), Adi™ CARB 50 (M) (Medium CC), and Adi™ CARB 150 (C) (Coarse CC) were courteously supplied by BCI Chemical Corporation, Sdn, Bhd. (Selangor Darul Ehsan, Malaysia). Triton™ X-100 (TX-100) (laboratory grade), a polyethoxylated (≈ 10.5 EO groups) octyl phenol (purity of 99 %+), was purchased from Sigma-Aldrich, Inc. (St. Louis, MO). Styrene (stabilized and at purity of 99 %), was purchased from Acros (New Jersey, USA). 2,2'-Azobisisobutyro-nitrile (AIBN) (purity of 98 %), was purchased from Sigma-Aldrich, Inc. (St. Louis, MO). Deionized water was obtained from a Millipore Direct-Q 3UV Water Purification System.

4.2.2 Qualitative analysis of the calcium carbonates

Since our substrate is naturally occurring calcium carbonate, in order to ensure that the experiment will not be affected by any impurity that might be present in the sample. Quantitative analysis of the metallic composition of three different grades, coarse, medium, and fine samples of CC supplied by BCI Chemical Corporation was performed using inductively coupled plasma mass spectrometry (ICP-MS). The ICP-MS results demonstrated that the amount of the other

metals present in the supplied CC are insignificant, thus their interference would be minimal. The CC grades all had similar compositions (about +/- 0.5 % of Mg ion).

4.2.3 Specific Surface Area Analysis of the calcium carbonates

The specific surface areas of the CC samples were obtained using a NOVA 2000 Multi Speed Gas Sorption Analyzer (NovaWin2) from Quantachrome Instruments (Boynton Beach, FL). The results were calculated using both the multi-point BET method and the Langmuir Adsorption method, performed in the accompanying software.

4.2.4 Surfactant adsorption

XFCC, having the highest specific surface area, was used as a representative of the other size grades for preliminary studies, the other three CC size grades were later treated using similar methods. A stock solution of TX-100 with a concentration of 10 mM, around 50 times the CMC (0.22-0.24 mM)^{*} was prepared by diluting a measured quantity of TX-100 (1.7 M) with an appropriate quantity of distilled water. A calibration curve for absorbance versus surfactant concentration was performed using a UV-1201s spectrophotometer (Shimadzu Co., Colombia, MA). Approximately 10 g of XFCC was weighed and added to 40 mL of solutions of varying surfactant concentrations. The samples were occasionally shaken once every hour and allowed to equilibrate at room temperature (25±2 °C) for 24 h. The vials were then centrifuged using a Fischer Scientific MARATHON 3200 centrifuge at 3000 rpm for 4 min. The supernatant was then removed by syringe, and filtered through a 0.2 micron PTFE syringe filter before UV-vis analysis. The amount of TX-100 in the bulk was determined by comparing the adsorption at 275 nm of the unknown solution with that of a calibration curve and the surfactant adsorption was

^{*} Sigma Product Information Sheet

calculated from the change in concentration. An adsorption isotherm was then generated by plotting the surfactant adsorption versus the equilibrium concentration.

The hydrodynamic radius of TX-100 in various solutions with varying surfactant concentration was determined through dynamic light scattering technique, using a Zetasizer Nano-ZS by Malvern Instrument Inc. (Westborough, MA).

4.2.5 Monomer adsolubilization

As it is important to admicellar polymerization that it operates below the critical micelle concentration, the adsorption isotherm was used to determine a feed concentration of the surfactant that would equilibrate at approximately 90 % of the CMC. At the appropriate feed concentration, samples were prepared by adding appropriate amounts of a stock TX-100 solution with distilled water and known quantities of styrene saturated water of a known concentration to 3 g samples of XFCC in 40 mL vials. Calibration of styrene concentrations versus UV-vis absorbance was performed similarly to TX-100 UV-vis calibration, but at 281 nm. A saturated styrene solution was prepared with distilled water. Styrene solubility in water is 2784 μM .[†] Samples of 3 g of XFCC were added to PTFE lined vials and constant TX-100 concentration, with varying styrene concentrations were added accordingly. The volume of bulk surfactant required to get the constant concentration, was obtained using

$$V_1 = C_2 * V_2 * \frac{1}{C_1} \quad \text{Eq. 1}$$

where C_1 is the saturation concentration of styrene in water and C_2 is the desired concentration (constant concentration) and V_2 is the total volume of solution (40 mL). The styrene

[†] Acros Product Information Sheet

concentration was varied in each vial but total solution volume and surfactant concentration was kept constant. The mixtures were shaken at intervals and left to equilibrate for 1 day. Samples were centrifuged and supernatant solution analyzed using UV-vis at 281 nm. Styrene adsolubilization was obtained using the change in concentration method, and the adsolubilization isotherm generated.

4.2.6 Admicellar polymerization

Samples adding up to a total volume of 40 mL containing 10 g XFCC, 310 μ M TX-100, 2.45 mM styrene, and 122 mM AIBN were prepared. The samples were allowed to equilibrate for 24 h before the addition of 0.08 mL of AIBN solution, to produce a monomer to initiator ratio of 10:1 was injected to each vial. And allowed to equilibrate for 24 h. Relatively, high initiator: monomer mole ratio levels for admicellar polymerization have always been used, possibly due to the fact that ethanol used to dissolve the AIBN may act to consume many of the radicals formed¹, but it is likely because the solutions were not purged of oxygen or inhibitor removed from the styrene, with the oxygen consuming most of the radicals. The sealed vial was placed in a thermostated water bath at 70 °C, for a 6 h polymerization. After polymerization, the mixture was centrifuged in order to easily decant the supernatant solution. The XFCC substrate was washed to remove the accessible TX-100 by adding water to the substrate, shaking vigorously, centrifuging, and then decanting the supernatant. The washing process was repeated five times, and treated substrate finally placed in an oven at 100 °C until dry.

4.2.7 Characterization of the treated calcium carbonate

BET N₂ surface area analysis of the treated substrates was done using a NOVA 2000 Multi Speed Gas Sorption Analyzer (NovaWin2) from Quantachrome Instruments, FTIR-ATR

analysis was done via a BRUKER TENSOR 27 IR Spectrometer, using resolution of 4 cm^{-1} and 64 scans, and thermal decomposition of the treated samples was examined using a TA Instruments thermogravimetric analyzer (TGA) Q 500 Series, heating at $10\text{ }^{\circ}\text{C}/\text{min}$ from room temperature to $500\text{ }^{\circ}\text{C}$.

4.2.8 Characterization of the polystyrene coated on calcium carbonate surface

Soxhlet extraction with refluxing tetrahydrofuran (THF) was used to extract the polymer from the treated CC. The resulting hot mixture was added to water to precipitate the polymer, filtered and then dried. The residual polymer was analyzed with FTIR-ATR using resolution of 4 cm^{-1} and 64 scans, and was analyzed with TGA, from room temperature to $500\text{ }^{\circ}\text{C}$ at $10\text{ }^{\circ}\text{C}/\text{min}$.

4.3 RESULTS AND DISCUSSION

4.3.1 Surface area of the calcium carbonates

Surface area results showed that the supplier reported values were apparently based on the Langmuir model, as the values were very comparable to those obtained from BET analysis using the Langmuir model but were about twice of those obtained from the multi-point BET results, which is usually an average of the surface area. See Table 4.1.

Table 4.1: Particle size properties of the four industrial CC size grades

Industrial CaCO₃	Particle size (diameter) μm	Specific surface area, m²/g (Laser Diffraction)	Specific surface area, m²/g (BET N₂) Multi-Point BET/Langmuir
Coarse	105.00	0.22	0.30/0.50
Medium	92.58	0.48	---
Fine	26.20	1.00	0.61/0.99
Extrafine	8.30	1.74	1.09/1.78

4.3.2 Surfactant adsorption

Slight adsorption drop was seen after the surfactant critical micelle concentration (CMC), which may have been due to impurities in the system. Although the tensiometer results of filtered supernatant solutions after adsorption on CC indicate that the CMC remains fairly stable after adsorption, (Table 4.2, Figures 4.1, 4.2). The Zetasizer results indicate that the hydrodynamic radius of changes with increasing surfactant concentration above the CMC. This implies that the aggregation number of TX-100 micelles changes with increasing surfactant concentration, as has been reported by Paradies.²⁸ The adsorption isotherms (Figure 4.3) were Langmuirian as expected, and the CMCs were comparable to those in the literature.

TX-100 has an area per molecule of 48 \AA^2 , i.e. $48 \times 10^{-20} \text{ m}^2/\text{molecule}$. The maximum amount of TX-100 that can be adsorbed on 1 gram of sample was calculated as shown below.

$$\frac{1.0 \frac{\text{m}^2}{\text{g}}}{48 \times 10^{-20} \frac{\text{m}^2}{\text{molecule}}} * \frac{1 \text{mole}}{6.022 \times 10^{23} \text{molecules}} = 3.46 \frac{\mu\text{mole}}{\text{g}}$$

This theoretical value is 10 times more than the experimental value ($\approx 0.34 \mu\text{mole/g}$) obtained from the adsorption isotherm, or 5 times more than what is needed for bilayer formation. Consequently, actual adsorption is lower than theoretical.

Table 4.2: Comparison of TX-100 CMC (approximate) before and after adsorption

TX-100 CMC (mM) Before Adsorption	TX-100 CMC (mM) After Adsorption
0.23	0.25
0.24	0.23
0.22	0.26
0.25	0.26

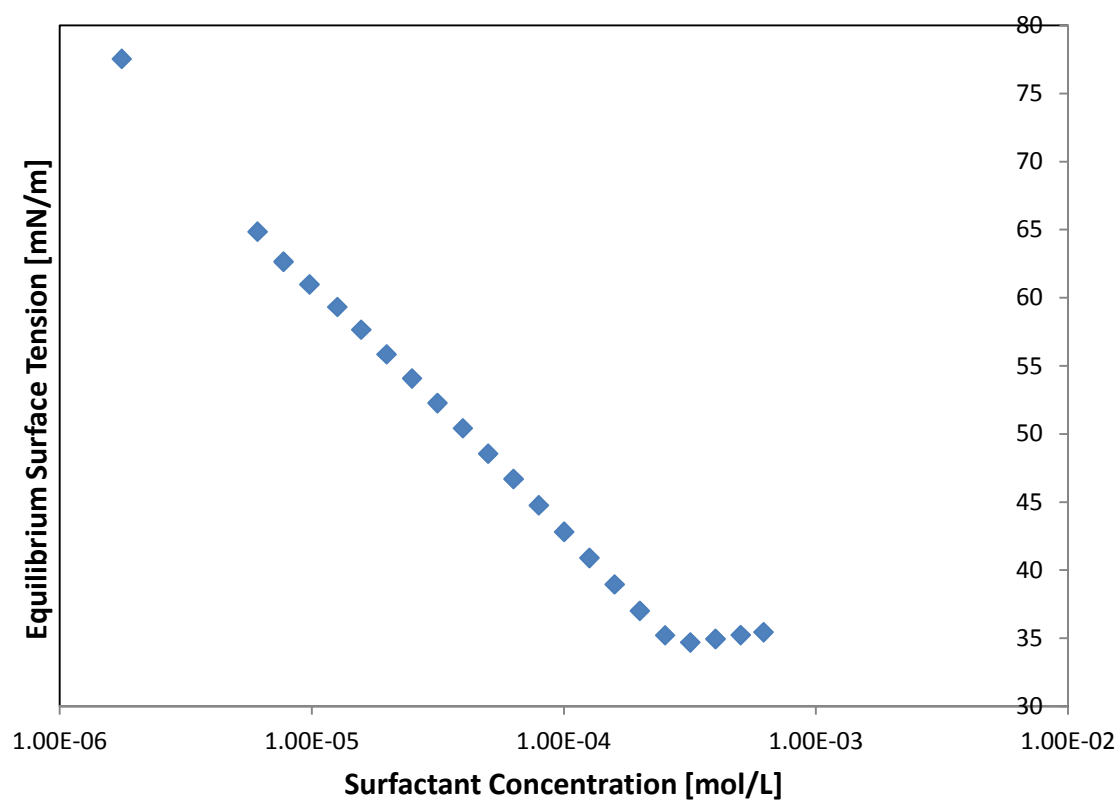


Figure 4.1: Tensiometer display during determination of TX-100 CMC before adsorption.

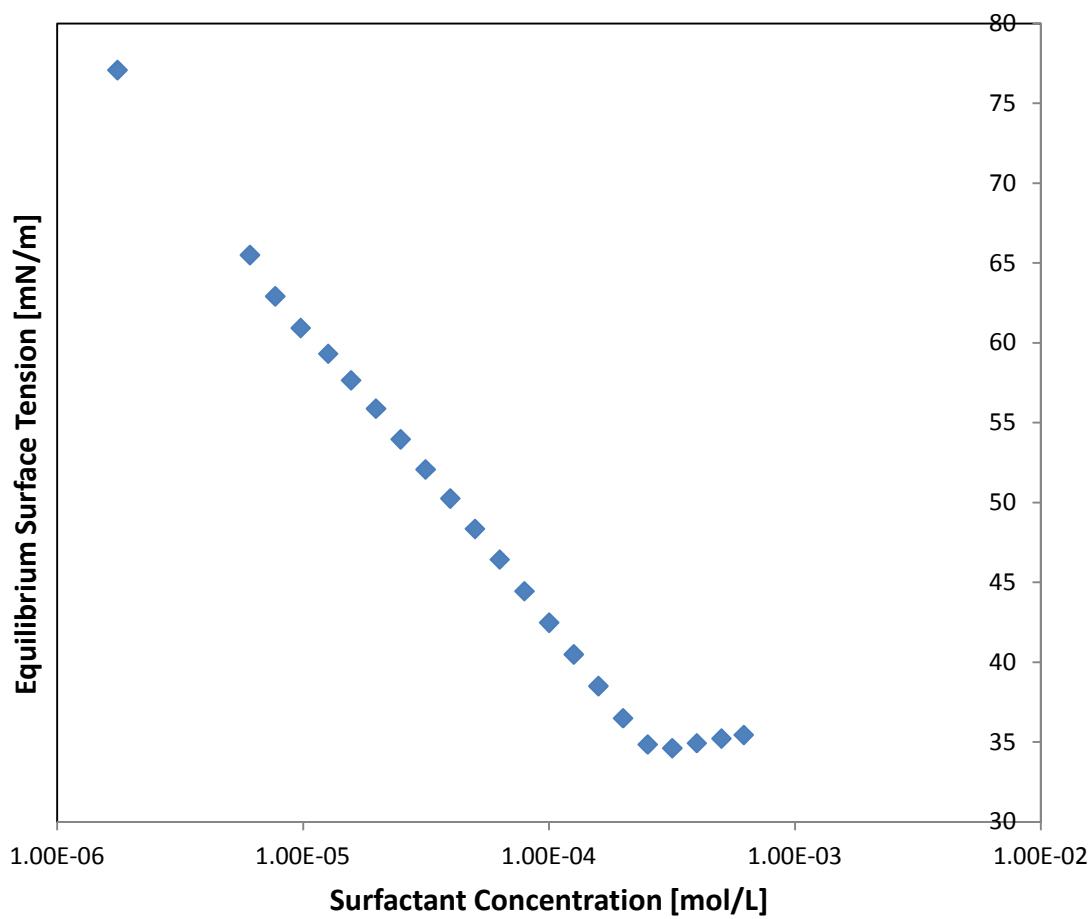


Figure 4.2: Tensiometer display during determination of TX-100 CMC after adsorption.

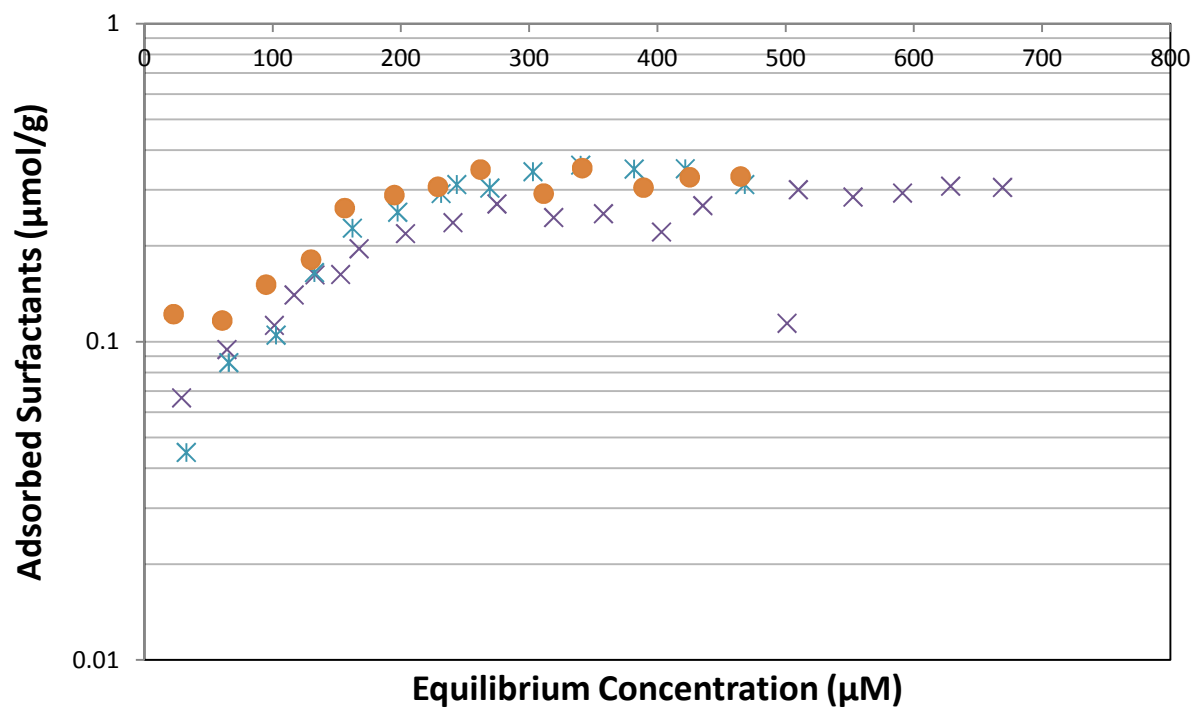


Figure 4.3: Adsorption isotherms of TX-100 on XFCC.

Changes in TX-100 Aggregation- Due to the slight drop in adsorption after the CMC, the aggregation number of the surfactant was determined using a Zetasizer. An hydrodynamic diameter of 7.5 nm will give an estimated weight of 72 kDa, since the average molecular weight of its monomer unit is 631 Da,²⁴ and therefore an aggregation number of 114, similar to reported values in literature.^{25, 26} It can be hypothesized from the Zetasizer results that there is a switch between oblate and prolate micelle ellipsoid and vice versa. Radius obtained at 1 mM was about 1.5 times those at higher concentrations (Table 4.3). This irregularity has been reported in the literature since the late 70s.^{27, 28}

Table 4.3: Hydrodynamic radius of TX-100 micelles at various surfactant concentrations

TX-100 Concentration (mM)	z-Average Radius (nm) (Before adsorption on XFCC) (± 0.01)	z-Average Radius (nm) (After adsorption on XFCC) (± 0.01)
1	5.896	7.037
1	5.666	7.025
1	5.999	7.114
1	5.939	7.021
3	4.837	-
3	4.482	-
3	4.55	-
4	4.249	-
4	4.183	-
4	4.165	-
5	4.629	-
5	4.627	-
5	4.756	-

4.3.3 Monomer adsolubilization and polymerization

The adsolubilization isotherm (Figure 4.4) indicates that there was effective adsolubilization of the styrene into the surfactant admicelle. Maximum adsolubilization was 18 $\mu\text{mol/g}$ and mole ratio of styrene monomer to TX-100 surfactant was about 50:1, this was confirmed from the material balance of the extracted polymer and adsolubilized styrene. This ratio is in sharp contrast to ratios obtained on other substrates by previous work, the highest being about 3:1.²⁹ This indicates that the ratio of adsolubilized monomer to adsorbed surfactant is higher on calcium carbonate (a relatively low surface area substrate) than on silica (e.g. Hi-Sil 233, which is around 100 times more porous and of relatively low solubility). It can also be due to the type of initiator if compared to emulsion polymerization situations where a study found that high monomer to polymer conversion was achieved under thermally pulsed conditions and an optimum hydrophobic initiator like AIBN.³¹ Furthermore, a previous work on admicellar polymerization of calcium carbonate (CC)²² showed sodium dodecyl sulfate (SDS) precipitated in the presence of calcium ions forming $\text{Ca}(\text{DS})_2$. The dissociated CC ions are not expected to interfere with our surfactant because it is nonionic. However, the salting out effect of these ions on our monomer solute was determined using the Setschenow *empirical* formula³⁴

$$\text{Log}\left(\frac{C_{iw}^{sat}}{C_{iw,salt}^{sat}}\right) = K_i^s [\text{salt}]_{tot} \quad \text{Eq. 2}$$

The *Setschenow or salting constant* (M^{-1}), K_i^s of ethylbenzene (having a similar molecular structure to styrene was used because the K_i^s of styrene was not available) and the total concentration of the CC, $[\text{salt}]_{tot}$, utilized in generating the adsolubilization isotherm were used.

$$\text{Log}\left(\frac{C_{iw}^{sat}}{C_{iw,salt}^{sat}}\right) = 0.29 \text{ L/mol} * 2.5 \text{ mol/L} = 0.725$$

$$\left(\frac{C_{iw}^{sat}}{C_{iw,salt}^{sat}}\right) = 5.3$$

This implies that the styrene monomer was 5.3 times less soluble in water. Thus, it is likely that more styrene monomers were driven to the admicelle due to the salting out effect of the dissociated CC ions (Ca^{2+}) and (CO_3^{2-}) on the styrene monomer.

Also, assuming a spherical particle, the size of the droplet that would give a monomer to surfactant mole ratio of 50 was determined by the relation below:

$$\frac{\frac{4}{3} * \pi * r^2 * \rho_{sty} * \frac{1}{MW_{sty}} * Avo}{\left(\frac{4 * \pi * r^2}{48 \text{ Angstrom}^2}\right)} = 50$$

ρ_{sty} = density of styrene, MW_{sty} = molecular mass of styrene, r = radius of the CC particle

Avo = Avogadro's number

The relation gave $r = 59.5 \text{ nm}$, a value that is within the micro emulsion range.

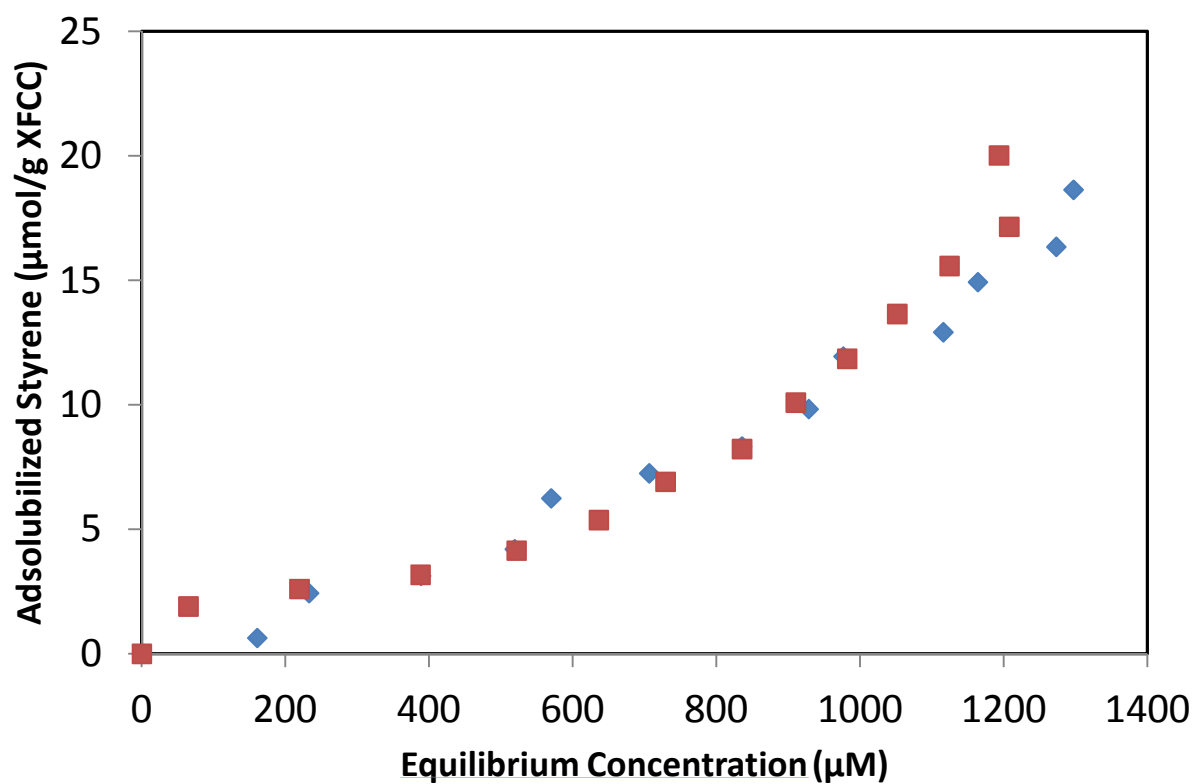


Figure 4.4: Adsolubilization isotherms of styrene in TX-100 admicelle on XFCC.

The partition coefficient K_{AS} as defined by Wu et al.³³ is an equilibrium constant, analogous to the partition coefficients used in solubilization studies:

$$K_{AS} = (\text{adsolubilized styrene molecule per adsorbed surfactant molecule}) / (\text{equilibrium concentration of styrene in the supernatant})$$

The approximate value of K_{AS} in this study at 25 °C was 20,830 M⁻¹, which is about 70 times the 300 M⁻¹ average of the SDS-styrene-alumina system³³ and around 50 times the 400 M⁻¹ value of the CTAB-styrene-silica system.¹

4.3.4 Characterization of the treated calcium carbonate

The FTIR-ATR spectra of the untreated CC and the treated CC were similar, there was no observed polystyrene peaks on the treated substrate, an indication that the polymer coating on the CC was below the detection limit of the IR instrument (see Figure 4.5 and Figure 4.6).

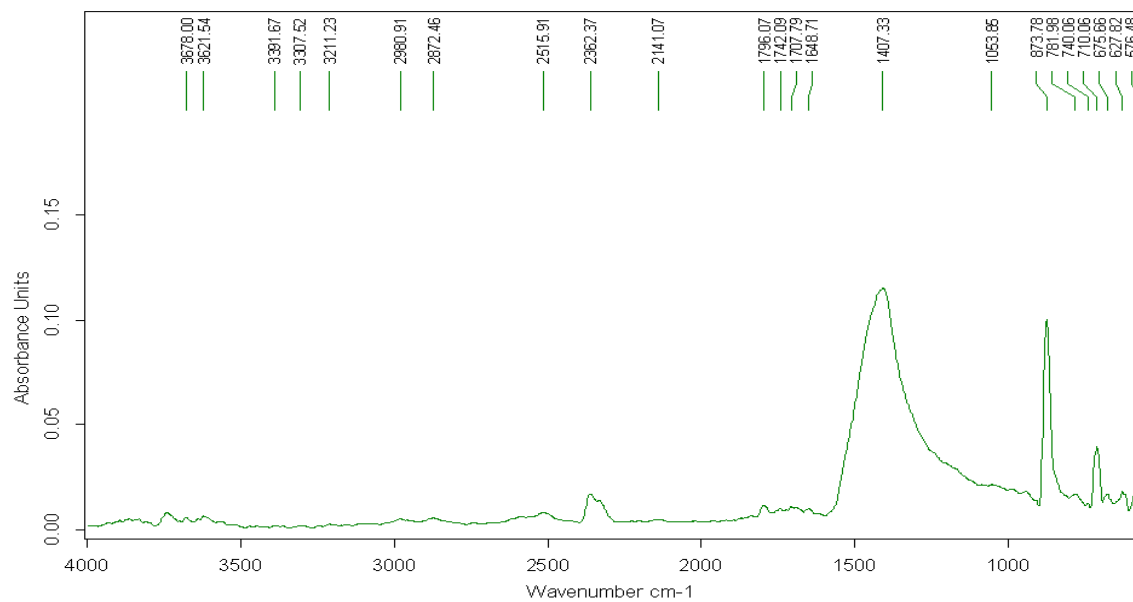


Figure 4.5: FTIR-ATR spectra of neat XFCC before treatment.

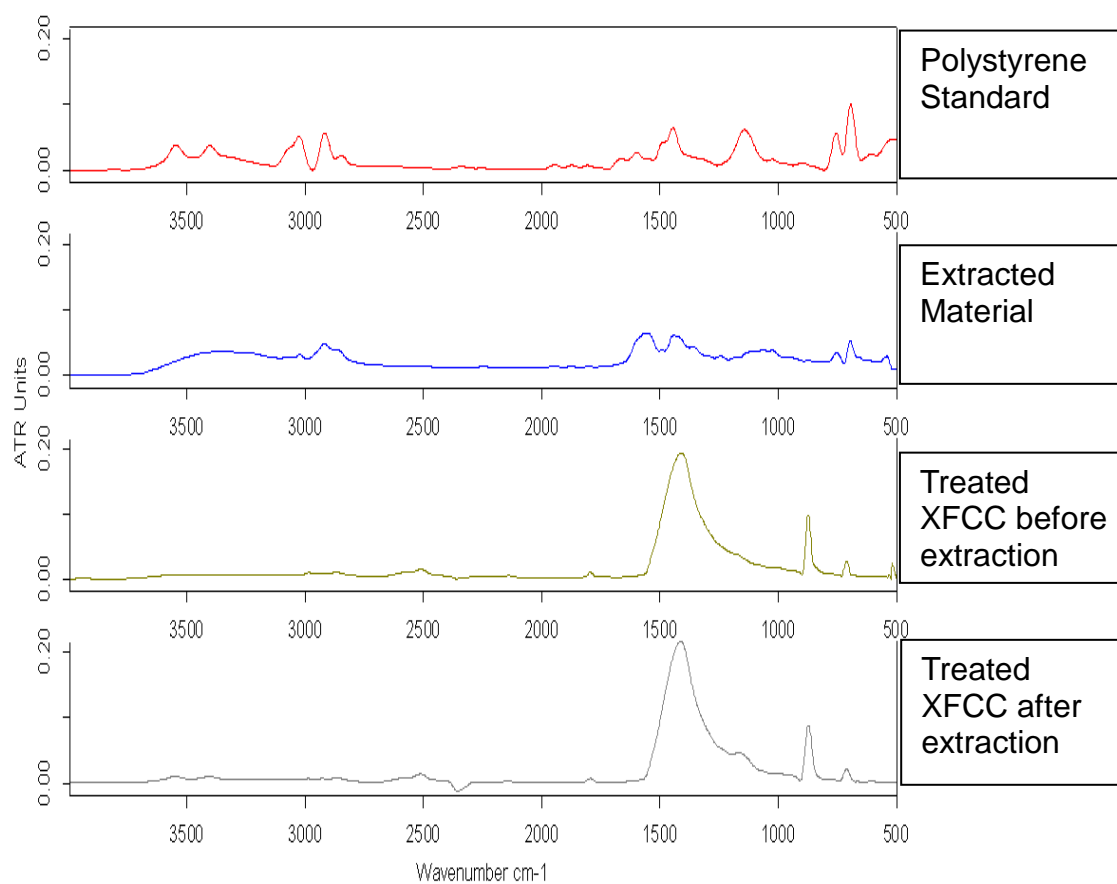


Figure 4.6: FTIR-ATR spectra of polystyrene standard, extracted polymer, treated XFCC before extraction, and treated XFCC after extraction.

Consequently, the experimental challenge to successfully detect the thin film coating *in situ* is quite significant. Physical observation of the dried treated CC substrates showed that the Coarse CC sample was more closely packed and had a rigid structure compared to the Fine and Extrafine CC. This is believed to be an indication of plasticization occurring as a result of the polymer (and the entrapped TX-100, which acts as a plasticizing agent) exceeding its glass transition temperature (T_g). Enhanced FTIR-ATR spectra (see Figure 4.7) were observed for treated CC when compared to the untreated CC, an indication of increased hydrophobicity.³⁰ However, the highest % decrease in specific surface area, up to 37 %, was from the XFCC. TGA results further reinforced the existence of a polymer thin film on the treated substrates. Thermal decomposition analysis of untreated Coarse, Fine and Extrafine CC samples respectively resulted in 1.3, 0.08 and 0.06 % weight loss. Whereas, the treated samples respectively had 3.2, 0.5 and 0.15 % weight loss, and a smoother and steeper weight loss region, indicating the simultaneous loss of the coated polymer with CO₂. See Table 4.5. Thermal decomposition graphs are given in Figures 4.8, 4.9 and 4.10. It is likely that a lower % weight loss difference indicates lower amount of coated material and invariably lower hydrophobicity. Therefore, the treated Coarse CC is more hydrophobic and expected to compatibilize with OBM better than the other CC size grades. Rungruang et al.⁷ obtained a % weight difference of about 0.2, which is comparable to that obtained for XFCC in this study.

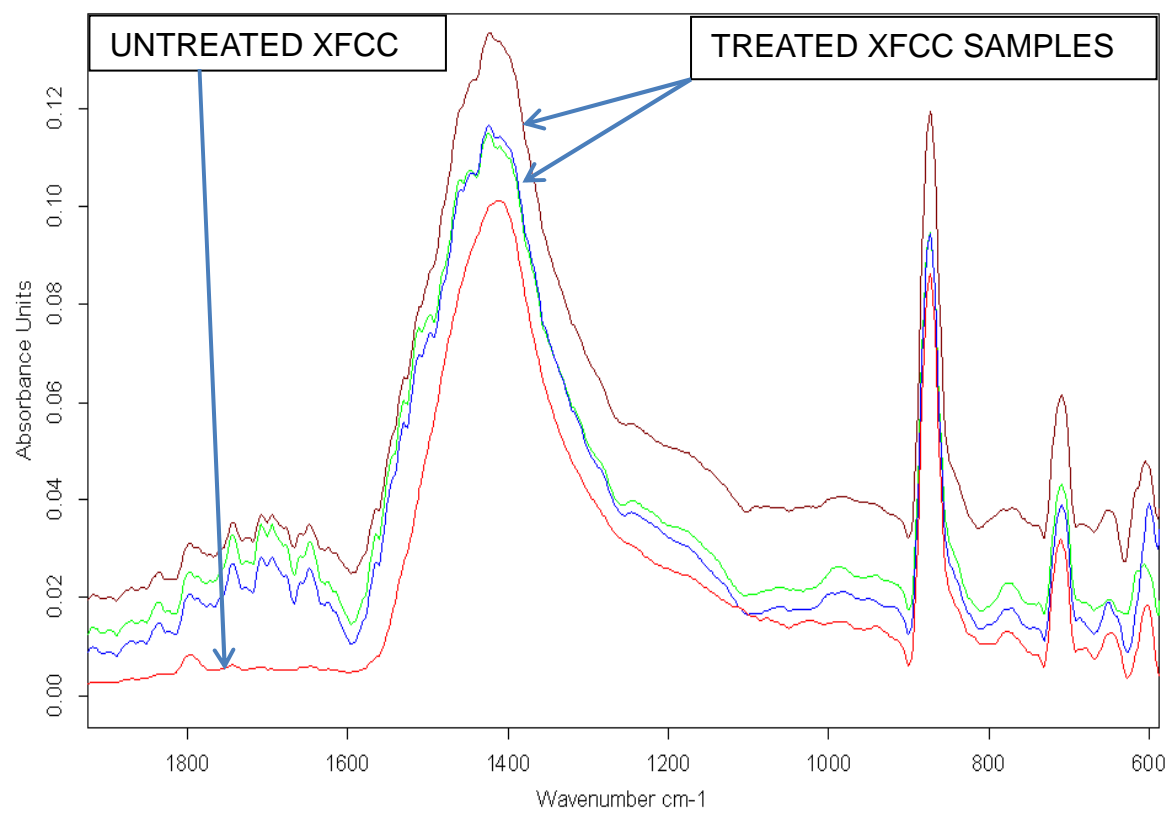


Figure 4.7: FTIR-ATR spectra of treated and untreated XFCC.

Table 4.4: Comparing BET N₂ specific surface areas of the untreated and treated industrial CC

Industrial CaCO₃	Specific surface area (m²/g) Multi-Point BET/Langmuir (UNTREATED)	Specific surface area (m²/g) Multi- Point BET/Langmuir (TREATED)	Approximate % Decrease in specific surface area
Coarse	0.297/0.498	0.207/0.367	30
Fine	0.608/0.987	0.434/0.755	29
Extrafine	1.091/1.776	0.686/1.178	37

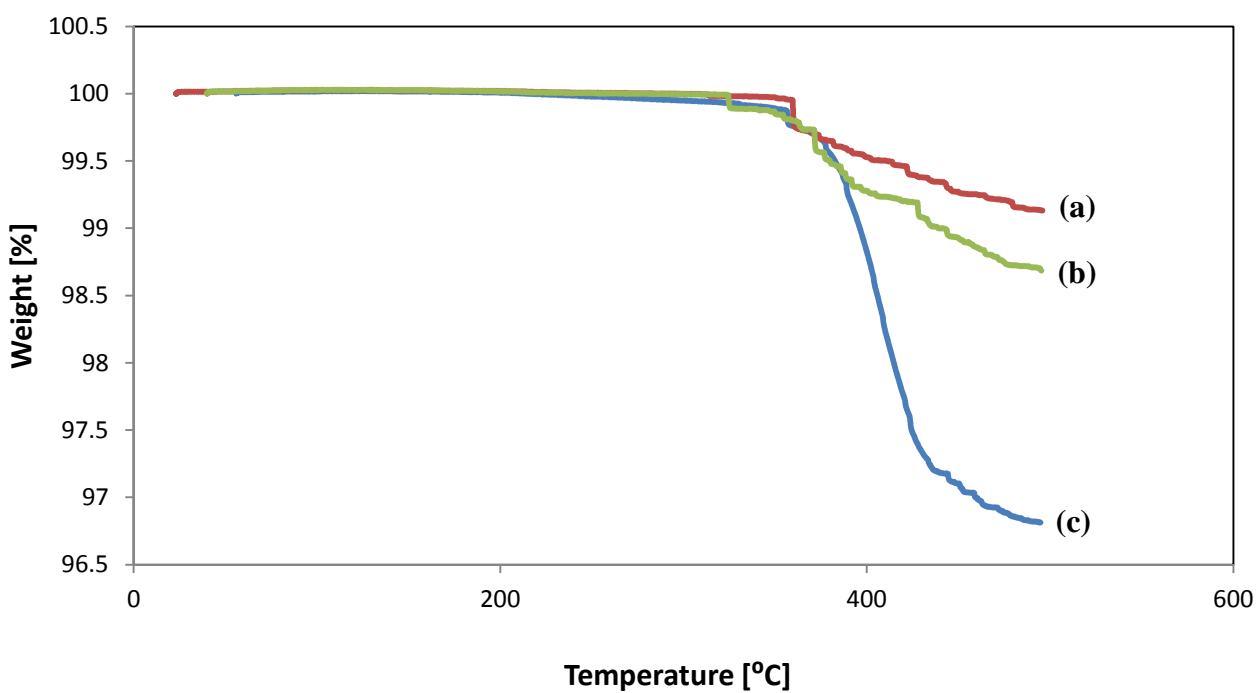


Figure 4.8: Thermal decomposition plots of untreated (b), treated (c), and after extraction treated (a) industrial Coarse CC.

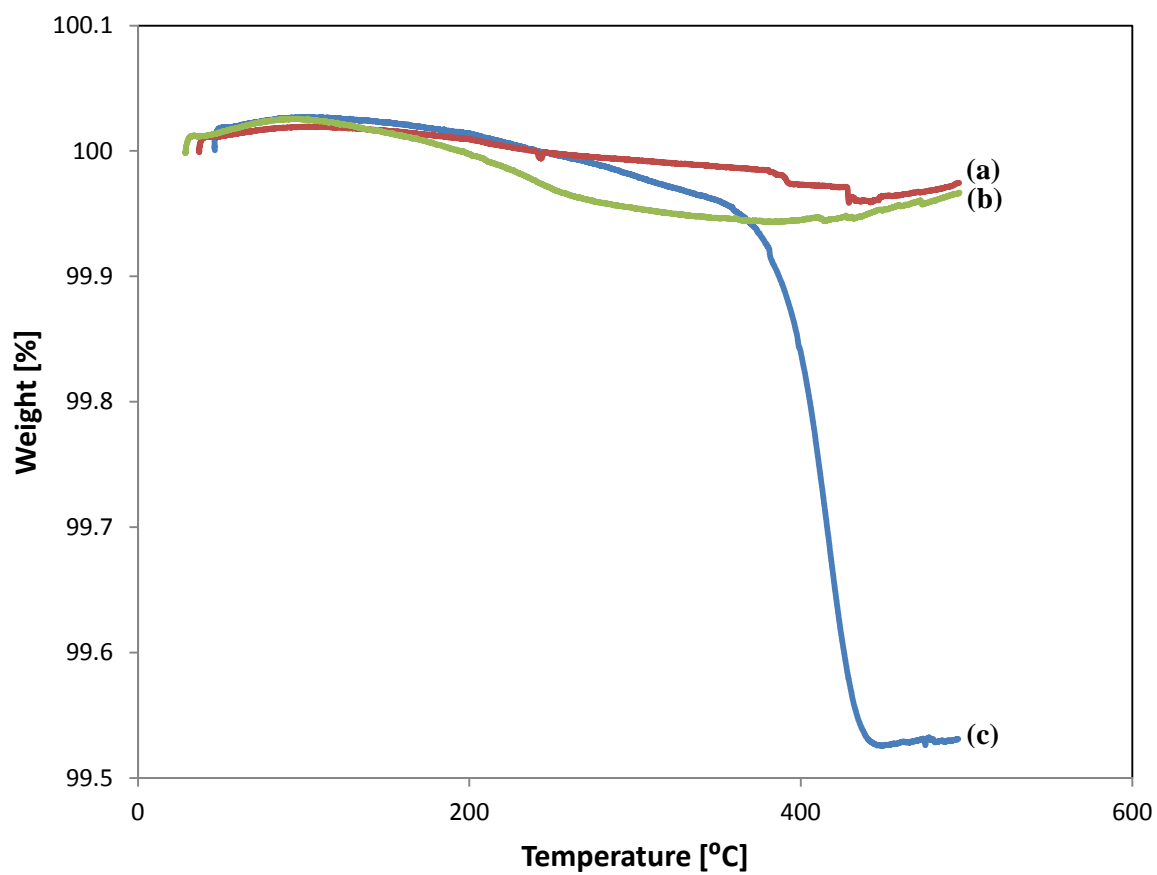


Figure 4.9: Thermal decomposition plots of untreated (b), treated (c), and after extraction treated (a) industrial Fine CC.

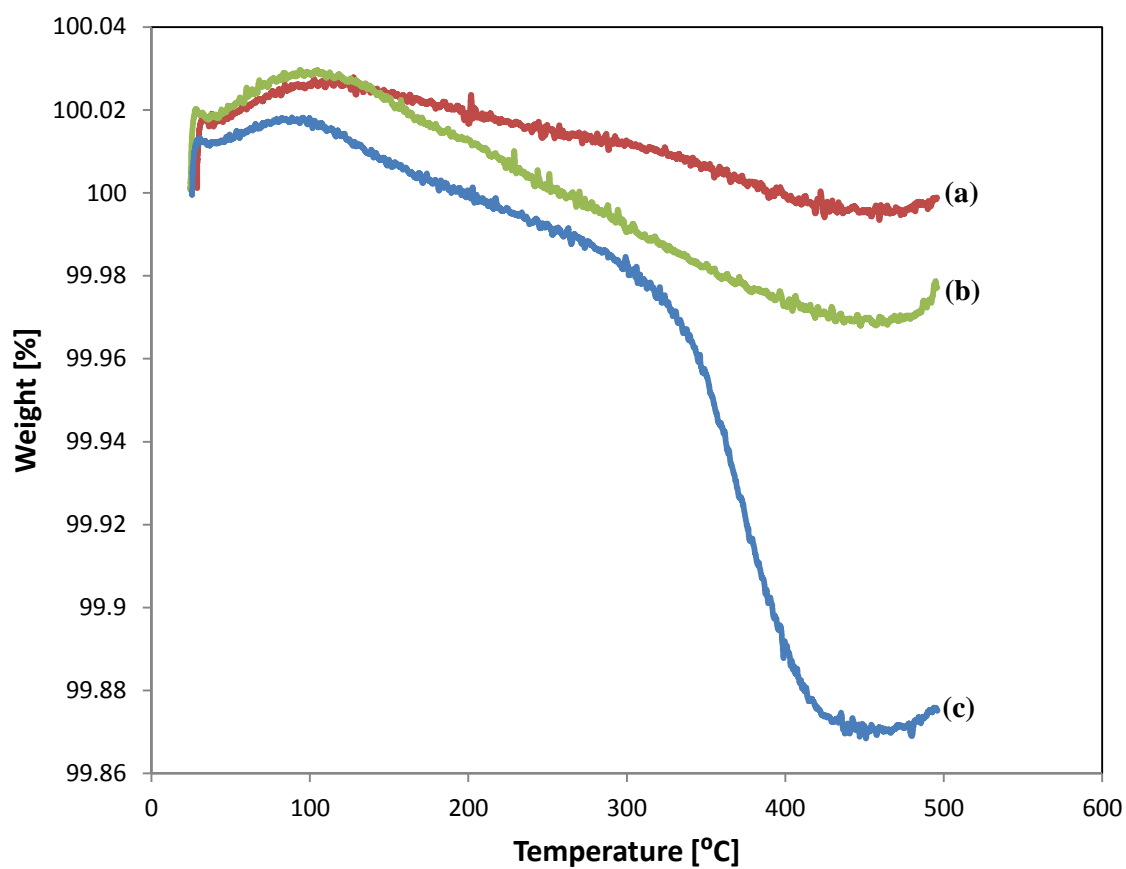


Figure 4.10: Thermal decomposition plots of untreated (b), treated (c), and after extraction treated (a) industrial XFCC.

4.3.5 Characterization of the extracted polymer

The polymerized material on Coarse, Fine and Extrafine CC was successfully extracted using a Soxhlet extractor. Soxhlet extraction attempts on the treated Medium CC were unsuccessful and resulted in no polymer upon precipitation in water.

Physical Appearance –The polymer extract from the Fine CC and XFCC are fibrous and loosely packed, they easily break up when touched. In contrast, the polymer extract from the Coarse CC was less fibrous, tightly packed, and had a more plastic behavior (see Figure 4.8). The reason for this difference is not yet understood, but effort is ongoing to characterize the extract with a gel permeation chromatography (GPC) system to determine if the molecular weights are different and if the amount of entrapped TX-100 varies.



Figure 4.11: Picture of dried polystyrene extract from treated Coarse CC.

Results in Table 4.4 shows that % extractions of coated material obtained from Soxhlet extraction were comparable to % weight loss of the various CC size grades. We expected the amount of recoverable polymer to be approximately equal to that of the added monomer and initiator. XFCC had a % extraction very similar to the expected results (based on the amount of adsolubilized monomer), Fine CC gave about 3 times the expected value and Coarse CC gave as high as 14 times of the expected extraction.

Table 4.5: Comparison of % extraction and % weight loss of treated CC samples

Industrial CaCO₃	Predicted % extraction based on added monomer and initiator	% Extraction (Soxhlet Extraction)	% Weight loss of treated sample - % Weight loss of treated sample after extraction (Thermo Gravimetric Analyzer, TGA)
Coarse	0.187	2.6	2.32
Fine	0.187	0.54	0.44
Extrafine	0.187	0.15	0.12

Infrared (IR) analysis – FTIR-ATR spectra of the extracts confirmed that the extracted polymer material was polystyrene, with an almost overlapping spectra band in some cases, see Figure 4.12.

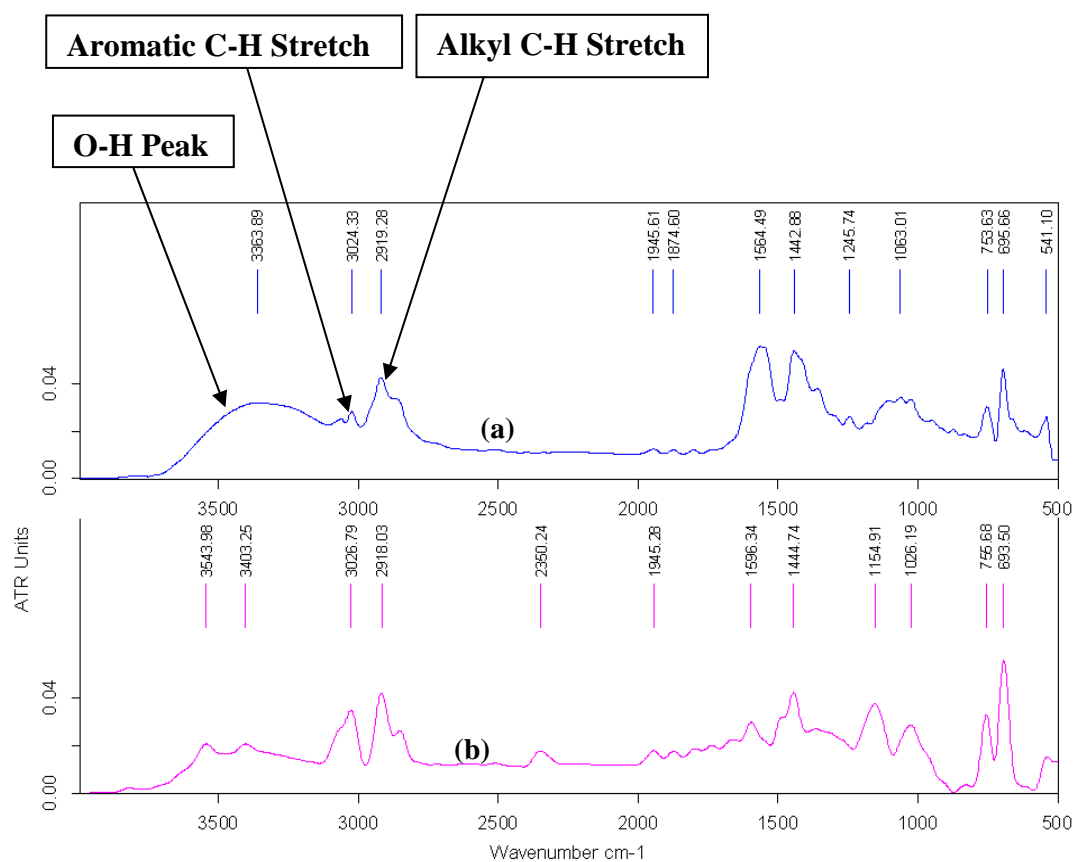


Figure 4.12: Comparison of the IR spectra of (a) extracted material and (b) polystyrene standard.

Thermal decomposition analysis – We expect the decomposition of half the TX-100, and all of the added monomer and initiator, but each sample left carbon black residue (see Figure 4.13). [Coarse CC (had the least residue): residue representing about 0.84 % of total burnt extract (99.16 % weight loss) (the PS standard had a 99.92 % weight loss)], [Fine CC: left residue of about 6.76 % of total burnt extract (93.24 % weight loss)], and [XFCC: left residue of about 17.24 % of total burnt extract (82.76 % weight loss)]. Thus, percent residue increased with decreasing particle size and increasing specific surface area of substrate. Thus, there are probably small amounts of CaCO_3 particulates in the samples. The very small residue and high % weight loss obtained from Coarse CC indicates that the polymer thin film on this substrate is almost pure polystyrene, unlike the ones coated on the Fine and XFCC. Figure 4.14 and Table 4.6 summarizes the % weight loss of the extracts. Three decomposition regions were observed (see Figure 4.13), confirming the presence of water and surfactant (TX-100 EO group (the TX-100 is believed to be present in the extract as part of the surfactant-polymer matrix, despite rinsing of the THF extract with water)), although, both are present in very small quantity. Phase 1 is water vaporization phase, 100 °C to about 240 °C (temperature at which TX-100 starts to decompose), Phase 2 is the TX-100 decomposition phase, 240 °C to about 350 °C (temperature at which PS starts to decompose), and Phase 3 is the PS decomposition phase starting at about 350 °C. One major concern of the applicability or viability of the treated CC is the high temperature and pressure usually encountered downhole while drilling, that the synthesized polymer could easily break off from the CC substrate. However, most downhole temperature sensing devices operate below 300 °C, an indication that downhole temperature is usually less than 300 °C. Thus, the problem of polymer decomposition will not occur since the polymer did not decompose until over 350 °C. Additionally, the coated polymer was difficult to extract, only 0.001 % extraction

by mass of substrate was achieved when hot THF was used, but when a boiling THF was refluxed, we had 0.15 to 2.6 % extraction.

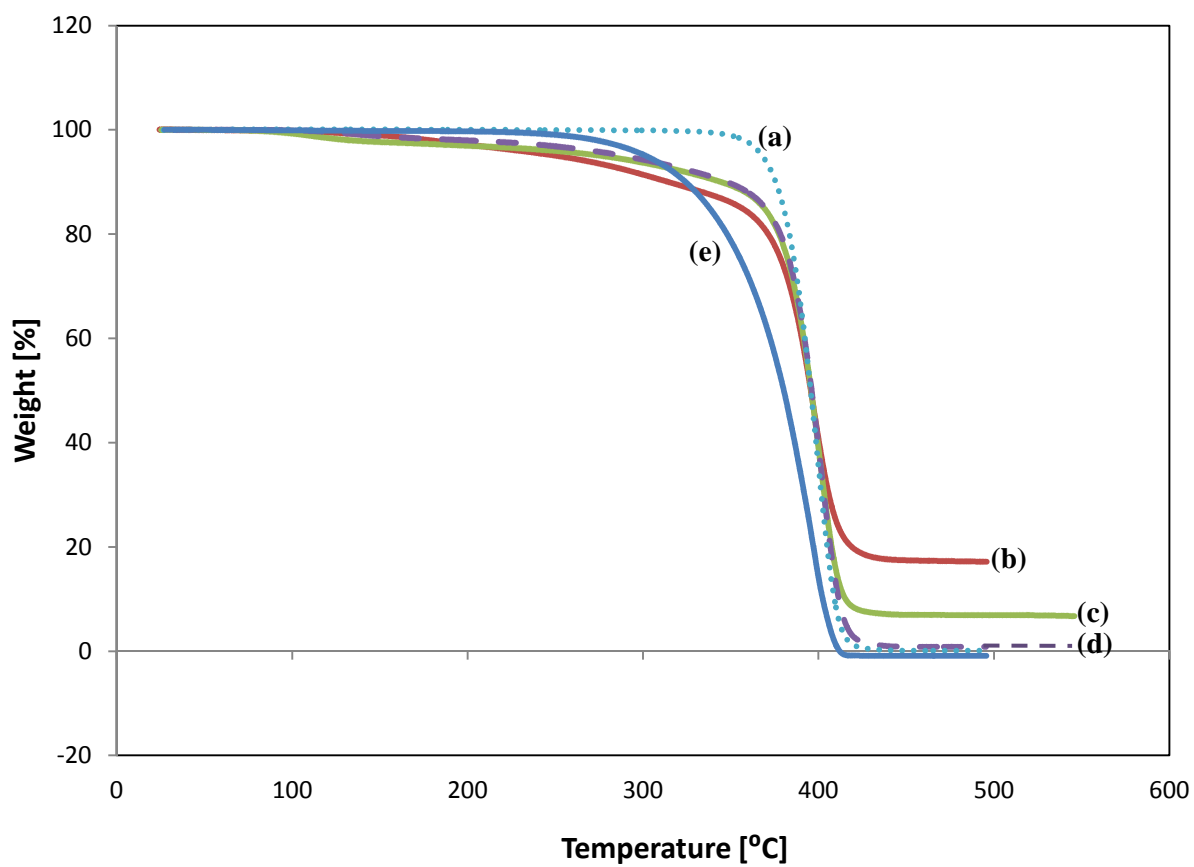


Figure 4.13: Thermal decomposition plots of polystyrene standard (a), XFCC extract (b), Fine CC extract (c), Coarse CC extract (d), and TX-100 (e).

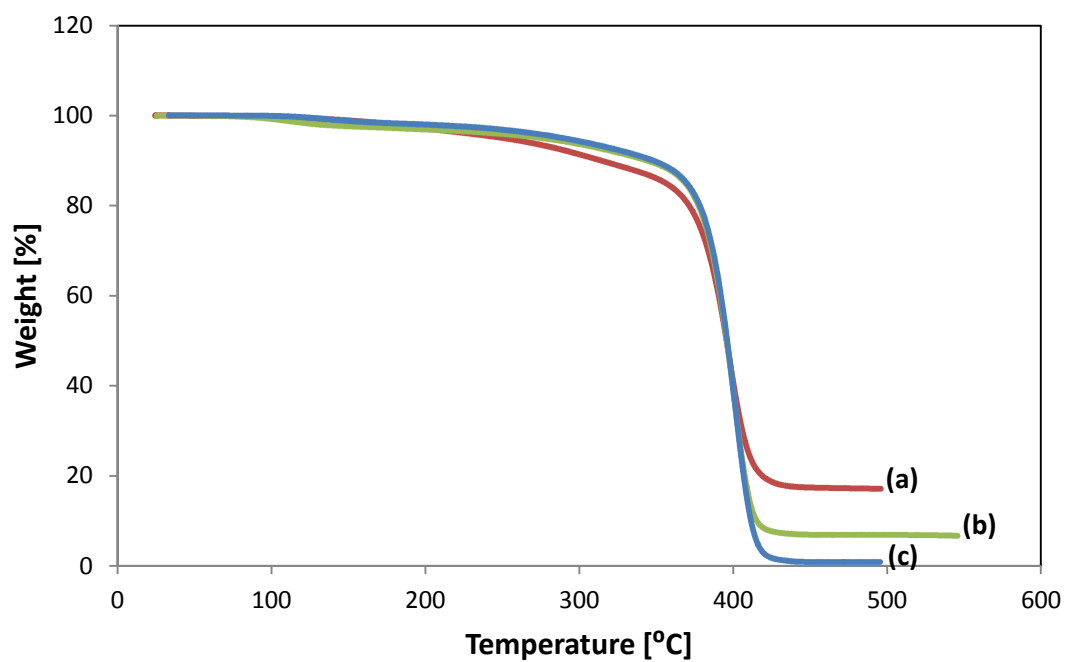


Figure 4.14: % Weight loss of extracted material: Extract from XFCC (a), Fine CC (b), and Coarse CC (c).

Table 4.6: Mass balance of the polymer extract

Industrial CaCO₃	Total % weight loss (T)	% Weight loss due to water (A)	% Weight loss due to TX-100 (B)	% Weight loss due to polystyrene (T-A-B)	Mass ratio of polymer to surfactant
Coarse	99.16	5	10	84.16	8.4:1
Fine	92.53	5	10	77.53	7.8:1
Extrafine	82.44	5	10	67.44	6.7:1

4.4 CONCLUSIONS

Calcium carbonate that is possibly more compatible with oil-based drilling mud (OBM) can be produced via admicellar polymerization using styrene monomers. At suitable time durations, near CMC surfactant concentration and styrene concentrations greater than 2.4 mM, Coarse , Fine, and Extrafine size grades of industrial calcium carbonate, with respective % weight loss of 1.3, 0.08, and 0.06 before treatment and respective % weight loss of 3.2, 0.5, and 0.15 after treatment, and respective average surface area % decrease of about 30, 29, and 37 after treatment, have been produced by admicellar polymerization process and are stable even under high temperature of up to 350 °C.

LIST OF REFERENCES

4.5 REFERENCES

1. O'Haver, J.H.; Harwell, J.H.; O'Rear, E.A.; Snodgrass, L. J.; Waddell, W. H. In situ Formation of Polystyrene in Adsorbed Surfactant Bilayers on Precipitated Silica. *Langmuir*. **1994**, 10(8), 2588-93.
2. Sakhalkar, S.S.; Hirt, D.E. Admicellar Polymerization of Polystyrene on Glass Fibers. *Langmuir*. **1995**, 3369-73.
3. Lai, C.L.; Harwell, J.H.; O'Rear, E.A.; Komatsuzaki, S; Arai, J.; Nakakawaji, T.; Ito, Y. Formation of Poly(tetrafluoroethylene) Thin Films on Alumina by Admicellar Polymerization. *Langmuir*. **1995**, 11(3), 905-11.
4. Wu, J.; Harwell, J.H.; O'Rear, E.A.; Christian, S.D. Application of Thin Films to Porous Mineral Oxides using Two-Dimensional Solvents. *AIChE Journal*. **1988**, 34(9), 1511-18.
5. Waddell, W.H.; O'Haver, J.H.; Evans, L.R.; Harwell, J.H. Organic Polymer-Surface Modified Precipitated Silica. *Journal of Applied Polymer Science*. **1995**, 55, 1627-1641.
6. O'Haver, J.H.; Harwell, J.H.; Evans, L.R.; Waddell, W.H. Polar Copolymer-Surface-Modified Precipitated Silica. *Journal of Applied Polymer Science*. **1996**, 59, 1427-1435.
7. Rungruang, P.; Grady, B.P.; Supaphol, P. Surface-Modified Calcium Carbonate Particles by Admicellar Polymerization to be used as Filler for Isotactic Polypropylene. *Colloids and Surfaces A: Physicochem. Eng. Aspects*. **2006**, 275, 114-125.
8. Pongprayoon, T.; Yanumet, N.; O'Rear, E.A. Admicellar polymerization of styrene on cotton. *J. Colloid Interface Sci*. **2002**, 249, 227-34.
9. Pongprayoon, T.; O'Rear, E.A.; Yanumet, N.; Yuan, W.L. Wettability of cotton modified by admicellar polymerization. *Langmuir*. **2003**, 19, 3770-8.

10. Tragoonwichian, S.; O'Rear, E.A.; Yanumet, N. Admicellar polymerization of 2-hydroxy-4-acryloyloxybenzophenone: The production of UV-protective cotton. *Colloids and Surfaces A: Physicochem. Eng. Aspects*. **2008**, 329, 87-94.
11. Wang, S.; Russo, T.; Qiao, G.G.; Solomon, D.H.; Shanks, R.A. Admicellar polymerization of styrene with Divinyl benzene on alumina particles: the synthesis of white reinforcing fillers. *J. Mater. Sci.* **2006**, 41, 7474-82.
12. Barraza, H.J.; Hwa, M.J.; Blakley, K.; O'Rear, E.A.; Grady, B.P. Wetting behavior of elastomer-modified modified glass fibers. *Langmuir*. **2001**, 17, 5288-96.
13. Yuan, W.L.; O'Rear, E.A.; Grady, B.P.; Glatzhofer, D.T. Nanometer-thick poly(pyrrole) films formed by admicellar polymerization under conditions of depleting adsolubilization. *Langmuir*. **2002**, 18, 3343-51.
14. Chibowski, S. Investigations of Interactions of Sodium Dodecyl Sulfate and Polyacrylamide Molecules on Calcium Carbonate Surface using Radiotracer Technique. *J. Colloid and Interface Science*. **1980**, 76, 2, p371-74.
15. Hu, Z.; Deng, Y. Superhydrophobic Surface Fabricated from Fatty Acid-Modified Precipitated Calcium Carbonate. *Ind. Eng. Chem. Res.* **2010**, 49, p5425-30.
16. Zhang, J.; Guo, J.; Li, T. Chemical Surface Modification of Calcium Carbonate Particles by Maleic Anhydride Grafting Polyethylene Wax. *International Journal Green Nanotechnology: Physics and Chemistry 1*. **2010**, p65-71.
17. Kurkarni, R.D.; Leung, P.S.; Goddard, E.D. Oil Dispersion Properties of Silanated Calcium Carbonate: A Rheological Study. *Colloid and Surfaces*. **1982**, 5, p321-32.

18. Razaei Gomari, K.A.; Hamouda, A.A. Effect of fatty acids, water composition and pH on the wettability alteration of calcite surface. *J. Petroleum Science and Engineering*. **2006**, 50, p140-50.
19. Ding, H.; Lu, S.; Deng, Y.; Du, G. Mehano-activated surface modification of calcium carbonate in wet stirred mill and its properties. *Trans. Nonferrous Met. Soc. China* 7. **2007**, p1100-04.
20. Wang, G.G.; Zhu, L.Q.; Liu, H.C.; Li, W.P. *Langmuir* dx.doi.org/10.1021/la202613r. **2011**.
21. Rungruang, P.; Grady, B.P.; Supaphol, P. Surface-Modified Calcium Carbonate Particles by Admicellar Polymerization to be used as Filler for Isotactic Polypropylene. *Colloids and Surfaces A: Physicochem. Eng. Aspects*. **2006**, 275, 114-125.
22. Cheah, P.L. Admicellar Polymerization of Calcium Carbonate and its Performance in Drilling Fluids. Masters Thesis, The University of Mississippi, 2012.
23. Schramm, L.L.; Marangoni, D.G. *Surfactants and Their Solutions: Basic Principles. Surfactants: Fundamental and Applications in the Petroleum Industry*. Schramm, L.L. Cambridge University Press, 2000.
24. Ash, M.; Ash, I. *Handbook of Industrial Surfactants*. Gower, UK. **1993**.
25. Tummino, P.J.; Gafni, A. Determination of the Aggregation Number of Detergent Micelles using Steady-State Fluorescence Quenching. *Biophys. J.* **1993**, 64, 1580.
26. Biaselle, C.J.; Millar, D.B. Studies on Triton™ X-100 Detergent Micelles. *Biophys. Chem.* **1975**, 3, 355.
27. Robson, R.J.; Dennis, E.A. The Size, Shape, and Hydration of Nonionic Surfactant Micelles. Triton™ X-100. *The Journal of Physical Chemistry*. **1977**, 81, 11.

28. Paradies, H.H. Shape and Size of a Nonionic Surfactant Micelle. Triton™ X-100 in Aqueous Solution. **1980**, 84, 6, 599-607.
29. Tan, Y.; O'Haver, J.H. Lipophilic linker impact on adsorption of and styrene adsolubilization in polyethoxylated octylphenols. Colloids and Surfaces A: Physicochem. Eng. Aspects. **2004**, 232, 101-11.
30. Lucas, P.; Solis, M.A.; Le Coq, D.; Juncker, C.; Riley, M.R.; Collier, J.; Boesewetter, D.E.; Boussard-Pledel, C.; Bureau, B. Infrared biosensors using hydrophobic chalcogenide fibers sensitized with live cells. Sensors and Actuators B Chemical. **2006**, 119, 355-62.
31. Tauer, K.; Hernandez, H.; Kozempel, S.; Lazareva, O.; Nazaran, P. Towards a consistent mechanism of emulsion polymerization—new experimental details. Colloid Polym Sci. **2008**, 286(5), p499-515.
32. Smith, W.V. and Ewart, R.H. (1948) J. Chem. Phys. 16:592.
33. Wu, J.; Harwell, J.H.; O'Rear, E.A. Two-dimensional reaction solvents: Surfactant bilayers in the formation of ultrathin films. Langmuir. **1987**, 3, 531-537.
34. Schwarzenbach, R.P.; Gschwend, P.H.; Imboden, D.M. Environmental Organic Chemistry. 2nd Edition. John Wiley & Sons, Inc. 2003.

CHAPTER FIVE

CONCLUSIONS AND RECOMMENDATIONS

5.1 CONCLUSIONS

This study has successfully shown that admicellar polymerization can be used to produce surface-modified industrial calcium carbonate (CC), a relatively soluble and low porous mineral substrate. Polystyrene has been coated on various size grades of industrial CC, with the Coarse CC size grade (AdiTM CARB 150 (C)) showing a greater promise for improved performance with the oil-based drilling mud (OBM). The highest polymer extraction was obtained from the Coarse CC, approximately 2.6 weight %, indicating a very high monomer to polymer conversion showing that Coarse CC was the most hydrophobic. The % extractions of all 3 size grades were comparable to the % weight loss when thermally decomposed after treatment. Extraction of the coated polymer was only possible when boiling THF was refluxed onto the treated substrate and not when treated substrate was dissolved in hot THF. This indicates that the organic polymer treatment is firmly attached even though it was not chemically bonded. It is very likely that the ability of the coated polymer to withstand high temperatures up to 350 °C (from the TGA analysis of the treated substrates) would offer a wider range of use for the modified substrate at moderate temperature and high temperature situations while maintaining its enhanced properties. Overall, the admicellar-treated industrial CC should be more compatible with the OBM, consequently increasing; parts per hundred mud of weighting agent, wellbore pressure, thin film low-permeability filter cake strength, overall homogeneity, cuttings removal, reuse, and overall

mud quality and performance. A pilot test of the performance of OBM formulated with admicellar-treated CC is under way at BCI Chemical, Malaysia.

5.2 RECOMMENDATIONS AND FUTURE WORK

It is recommended that nonionic surfactant be used for future work on admicellar polymerization of industrial calcium carbonate in order to avoid precipitation, like those recently reported by Poh Lee Cheah.¹ The high conversion of monomer to polymer obtained in this work is believed to be due to the high preferential partitioning of styrene monomers (due to salting out effect of Ca^{2+} and CO_3^{2-} (from dissociation of CC in solution) on the styrene solute) into the TX-100 admicellar core and subsequent swelling. See Figure 5.1. A further work to examine the ionization effect of salts on monomer adsolubilization and to fully explain the high conversion can be explored.

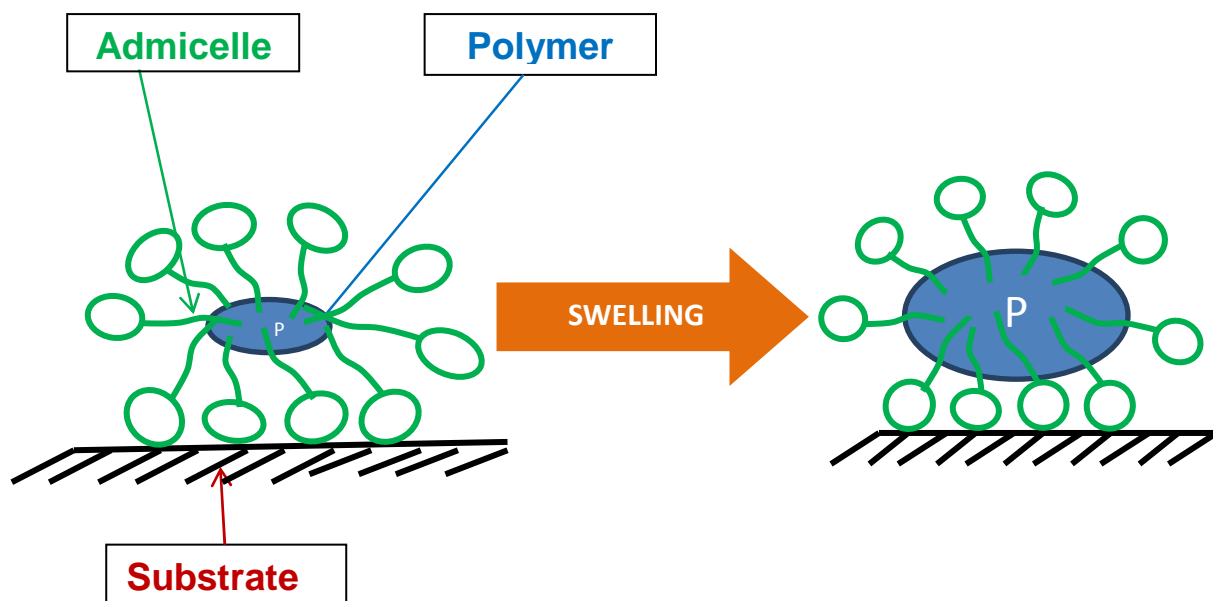


Figure 5.1: Suggested explanation for the high polymer conversion.

Admicellar polymerization of co-polymers and other monomers can be explored and compared with the present work to see which one gives better compatibility with OBM. A double coating via repeat admicellar polymerization like the one done by Tragoonwichian² on cotton can be explored to see if it results in increased hydrophobicity or film durability. Lastly, the possible use of treated calcium carbonate shows a great promise for other applications, especially with materials where it is used as fillers. Only a single work, admicellar-treated CC for use as filler in isotactic polypropylene,³ is been published in this regard, hence, there are a lot of application areas that can be explored in this regard. Calcium carbonate is widely used as an extender in paints, particularly in matte emulsion paints where typically 30 % by weight of the paint is chalk or marble, a hydrophobic chalk can help prevent chalking. As a popular filler in plastics, around 15 to 20 % loading of chalk is used in unplasticized polyvinyl chloride (uPVC) drain pipe, 5 to 15 % of stearate coated chalk or marble in uPVC window profile, PVC cables can use CC at loadings of up to 70 phr (parts per hundred resin) to improve mechanical properties (tensile strength and elongation) and electrical properties (volume resistivity), it is very likely that this loadings can be increased using admicellar-treated CC.

LIST OF REFERENCES

5.3 REFERENCES

1. Poh Lee Cheah. Masters Thesis, The University of Mississippi, 2012.
2. S. Tragoonwichian et al. Colloids and Surfaces A: Physicochem. Eng. Aspects 349 (2009) 170-175.
3. P. Rungruang et al. Colloids and Surfaces A: Physicochem. Eng. Aspects 275 (2006) 114-125.

LIST OF APPENDICES

APPENDIX A

A.1 Inductively coupled plasma mass spectrometry (ICP-MS) Analysis

This analysis was to detect the presence of other metallic elements in the industrial grade CaCO_3 samples supplied by BCI Chemical Corporation, to see if the amount of these elements is significant enough to affect our results. But, it was found that these elements were present in trace amount and thus will not affect our results. The analysis was done in one of the instrumentation laboratories in the Chemistry Department of The University of Mississippi.

Table A.1: ICP-MS analysis of coarse, medium, and fine CaCO₃ samples

Conc Unit(ppb)	Blank	CaCO ₃ 25(F)		CaCO ₃ 50 (coarse)		CaCO ₃ 50(m)	
Isotope	Measured conc	Measured conc	Conc in sample	Measured conc	Conc in sample	Measured conc	Conc in sample
Ba137(LR)	-0.003	-0.317	-0.141	-0.345	-0.172	-0.355	-0.157
Ag107(LR)	0.093	-0.110	-0.049	-0.112	-0.056	-0.114	-0.050
Sr88(LR)	0.052	20.487	9.130	8.286	4.135	15.294	6.767
Cs133(LR)	-0.024	-0.018	-0.008	-0.023	-0.011	-0.024	-0.011
Mg24(MR)	0.311	251.086	111.892	398.965	199.084	325.350	143.960
Ca44(MR)	17.110	28266.839	12596.631	19515.764	9738.405	27565.028	12196.915
V51(MR)	0.020	-0.021	-0.009	-0.004	-0.002	-0.020	-0.009
Cr52(MR)	0.029	0.023	0.010	0.032	0.016	0.023	0.010
Mn55(MR)	0.075	4.529	2.018	2.343	1.169	3.571	1.580
Co59(MR)	0.061	0.052	0.023	0.051	0.025	0.052	0.023
Ni60(MR)	0.029	-0.075	-0.033	-0.073	-0.036	-0.073	-0.032
Cu63(MR)	15.391	0.158	0.070	-0.008	-0.004	0.003	0.001
Zn66(MR)	7.444	0.120	0.053	0.000	0.000	-0.013	-0.006
Al27(MR)	0.414	0.988	0.440	1.761	0.879	-0.486	-0.215
Cu65(MR)	15.304	0.175	0.078	0.018	0.009	0.025	0.011
Na23(MR)	-0.406	-1.463	-0.652	-1.279	-0.638	-1.332	-0.589
Fe56(HR)	0.702	8.542	3.807	9.719	4.850	9.240	4.088
K39(HR)	60.737	59.306	26.429	60.768	30.323	62.629	27.712

A.2 Surface Area/Particle Size Analysis from BCI Chemical Corporation

The result they got is comparable to what I got from the BET analysis (Langmuir report summary), whose reported values are bit higher than the Multi-Point BET report.



BCI CHEMICAL CORPORATION SDN. BHD. (Co. No 441454-X)

No.27, Jalan P/21, Selaman Industrial Park, Sec 10, 43650 Bandar Baru Bangi, Selangor Darul Ehsan
Tel : 603-8922 1822 Fax : 603-8922 3088
Email : sales@bcichemical.com.my

Result: Sieve ASTM E11:61 Report

Sample Name:
AdiCARB 150 (C)
C124 (HKK) - 230310 [SAM]

SOP Name:

Measured:
Saturday, April 03, 2010 11:14:15 AM

Measured by:
Administrator

Analysed:
Saturday, April 03, 2010 11:14:16 AM

Sample bulk lot ref:

Result Source:
Averaged

Particle Name:
CaCO₃ (calcite)
Particle RI:
1.572
Dispersant Name:
Water

Accessory Name:
Hydro 2000MU (A)
Absorption:
0.1
Dispersant RI:
1.330

Analysis model:
General purpose
Size range:
0.020 to 2000.000 μ m
Weighted Residual:
1.870 %

Sensitivity:
Normal
Obscuration:
15.29 %
Result Emulation:
Off

Concentration:
0.0661 %Vol

Span :
2.460
Surface Weighted Mean D[3,2]:
27.680 μ m

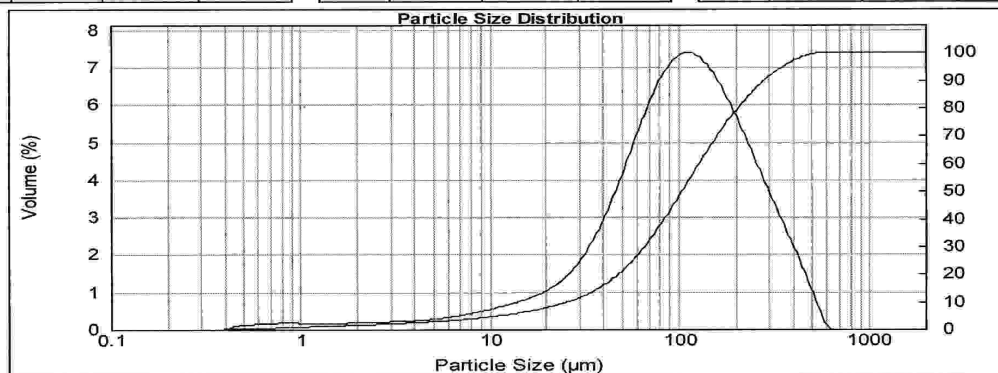
Uniformity:
0.743
Vol. Weighted Mean D[4,3]:
133.726 μ m

Result units:
Volume
Density:
1.000 g/cm³

Specific Surface Area:
0.218 m²/g

d(0.1): 26.279 μ m d(0.5): 105.002 μ m d(0.9): 284.635 μ m

Mesh No	Aperture μ m	Volume In %	Vol Below %	Mesh No	Aperture μ m	Volume In %	Vol Below %	Mesh No	Aperture μ m	Volume In %	Vol Below %
10	2000	0.00	100.00	35	500	1.62	99.32	120	125	7.95	58.40
12	1700	0.00	100.00	40	425	2.82	97.70	140	106	7.75	50.46
14	1400	0.00	100.00	45	355	3.58	94.89	170	90	8.04	42.70
16	1180	0.00	100.00	50	300	4.93	91.31	200	75	6.74	34.66
18	1000	0.00	100.00	60	250	6.24	86.38	230	63	5.56	27.92
20	850	0.00	100.00	70	212	6.24	80.97	270	53	4.21	22.35
25	710	0.00	100.00	80	180	7.83	74.74	325	45	3.37	18.14
30	600	0.00	100.00	100	150	8.51	66.91	400	38		14.77
35	500	0.68	99.32	120	125		58.40				



Operator notes: Add 5 drops of 15% Sodium Hexametaphosphate solution.



BCI CHEMICAL CORPORATION SDN. BHD.(Co. No 441454-X)
No.27, Jalan P/21, Selaman Industrial Park, Sec 10, 43650 Bandar Baru Bangi, Selangor Darul Ehsan
Tel : 603-8922 1822 Fax : 603-8922 3088
Email : sales@bcichemical.com.my

Result: Sieve ASTM E11:61 Report

Sample Name:
AdiCARB 50 (M)
C103 (OM) - 230310 [SAM]

SOP Name:

Measured by:
Administrator

Result Source:
Averaged

Measured:
Saturday, April 03, 2010 10:40:08 AM

Analysed:
Saturday, April 03, 2010 10:40:09 AM

Sample bulk lot ref:

Particle Name:
CaCO₃ (calcite)

Particle RI:
1.572

Dispersant Name:
Water

Accessory Name:
Hydro 2000MU (A)

Absorption:
0.1

Dispersant RI:
1.330

Analysis model:
General purpose

Size range:
0.020 to 2000.000 um

Weighted Residual:
2.941 %

Sensitivity:
Normal

Obscuration:
17.12 %

Result Emulation:
Off

Concentration:
0.0342 %Vol

Span :
3.173

Uniformity:
0.965

Result units:
Volume

Specific Surface Area:
0.483 m²/g

Surface Weighted Mean D[3,2]:
12.413 um

Vol. Weighted Mean D[4,3]:
125.759 um

Density:
1.000 g/cm³

d(0.1): 6.968 um

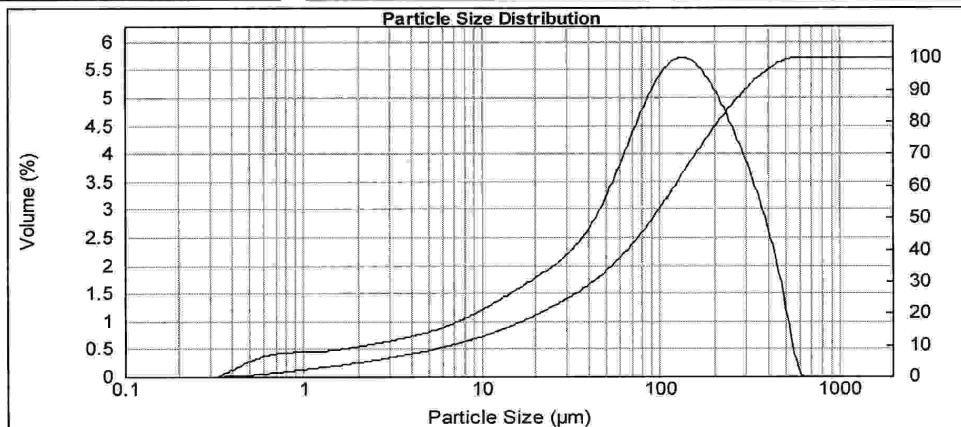
d(0.5): 92.578 um

d(0.9): 300.725 um

Mesh No	Aperture µm	Volume In %	Vol Below %
10	2000	0.00	100.00
12	1700	0.00	100.00
14	1400	0.00	100.00
16	1180	0.00	100.00
18	1000	0.00	100.00
20	850	0.00	100.00
25	710	0.00	100.00
30	600	0.00	100.00
35	500	0.76	99.24

Mesh No	Aperture µm	Volume In %	Vol Below %
35	500	2.02	99.24
40	425	3.34	97.22
45	355	3.94	93.88
50	300	5.02	89.94
60	250	5.14	84.91
70	212	5.68	79.77
80	180	6.61	74.19
100	150	6.79	67.58
120	125		60.79

Mesh No	Aperture µm	Volume In %	Vol Below %
120	125	6.05	60.79
140	106	5.70	54.74
170	90	5.78	49.05
200	75	4.84	43.27
230	63	4.12	38.43
270	53	3.35	34.31
325	45	3.00	30.96
400	38		27.96



Operator notes: Add 5 drops of 15% Sodium Hexametaphosphate solution.

**BCI CHEMICAL CORPORATION SDN. BHD.(Co. No 441454-X)**

No.27, Jalan P/21, Selaman Industrial Park, Sec 10, 43650 Bandar Baru Bangi, Selangor Darul Ehsan
Tel : 603-8922 1822 Fax : 603-8922 3088
Email : sales@bcichemical.com.my

Result: Sieve ASTM E11:61 Report

Sample Name:
AdiCARB 25 (F)
C133 (KPM) - 230310 [SAM]

SOP Name:

Measured:
Saturday, April 03, 2010 10:28:48 AM

Measured by:
Administrator

Analysed:
Saturday, April 03, 2010 10:28:49 AM

Sample bulk lot ref:

Result Source:
Averaged

Particle Name:
CaCO₃ (calcite)
Particle RI:
1.572
Dispersant Name:
Water

Accessory Name:
Hydro 2000MU (A)
Absorption:
0.1
Dispersant RI:
1.330

Analysis model:
General purpose
Size range:
0.020 to 2000.000 μ m
Weighted Residual:
1.988 %

Sensitivity:
Normal
Obscuration:
17.30 %
Result Emulation:
Off

Concentration:
0.0168 %Vol

Span :
2.442

Uniformity:
0.761

Result units:
Volume

Specific Surface Area:
0.997 m²/g

Surface Weighted Mean D[3,2]:
6.019 μ m

Vol. Weighted Mean D[4,3]:
30.592 μ m

Density:
1.000 g/cm³

d(0.1): 2.305 μ m

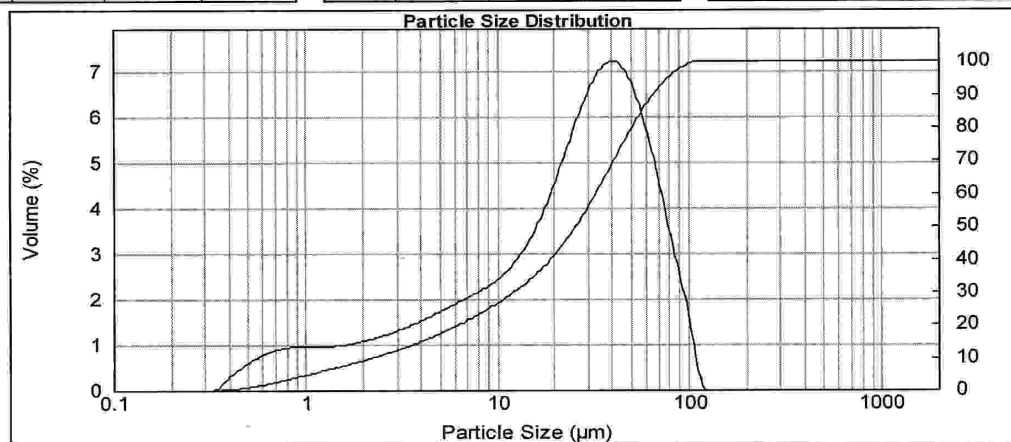
d(0.5): 26.181 μ m

d(0.9): 66.246 μ m

Mesh No	Aperture μ m	Volume In %	Vol Below %
10	2000	0.00	100.00
12	1700	0.00	100.00
14	1400	0.00	100.00
16	1180	0.00	100.00
18	1000	0.00	100.00
20	850	0.00	100.00
25	710	0.00	100.00
30	600	0.00	100.00
35	500	0.00	100.00

Mesh No	Aperture μ m	Volume In %	Vol Below %
35	500	0.00	100.00
40	425	0.00	100.00
45	355	0.00	100.00
50	300	0.00	100.00
60	250	0.00	100.00
70	212	0.00	100.00
80	180	0.00	100.00
100	150	0.00	100.00
120	125	0.00	100.00

Mesh No	Aperture μ m	Volume In %	Vol Below %
120	125	0.32	100.00
140	106	0.32	99.68
170	90	2.07	97.61
200	75	3.90	93.71
230	63	5.44	88.27
270	53	6.80	81.47
325	45	7.33	74.14
400	38	7.94	66.20



Operator notes: Add 5 drops of 15% Sodium Hexametaphosphate solution.



BCI CHEMICAL CORPORATION SDN. BHD.(Co. No 441454-X)
No.27, Jalan P/21, Selaman Industrial Park, Sec 10, 43650 Bandar Baru Bangi . Selangor Darul Ehsan
Tel : 603-8922 1822 Fax : 603-8922 3088
Email : sales@bcichemical.com.my

Result: Sieve ASTM E11:61 Report

Sample Name:
AdiCARB 5 (XF)
C232 (OM) - 230310 [SAM]

SOP Name:

Measured:
Saturday, April 03, 2010 10:17:11 AM

Measured by:
Administrator

Analysed:
Saturday, April 03, 2010 10:17:13 AM

Sample bulk lot ref:

Result Source:
Averaged

Particle Name:
CaCO₃ (calcite)
Particle RI:
1.572
Dispersant Name:
Water

Accessory Name:
Hydro 2000MU (A)
Absorption:
0.1
Dispersant RI:
1.330

Analysis model:
General purpose
Size range:
0.020 to 2000.000 um
Weighted Residual:
1.887 %

Sensitivity:
Normal
Obscuration:
17.96 %
Result Emulation:
Off

Concentration:
0.0098 %Vol

Span :
1.976

Uniformity:
0.605

Result units:
Volume

Specific Surface Area:
1.74 m²/g

Surface Weighted Mean D[3,2]:
3.450 um

Vol. Weighted Mean D[4,3]:
8.953 um

Density:
1.000 g/cm³

d(0.1): 1.220 um

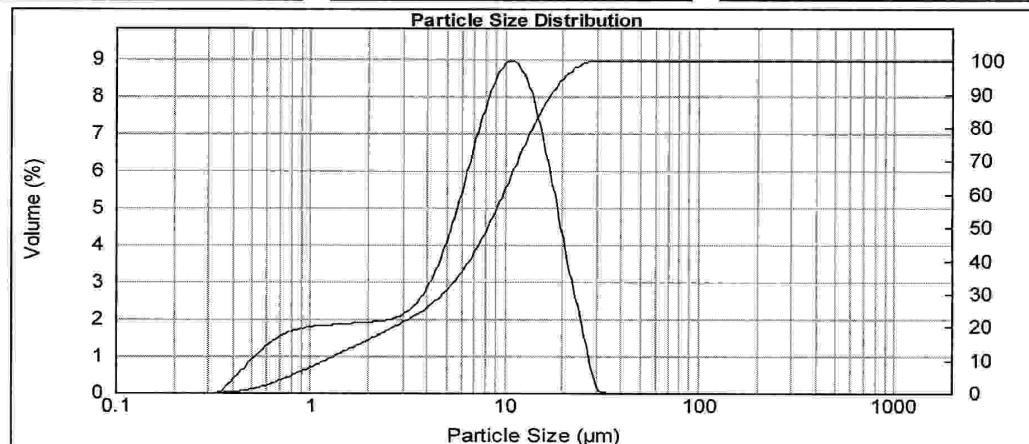
d(0.5): 8.274 um

d(0.9): 17.569 um

Mesh No	Aperture µm	Volume In %	Vol Below %
10	2000	0.00	100.00
12	1700	0.00	100.00
14	1400	0.00	100.00
16	1180	0.00	100.00
18	1000	0.00	100.00
20	850	0.00	100.00
25	710	0.00	100.00
30	600	0.00	100.00
35	500	0.00	100.00

Mesh No	Aperture µm	Volume In %	Vol Below %
35	500	0.00	100.00
40	425	0.00	100.00
45	355	0.00	100.00
50	300	0.00	100.00
60	250	0.00	100.00
70	212	0.00	100.00
80	180	0.00	100.00
100	150	0.00	100.00
120	125	0.00	100.00

Mesh No	Aperture µm	Volume In %	Vol Below %
120	125	0.00	100.00
140	106	0.00	100.00
170	90	0.00	100.00
200	75	0.00	100.00
230	63	0.00	100.00
270	53	0.00	100.00
325	45	0.00	100.00
400	38	0.00	100.00



Operator notes: Add 5 drops of 15% Sodium Hexametaphosphate solution.

A.3 BET N₂ Surface Area/Pore Volume Analysis

- Weigh BET cell, note the cell number, add sample to cell and obtain sample mass.
 - Adjust the nitrogen cylinder gas pressure to between 10-15 psi/bar. Switch on the pump and then the BET machine.
 - Fix the cell+sample in 1st bag, make sure other screws inside the instrument are well fixed and tight. Select Start (on the control panel), choose degas station, load degasser (system starts pressurizing), press any key.
 - Set heating mantle to 300°C (after evacuation), switch button (inside) to start.
 - Wait for temperature to reach 300°C (about 10-15minutes), record the time when temperature gets to 300°C. Turn off switch button (inside) after 3 hours. Record time when temperature gets to 25°C from 300°C (not necessary though, just to know how long it takes)
- Start Analysis:
- When the temperature gets to 25°C, open the instrument and remove the cell. Weigh to check weight loss –record out-gassed mass, now fix the cell in the analysis chamber. Clean the nitrogen flask and pour liquid nitrogen up to a point very close to the top of the Dewar flask (designed to provide very good thermal insulation), then fix the flask containing nitrogen in the analysis chamber.
 - Turn on the BET computer/workstation, double click to open the NovaWin software (Quantachrome) -check if it shows connected. Click Operation, click Start Analysis.
 - In the dialogue box, type in your name, select Station tab -type in file name (e.g. caco3XFdate), ID (date), out-gassed weight, cell number. Click on Start, choose Yes.
 - Check the instruction on the instrument, when prompted to Unload degasser, press Yes. Press any key to continue. Close the instrument as the analysis starts.

- Check when analysis is complete. Open the instrument, remove Dewar flask and pour back remaining nitrogen in storage cylinder –don't decant everything, retain the bottoms.
- Turn off the instrument, the pump, and the nitrogen gas cylinder.
- Get the results, graphs and tables from the computer (NovaWin software). Right click on the isotherm graph, click Edit Data.
- **For Surface Area Analysis:** Select 0.05-0.35, select M,S, and L (check 'on'). Click Apply, click Ok. Select Tables, Graphs, etc -BET, Langmuir, etc.
- **For Pore Volume Analysis:** Check all points, select Table, BJH then Adsorption.

NOTES:

- BET analysis can be used for; surface area and pore volume determination. It has a range 0.05-0.95 for relative pressure, P/P_o (pressure/atmospheric pressure).
- Pore region: 0-20 Å (Micropore), 20-500 Å (Mesopore), 500Å above (Macropore). BET can only analyze micropore and mesopore regions.

Un Treated

Quantachrome NovaWin2 - Data Acquisition and Reduction
for NOVA instruments
©1994-2007, Quantachrome Instruments
version 9.0



Analysis		Report	
Operator: OJO	Date: 2011/07/28	Operator:	Date: 7/29/2011
Sample ID: 07_28_11	Filename:	C:\QCdata\Physisorb\CaCO3_XFine\7_28_11.qps	
Sample Desc: Surface Area/Pore volume	Comment:	Degassed @ 300 deg C for 3 hrs	
Sample weight: 3.8792 g	Sample Volume: 1.55235 cc		
Outgas Time: 3.0 hrs	Outgas Temp: 300.0 C		
Analysis gas: Nitrogen	Bath Temp: 77.3 K		
Press. Tolerance: 0.100/0.100 (ads/des)	Equil time: 240/240 sec (ads/des)	Equil timeout: 480/480 sec (ads/des)	
Analysis Time: 166.2 min	End of run: 2011/07/28 0:00:00	Instrument: Nova Station A	
Cell ID: 5			

Multi-Point BET

Data Reduction Parameters Data

Adsorbate	Nitrogen	Temperature	77.350K	
	Molec. Wt.: 28.013 g	Cross Section:	16.200 Å²	Liquid Density: 0.808 g/cc

Multi-Point BET Data

Relative Pressure	Volume @ STP	1 / [W((Po/P) - 1)]	Relative Pressure	Volume @ STP	1 / [W((Po/P) - 1)]
[P/Po]	[cc/g]		[P/Po]	[cc/g]	
4.82512e-02	0.2501	1.6219e+02	2.39202e-01	0.3295	7.6351e+02
9.61000e-02	0.2733	3.1130e+02	2.86691e-01	0.3507	9.1685e+02
1.44217e-01	0.2897	4.6535e+02	3.33968e-01	0.3731	1.0752e+03
1.92137e-01	0.3069	6.1996e+02			

BET summary

Slope = 3186.213
Intercept = 6.149e+00
Correlation coefficient, r = 0.999950
C constant = 519.202
Surface Area = 1.091 m²/g

Quantachrome NovaWin2 - Data Acquisition and Reduction
for NOVA instruments
©1994-2007, Quantachrome Instruments
version 9.0



Analysis

Operator: OJO
Sample ID: 07_28_11
Sample Desc: Surface Area/Pore volume
Sample weight: 3.8792 g
Outgas Time: 3.0 hrs
Analysis gas: Nitrogen
Press. Tolerance: 0.100/0.100 (ads/des)
Analysis Time: 166.2 min
Cell ID: 5

Date: 2011/07/28

Filename:

Comment:

Sample Volume:

Outgas Temp:

Bath Temp:

Equil time:

End of run:

Report

Operator:

C:\QCdata\Physisorb\CaCO3_XFine_7_28_11.qps

Degassed @ 300 deg C for 3 hrs

1.55235 cc

300.0 C

77.3 K

240/240 sec (ads/des)

2011/07/28 0:00:00

Date: 7/29/2011

Equil timeout: 480/480 sec (ads/des)

Instrument: Nova Station A

Langmuir

Data Reduction Parameters Data

Adsorbate	Nitrogen	Temperature	77.350K	Liquid Density:	0.808 g/cc
	Molec. Wt.: 28.013 g	Cross Section:	16.200 Å²		

Langmuir Data

P/Po	P/Po/W [(g/g)]	P/Po	P/Po/W [(g/g)]
4.82512e-02	1.5437e+02	2.39202e-01	5.8088e+02
9.61000e-02	2.8139e+02	2.86691e-01	6.5399e+02
1.44217e-01	3.9824e+02	3.33968e-01	7.1612e+02
1.92137e-01	5.0084e+02		

Langmuir summary

Surface Area = 1.776 m²/g

Analysis		Report	
Operator: QJO	Date: 2011/07/27	Operator:	Date: 7/27/2011
Sample ID: 07_27_11	Filename:	C:\QCdata\Physisorb\CaCO3_Fine\7_27_11.qps	
Sample Desc: Surface Area/Pore volume	Comment:	Degassed @ 300 deg C for 3 hrs	
Sample weight: 4.927 g	Sample Volume:	1.95036 cc	
Outgas Time: 3.0 hrs	Outgas Temp:	300.0 C	
Analysis gas: Nitrogen	Bath Temp:	77.3 K	
Press. Tolerance: 0.100/0.100 (ads/des)	Equil time:	240/240 sec (ads/des)	Equil timeout: 480/480 sec (ads/des)
Analysis Time: 176.9 min	End of run:	2011/07/27 0:00:00	Instrument: Nova Station A
Cell ID: 5			

Multi-Point BET

Data Reduction Parameters Data

Adsorbate	Nitrogen	Temperature	77.350K	Liquid Density:	0.808 g/cc
	Molec. Wt.: 28.013 g	Cross Section:	16.200 Å²		

Multi-Point BET Data

Relative Pressure [P/Po]	Volume @ STP [cc/g]	1 / [W((Po/P) - 1)]	Relative Pressure [P/Po]	Volume @ STP [cc/g]	1 / [W((Po/P) - 1)]
4.69666e-02	0.1425	2.7661e+02	2.40310e-01	0.1844	1.3729e+03
9.60930e-02	0.1534	5.5441e+02	2.87735e-01	0.1959	1.6498e+03
1.44683e-01	0.1633	8.2870e+02	3.34984e-01	0.2092	1.9268e+03
1.92793e-01	0.1735	1.1012e+03			

BET summary

Slope =	5722.537
Intercept =	3.120e+00
Correlation coefficient, r =	0.999969
C constant =	1835.270
Surface Area =	0.608 m²/g

Analysis		Report	
Operator: OJO	Date: 2011/07/27	Operator:	Date: 7/27/2011
Sample ID: 07_27_11	Filename:	C:\QCdata\Physisorb\CaCO3_Fine_7_27_11.qps	
Sample Desc: Surface Area/Pore volume	Comment:	Degassed @ 300 deg C for 3 hrs	
Sample weight: 4.927 g	Sample Volume:	1.95036 cc	
Outgas Time: 3.0 hrs	Outgas Temp:	300.0 C	
Analysis gas: Nitrogen	Bath Temp:	77.3 K	
Press. Tolerance: 0.100/0.100 (ads/des)	Equil time:	240/240 sec (ads/des)	Equil timeout: 480/480 sec (ads/des)
Analysis Time: 176.9 min	End of run:	2011/07/27 0:00:00	Instrument: Nova Station A
Cell ID: 5			

Langmuir

Data Reduction Parameters Data

Adsorbate	Nitrogen	Temperature	77.350K	Liquid Density:	0.808 g/cc
	Molec. Wt.: 28.013 g	Cross Section:	16.200 Å²		

Langmuir Data

P/Po	P/Po/W [(g/g)]	P/Po	P/Po/W [(g/g)]
4.69666e-02	2.6362e+02	2.40310e-01	1.0430e+03
9.60930e-02	5.0113e+02	2.87735e-01	1.1751e+03
1.44683e-01	7.0880e+02	3.34984e-01	1.2814e+03
1.92793e-01	8.8891e+02		

Langmuir summary

Surface Area = 0.987 m²/g

Analysis		Report	
Operator: OJO	Date: 2011/07/21	Operator: [redacted]	Date: 7/22/2011
Sample ID: 07_21_11	Filename: C:\QCdata\Physisorb\CaCO3_Coarse_7_21_11.qps		
Sample Desc: Surface Area/Pore volume	Comment: Degassed @ 300 deg C for 3 hrs		
Sample weight: 7.9694 g	Sample Volume: 3.16734 cc		
Outgas Time: 3.0 hrs	Outgas Temp: 300.0 C		
Analysis gas: Nitrogen	Bath Temp: 77.3 K		
Press. Tolerance: 0.100/0.100 (ads/des)	Equil time: 240/240 sec (ads/des)	Equil timeout: 480/480 sec (ads/des)	
Analysis Time: 178.3 min	End of run: 2011/07/21 0:00:00	Instrument: Nova Station A	
Cell ID: 5			

Multi-Point BET

Data Reduction Parameters Data

Adsorbate	Nitrogen	Temperature	77.350K	Liquid Density:	0.808 g/cc
	Molec. Wt.: 28.013 g	Cross Section:	16.200 Å²		

Multi-Point BET Data

Relative Pressure [P/Po]	Volume @ STP [cc/g]	1 / [W((Po/P) - 1)]	Relative Pressure [P/Po]	Volume @ STP [cc/g]	1 / [W((Po/P) - 1)]
4.77924e-02	0.0595	6.7515e+02	2.40684e-01	0.0870	2.9164e+03
9.66224e-02	0.0670	1.2780e+03	2.88032e-01	0.0935	3.4631e+03
1.44838e-01	0.0737	1.8398e+03	3.35634e-01	0.1002	4.0355e+03
1.92864e-01	0.0800	2.3898e+03			

BET summary

Slope = 11569.519
 Intercept = 1.457e+02
 Correlation coefficient, r = 0.999900
 C constant = 80.415
 Surface Area = 0.297 m²/g

Analysis

Operator: OJO
Sample ID: 07_21_11
Sample Desc: Surface Area/Pore volume
Sample weight: 7.9694 g
Outgas Time: 3.0 hrs
Analysis gas: Nitrogen
Press. Tolerance: 0.100/0.100 (ads/des)
Analysis Time: 178.3 min
Cell ID: 5

Date: 2011/07/21

Filename:

Comment: Degassed @ 300 deg C for 3 hrs

Sample Volume: 3.16734 cc

OutgasTemp: 300.0 C

Bath Temp: 77.3 K

Equil time: 240/240 sec (ads/des)

End of run: 2011/07/21 0:00:00

Report

Operator:

Date: 7/22/2011

C:\QCdata\Physisorb\CaCO3_Coarse_7_21_11.qps

Equil timeout: 480/480 sec (ads/des)
Instrument: Nova Station A

Langmuir

Data Reduction Parameters Data

<u>Adsorbate</u>	Nitrogen	Temperature	77.350K	
	Molec. Wt.: 28.013 g	Cross Section:	16.200 Å²	Liquid Density: 0.808 g/cc

Langmuir Data

P/Po	P/Po/W [(g/g)]	P/Po	P/Po/W [(g/g)]
4.77924e-02	6.4288e+02	2.40684e-01	2.2145e+03
9.66224e-02	1.1545e+03	2.88032e-01	2.4656e+03
1.44838e-01	1.5734e+03	3.35634e-01	2.6811e+03
1.92864e-01	1.9289e+03		

Langmuir summary

Surface Area = 0.498 m²/g

Treated

Quantachrome NovaWin2 - Data Acquisition and Reduction
for NOVA instruments
©1994-2007, Quantachrome Instruments
version 9.0



Analysis

Operator:Gbenga Ojo
Sample ID: 11812
Sample Desc: surface area and pore volume
Sample weight: 3.4708 g
Outgas Time: 5.5 hrs
Analysis gas: Nitrogen
Press. Tolerance: 0.100/0.100 (ads/des)
Analysis Time: 136.3 min
Cell ID: 4

Date:2012/11/09

Filename:

Comment:

Sample Volume:

OutgasTemp:

Bath Temp:

Equil time:

End of run:

Report

Operator:

C:\QCdata\Physisorb\TreatedXFCC

Degassed @ 300 deg C for 3 hrs

1.26953 cc

300.0 C

77.3 K

240/240 sec (ads/des)

2012/11/09 0:00:00

Date:11/10/2012

11082012.qps

Equil timeout: 480/480 sec (ads/des)

Instrument: Nova Station A

Multi-Point BET

Data Reduction Parameters Data

Adsorbate	Nitrogen	Temperature	77.350K	Liquid Density:	0.808 g/cc
	Molec. Wt.: 28.013 g	Cross Section:	16.200 Å²		

Multi-Point BET Data

Relative Pressure	Volume @ STP	1 / [W((Po/P) - 1)]	Relative Pressure	Volume @ STP	1 / [W((Po/P) - 1)]
[P/Po]	[cc/g]		[P/Po]	[cc/g]	
9.81752e-02	0.1560	5.5823e+02	2.26370e-01	0.1973	1.1864e+03
1.49440e-01	0.1721	8.1699e+02	2.52225e-01	0.2038	1.3240e+03
2.00169e-01	0.1902	1.0529e+03	3.02325e-01	0.2183	1.5882e+03

BET summary

Slope = 5012.986
Intercept = 6.120e+01
Correlation coefficient, r = 0.999677
C constant = 82.914
Surface Area = 0.686 m²/g

Quantachrome NovaWin2 - Data Acquisition and Reduction
for NOVA instruments
©1994-2007, Quantachrome Instruments
version 9.0



Analysis

Operator: Gbenga Ojo
Sample ID: 11812
Sample Desc: surface area and pore volume
Sample weight: 3.4708 g
Outgas Time: 5.5 hrs
Analysis gas: Nitrogen
Press. Tolerance: 0.100/0.100 (ads/des)
Analysis Time: 136.3 min
Cell ID: 4

Date: 2012/11/09

Filename:

Comment:

Sample Volume:

Outgas Temp:

Bath Temp:

Equil time:

End of run:

Report

Operator:

C:\QCdata\Physisorb\TreatedXFCC\11082012.qps

Degassed @ 300 deg C for 3 hrs

1.26953 cc

300.0 C

77.3 K

240/240 sec (ads/des)

2012/11/09 0:00:00

Date: 11/10/2012

Equil timeout: 480/480 sec (ads/des)

Instrument: Nova Station A

Langmuir

Data Reduction Parameters Data

Adsorbate	Nitrogen	Temperature	77.350K	Liquid Density:	0.808 g/cc
	Molec. Wt.: 28.013 g	Cross Section:	16.200 Å²		

Langmuir Data

P/Po	P/Po/W [(g/g)]	P/Po	P/Po/W [(g/g)]
9.81752e-02	5.0342e+02	2.26370e-01	9.1780e+02
1.49440e-01	6.9490e+02	2.52225e-01	9.9002e+02
2.00169e-01	8.4215e+02	3.02325e-01	1.1081e+03

Langmuir summary

Surface Area = 1.178 m²/g

Analysis

Operator:Gbenga Ojo

Date:2012/11/10

Sample ID: 11812

Filename:

Sample Desc: surface area and pore volume

Comment:

Sample weight: 4.6324 g

Sample Volume: 1.73534 cc

Outgas Time: 5.5 hrs

OutgasTemp: 300.0 C

Analysis gas: Nitrogen

Bath Temp: 77.3 K

Press. Tolerance: 0.100/0.100 (ads/des)

Equil time: 240/240 sec (ads/des)

Analysis Time: 133.0 min

End of run: 2012/11/10 0:00:00

Equil timeout: 480/480 sec (ads/des)

Cell ID: 4

Instrument: Nova Station A

Multi-Point BET

Data Reduction Parameters Data

Adsorbate	Nitrogen	Temperature	77.350K	Liquid Density:	0.808 g/cc
	Molec. Wt.: 28.013 g	Cross Section:	16.200 Å²		

Multi-Point BET Data

Relative Pressure	Volume @ STP	1 / [W((Po/P) - 1)]	Relative Pressure	Volume @ STP	1 / [W((Po/P) - 1)]
[P/Po]	[cc/g]		[P/Po]	[cc/g]	
9.72506e-02	0.0948	9.0912e+02	2.26426e-01	0.1220	1.9193e+03
1.48925e-01	0.1062	1.3187e+03	2.52281e-01	0.1267	2.1313e+03
2.00063e-01	0.1171	1.7081e+03	3.02346e-01	0.1373	2.5259e+03

BET summary

Slope = 7873.840
Intercept = 1.415e+02
Correlation coefficient, r = 0.999955
C constant= 56.649
Surface Area = 0.434 m²/g

**Quantachrome NovaWin2 - Data Acquisition and Reduction
for NOVA instruments
©1994-2007, Quantachrome Instruments
version 9.0**



Analysis

Operator:Gbenga Ojo

Sample ID: 11812

Sample Desc: surface area and pore volume

Sample weight: 4.6324 g

Outgas Time: 5.5 hrs

Analysis gas: Nitrogen

Press. Tolerance: 0.100/0.100 (ads/des)

Analysis Time: 133.0 min

Cell ID: 4

Date:2012/11/10

Filename:

Comment:

Sample Volume: 1.73534 cc

OutgasTemp: 300.0 C

Bath Temp: 77.3 K

Equil time: 240/240 sec (ads/des)

End of run: 2012/11/10 0:00:00

Report

Operator:

C:\QCdata\Physisorb\TreatedFineCC_11082012.qps

Degassed @ 300 deg C for 3 hrs

Date:11/10/2012

Equil timeout: 480/480 sec (ads/des)

Instrument: Nova Station A

Langmuir

Data Reduction Parameters Data

<u>Adsorbate</u>	Nitrogen	Temperature	77.350K	Liquid Density:	0.808 g/cc
	Molec. Wt.: 28.013 g	Cross Section:	16.200 Å²		

Langmuir Data

P/Po	P/Po/W	P/Po	P/Po/W
	[(g/g)]		[(g/g)]
9.72506e-02	8.2071e+02	2.26426e-01	1.4848e+03
1.48925e-01	1.1223e+03	2.52281e-01	1.5936e+03
2.00063e-01	1.3664e+03	3.02346e-01	1.7622e+03

Langmuir summary

Surface Area = 0.755 m²/g

Analysis

Operator: Gbenga Ojo

Sample ID: 110912

Sample Desc: surface area and pore volume

Sample weight: 4.9858 g

Outgas Time: 5.5 hrs

Analysis gas: Nitrogen

Press. Tolerance: 0.100/0.100 (ads/des)

Analysis Time: 144.7 min

Cell ID: 4

Date: 2012/11/10

Filename:

Comment:

Sample Volume: 1.94734 cc

Outgas Temp: 300.0 C

Bath Temp: 77.3 K

Equil time: 240/240 sec (ads/des)

End of run: 2012/11/10 0:00:00

Report

Operator:

Date: 11/10/2012

File: C:\QCdata\Physisorb\TreatedCoarseCC\11092012.qps

Comment: Degassed @ 300 deg C for 3 hrs

Equil timeout: 480/480 sec (ads/des)

Instrument: Nova Station A

Multi-Point BET

Data Reduction Parameters Data

Adsorbate	Nitrogen	Temperature	77.350K	Liquid Density:	0.808 g/cc
	Molec. Wt.: 28.013 g	Cross Section:	16.200 Å²		

Multi-Point BET Data

Relative Pressure [P/Po]	Volume @ STP [cc/g]	1 / [W((Po/P) - 1)]	Relative Pressure [P/Po]	Volume @ STP [cc/g]	1 / [W((Po/P) - 1)]
5.00370e-02	0.0279	1.5113e+03	2.27979e-01	0.0507	4.6574e+03
1.01302e-01	0.0333	2.7048e+03	2.53382e-01	0.0544	4.9920e+03
1.52017e-01	0.0400	3.5829e+03	3.03426e-01	0.0623	5.5974e+03
2.02407e-01	0.0471	4.3080e+03			

BET summary

Slope = 15867.572
Intercept = 9.823e+02
Correlation coefficient, r = 0.992700
C constant = 17.154
Surface Area = 0.207 m²/g

Analysis

Operator: Gbenga Ojo

Sample ID: 110912

Sample Desc: surface area and pore volume

Sample weight: 4.9858 g

Outgas Time: 5.5 hrs

Analysis gas: Nitrogen

Press. Tolerance: 0.100/0.100 (ads/des)

Analysis Time: 144.7 min

Cell ID: 4

Date: 2012/11/10

Filename:

Comment: Degassed @ 300 deg C for 3 hrs

Sample Volume: 1.94734 cc

Outgas Temp: 300.0 C

Bath Temp: 77.3 K

Equil time: 240/240 sec (ads/des)

End of run: 2012/11/10 0:00:00

Report

Operator:

Date: 11/10/2012

File: C:\QCdata\Physisorb\reatedCoarseCC_11092012.qps

Equil timeout: 480/480 sec (ads/des)
Instrument: Nova Station A

Langmuir

Data Reduction Parameters Data

Adsorbate	Nitrogen	Temperature	77.350K	Liquid Density:	0.808 g/cc
	Molec. Wt.: 28.013 g	Cross Section:	16.200 Å²		

Langmuir Data

P/Po	P/Po/W [(g/g)]	P/Po	P/Po/W [(g/g)]
5.00370e-02	1.4356e+03	2.27979e-01	3.5956e+03
1.01302e-01	2.4308e+03	2.53382e-01	3.7271e+03
1.52017e-01	3.0383e+03	3.03426e-01	3.8990e+03
2.02407e-01	3.4360e+03		

Langmuir summary

Surface Area = 0.367 m²/g

APPENDIX B

B.1 UV-Vis Calibration

1. Prepare a bulk solution of Triton X-100 having a concentration of 10 mM, around 50 times the CMC (0.22-0.24 mM) by diluting a measured quantity of neat Triton X-100 (1.7 M) with distilled water.
2. Prepare 5 samples of varying surfactant concentrations by diluting measured amounts of the bulk Triton X-100 with the appropriate quantity of water. (Table B.1, B.2).
3. Measure the light absorbance using the UV-1201s Spectrophotometer (Shimadzu Co., Colombia MA) at a wave length, $\lambda=275$ nm (UV absorption wave length of Triton X-100 in water).
 - a. Turn on spectrophotometer and allow to boot
 - b. Press the “return” key
 - c. Press 1 for photometric measurement
 - d. Press “go to λ ”
 - e. Set wavelength
 - f. Press F3 for data display
 - g. Pour the base sample (usually distilled water, with zero concentration of surfactant, for baseline correction) in the UV-Vis cuvette (not less than half way), place cuvette in the spectrophotometer and press auto zero
 - h. Press start to take reading of your base sample (should be zero)
4. Obtain the absorbance for all 5 concentrations. (Table B.1, B.2)
5. Plot a graph of the absorbance versus concentration. (Figure B.1, B.2)
6. Find the equation of the line. Usually, the origin should be at (0, 0) so the plot can fully obey the Beer-Lambert Law, $A = \epsilon l c$ (where A=Absorbance, ϵ =molar absorptivity, and

l =path length, usually the width of the cuvette, c =molar concentration). But, the origin was not forced to zero; this is to allow for correction of experimental, instrumental or operator error. Thus, the constant of the equation is used in the calculation.

Table B.1: UV-Vis absorbance of varying surfactant concentrations (1)

TX-100 Conc. (mM)	KABS
0	0
0.1	0.1395
0.2	0.2821
0.4	0.5669
0.5	0.7003
0.6	0.8435

Table B.2: UV-Vis absorbance of varying surfactant concentrations (2)

TX-100 Conc. (mM)	KABS
0	0
0.1	0.0922
0.2	0.1924
0.3	0.2733
0.4	0.3628
0.5	0.4583

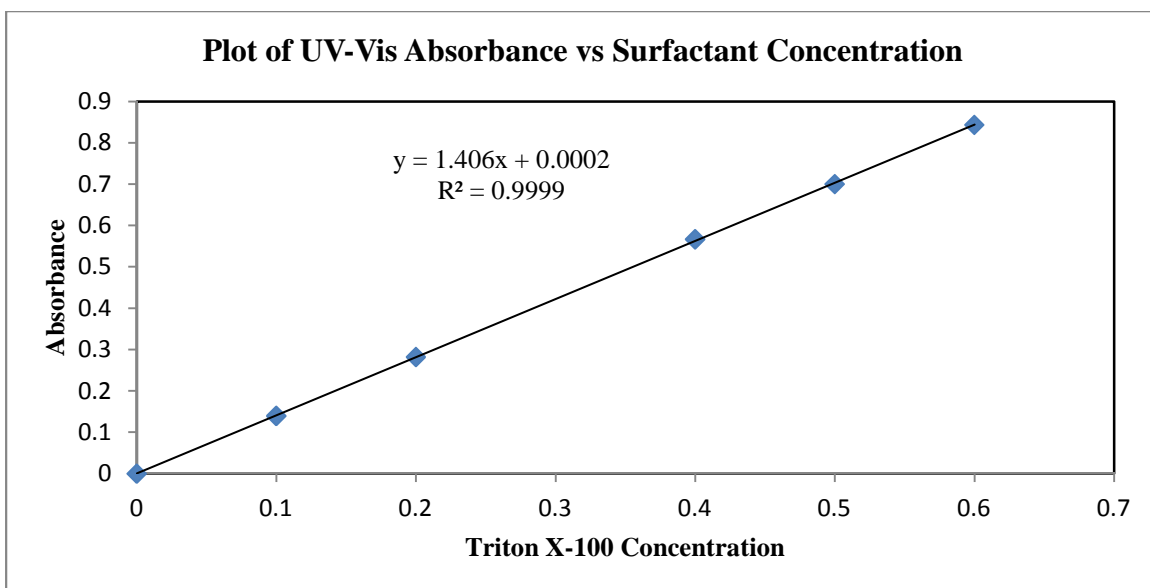


Figure B.1: UV-Vis absorbance against surfactant concentration (from Table B.1).

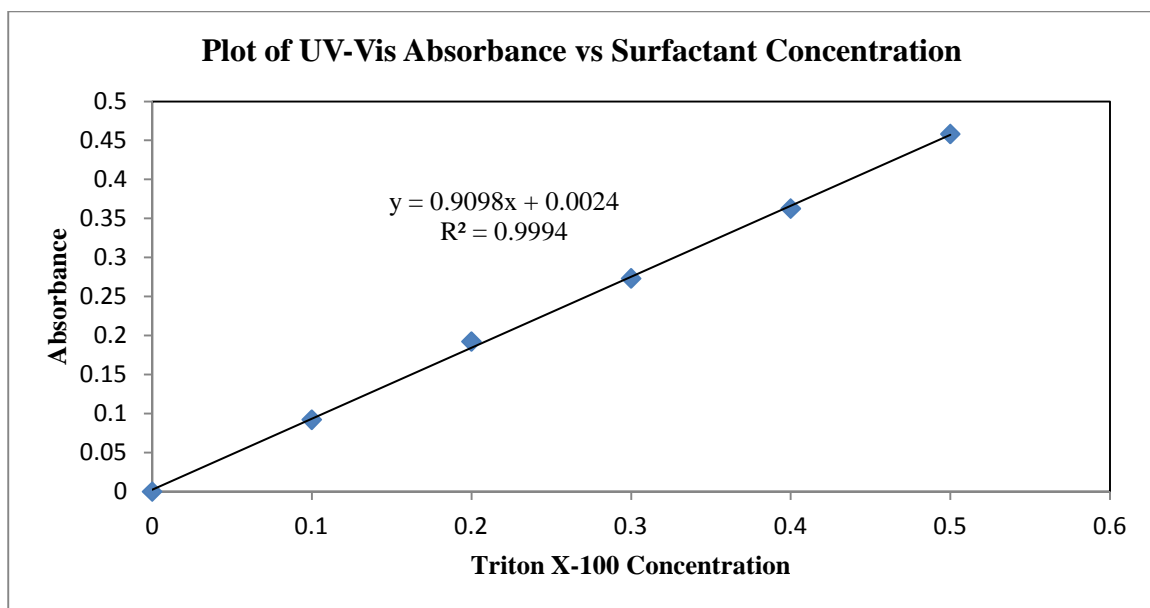


Figure B.2: UV-Vis absorbance against surfactant concentration (from Table B.2).

APPENDIX C

C.1 Some of the Experimental Data used to Generate the Adsorption Isotherms

4th ADSORPTION ISOTHERM (XFINE)													
Sample Number	ml of 0.010M (10mM)	ml DI Water	bulk Concentration (mM)	bulk Concentration (μM)	Xfine CaCO ₃ (g)	ABS	K* ABS	equil conc (mM) (kabs+y)/1.2989	equil conc (μM)	adsorption conc (μM)	μmoles adsorbed	Adsorption per gram (μmoles/g)	
1	0	30	0	0	5.0123	0	0	-0.000142	0.142248	0.142248	0.004267	0.0008514	
2	0.129	29.871	0.043	43	5.0021	0.032	0.032	0.0226174	22.617354	20.38265	0.611479	0.1222445	
3	0.24	29.76	0.08	80	5.0043	0.085	0.0853	0.0605263	60.526316	19.47368	0.584211	0.1167417	
4	0.36	29.64	0.12	120	5.0055	0.133	0.1334	0.0947368	94.736842	25.26316	0.757895	0.1514124	
5	0.48	29.52	0.16	160	5.0055	0.183	0.1826	0.1297297	129.72973	30.27027	0.908108	0.1814221	
6	0.6	29.4	0.2	200	5.0047	0.22	0.2196	0.1560455	156.04552	43.95448	1.318634	0.2634792	
7	0.729	29.271	0.243	243	5.0032	0.274	0.274	0.1947368	194.73684	48.26316	1.447895	0.2893937	
8	0.84	29.16	0.28	280	5.0039	0.322	0.3218	0.228734	228.734	51.266	1.53798	0.3073563	
9	0.96	29.04	0.32	320	5.0015	0.369	0.3685	0.2619488	261.94879	58.05121	1.741536	0.3482028	chosen for adsolubiliz
10	1.08	28.92	0.36	360	5.0076	0.438	0.4377	0.3111664	311.16643	48.83357	1.465007	0.2925567	
11	1.2	28.8	0.4	400	5.0087	0.48	0.48	0.3412518	341.25178	58.74822	1.762447	0.3518771	
12	1.32	28.68	0.44	440	5.0026	0.547	0.5472	0.3890469	389.04694	50.95306	1.528592	0.3055595	
13	1.44	28.56	0.48	480	5.0064	0.598	0.5978	0.4250356	425.03556	54.96444	1.648933	0.329365	
14	1.56	28.44	0.52	520	5.008	0.654	0.6536	0.4647226	464.72262	55.27738	1.658321	0.3311345	

5th ADSORPTION ISOTHERM (XFINE)

Sample Number	ml of 0.010M (10mM)	ml DI Water	bulk Concentration (mM)	bulk Concentration (μ M)	Xfine CaCO ₃ (g)	ABS	K*ABS	equil conc (mM) (kabs-y)/1.2989	equil conc (μ M)	adsorption conc (μ M)	μ moles adsorbed	5th Adsorption per gram (μ moles/g)
1	0	30	0	0	5.0024	0	0.0004	0.0001422	0.1422475	0.142247511	0.004267425	0.000853076
2	0.12	29.88	0.04	40	5.003	0.046	0.0459	0.0325036	32.503556	7.496443812	0.224893314	0.044951692
3	0.24	29.76	0.08	80	5.0022	0.093	0.0925	0.0656472	65.647226	14.35277383	0.430583215	0.086078768
4	0.36	29.64	0.12	120	5.0016	0.144	0.1443	0.1024893	102.48933	17.51066856	0.525320057	0.105030402
5	0.48	29.52	0.16	160	5.0046	0.186	0.1864	0.1324324	132.43243	27.56756757	0.827027027	0.165253372
6	0.6	29.4	0.2	200	5.0029	0.228	0.2289	0.1620199	162.01991	37.98008535	1.13940256	0.227748418
7	0.72	29.28	0.24	240	5.003	0.278	0.2777	0.1973684	197.36842	42.63157895	1.278947368	0.255636092
8	0.84	29.16	0.28	280	5.0028	0.325	0.3253	0.2312233	231.22333	48.77667141	1.463300142	0.292496231
	0.9099985	29.880002	0.29555	295.55	5.0027	0.343	0.3425	0.2434566	243.45661	52.09338549	1.562801565	0.312391621
9	0.96	29.04	0.32	320	5.004	0.379	0.3787	0.2692034	269.20341	50.79658606	1.523897582	0.304535888
10	1.08	28.92	0.36	360	5.0019	0.426	0.426	0.302845	302.84495	57.15504979	1.714651494	0.342800035
11	1.2	28.8	0.4	400	5.0029	0.478	0.4783	0.3400427	340.04267	59.95732575	1.798719772	0.359535424
12	1.32	28.68	0.44	440	5.0029	0.537	0.5369	0.3817212	381.72119	58.27880512	1.748364154	0.349470138
13	1.44	28.56	0.48	480	5.0025	0.593	0.593	0.4216216	421.62162	58.37837838	1.751351351	0.350095223
14	1.56	28.44	0.52	520	5.0024	0.658	0.6581	0.4679232	467.92319	52.07681366	1.56230441	0.312310973

6th ADSORPTION ISOTHERM (XFINE)

Sample Number	ml of 0.010M (10mM)	ml DI Water	bulk Concentration (mM)	bulk Concentration (μ M)	Xfine CaCO ₃ (g)	K* ABS	equil conc (mM) (kabs-0.0002)/1.406	equil conc (μ M)	adsorption conc (μ M)	μ moles adsorbed	6th Adsorption per gram (micromoles/g)
1	0	30	0	0	5.0026	0.0002	0	0	0	0	0
2	0.12	29.88	0.04	40	5.0022	0.0408	0.028876 245	28.87624 467	11.12375 5	0.33371 27	0.06671 3178
3	0.24	29.76	0.08	80	5.0003	0.0905	0.064224 751	64.22475 107	15.77524 9	0.47325 75	0.09464 5815
4	0.36	29.64	0.12	120	5.0019	0.1425	0.101209 104	101.2091 038	18.79089 6	0.56372 69	0.11270 255
4a	0.42	29.58	0.14	140	5.0017	0.1641	0.116571 835	116.5718 35	23.42816 5	0.70284 5	0.14052 1213
5	0.48	29.52	0.16	160	5.0009	0.1871	0.132930 299	132.9302 987	27.06970 1	0.81209 1	0.16238 8978
5a	0.54	29.46	0.18	180	5.0002	0.2151	0.152844 95	152.8449 502	27.15505	0.81465 15	0.16292 3782
6	0.6	29.4	0.2	200	5.0021	0.2354	0.167283 073	167.2830 725	32.71692 7	0.98150 78	0.19621 9153
7	0.72	29.28	0.24	240	5.0018	0.2863	0.203485 064	203.4850 64	36.51493 6	1.09544 81	0.21901 0772
8	0.84	29.16	0.28	280	5.003	0.3383	0.240469 417	240.4694 168	39.53058 3	1.18591 75	0.23704 1275
9	0.96	29.04	0.32	320	5.0026	0.3865	0.274751 067	274.7510 669	45.24893 3	1.35746 8	0.27135 2496
10	1.08	28.92	0.36	360	5.0019	0.4487	0.318990 043	318.9900 427	41.00995 7	1.23029 87	0.24596 6277
11	1.2	28.8	0.4	400	5.0006	0.5033	0.357823 613	357.8236 131	42.17638 7	1.26529 16	0.25302 7958
12	1.32	28.68	0.44	440	5.0029	0.5669	0.403058 321	403.0583 215	36.94167 9	1.10825 04	0.22152 1589
13	1.44	28.56	0.48	480	5.0026	0.6122	0.435277 383	435.2773 826	44.72261 7	1.34167 85	0.26819 6242
14	1.56	28.44	0.52	520	5.0028	0.7045	0.500924 609	500.9246 088	19.07539 1	0.57226 17	0.11438 829
15	1.68	28.32	0.56	560	5.0028	0.717	0.509815 078	509.8150 782	50.18492 2	1.50554 77	0.30094 1004
16	1.8	28.2	0.6	600	5.0024	0.7769	0.552418 208	552.4182 077	47.58179 2	1.42745 38	0.28535 3784
17	1.92	28.08	0.64	640	5.0019	0.8312	0.591038 407	591.0384 068	48.96159 3	1.46884 78	0.29365 7969
18	2.04	27.96	0.68	680	5.002	0.8839	0.628520 626	628.5206 259	51.47937 4	1.54438 12	0.30875 2744
19	2.16	27.84	0.72	720	5.0011	0.9408	0.668990 043	668.9900 427	51.00995 7	1.53029 87	0.30599 2426

8th ADSORPTION ISOTHERM (XFINE)					1/9/2012							
Sample Number	ml of 0.010M (10mM)	ml DI Water	bulk Concentration (mM)	bulk Concentration (microM)	Xfine CaCO3 (g)	ABS	K*ABS	equil conc (mM) (kabs+0.0016)/1.3797	equil conc (μM) (kabs+0.0016)/1.3797	adsorption conc (microM)	micromoles adsorbed	8th Adsorption per gram (micromoles/g)
Blank	0	20	0	0	3.0165	0	0.0004	0.001449 59	1.44959 049	1.44959 0491	0.0289918 1	0.009611 076
1	0.48	19.52	0.24	240	3.0492	0.286	0.2865	0.208814	208.813 51	31.1864 8982	0.6237297 96	0.204555 226
2	0.72	19.28	0.36	360	3.0135	0.442	0.4418	0.321374	321.374 212	38.6257 8821	0.7725157 64	0.256351 672
3	0.96	19.04	0.48	480	3.0096	0.611	0.6106	0.44372	443.719 649	36.2803 508	0.7256070 16	0.241097 493
4	1.2	18.8	0.6	600	3.0239	0.804	0.8042	0.58404	584.040 009	15.9599 913	0.3191998 26	0.105558 989
5	1.44	18.56	0.72	720	3.0655	0.971	0.9709	0.704863	704.863 376	15.1366 239	0.3027324 78	0.098754 682
6	1.68	18.32	0.84	840	3.0439	0.918	0.9177	0.666304	666.304 269	173.695 731	3.4739146 19	1.141270 942

C.2 Styrene Concentration/UV-Vis Absorbance Calibration

Table C.1: Styrene concentration/UV-Vis absorbance calibration result

s/n	Surfactant vol ml	water vol ml	styrene volume	c2 μM	c2 mM	UV-Vis K*ABS
1	1	39	0	0	0	0.0002
3	1	33	6	417.668	0.417668	0.0712
4	1	30	9	626.501	0.626501	0.0907
6	1	24	15	1044.169	1.044169	0.1587

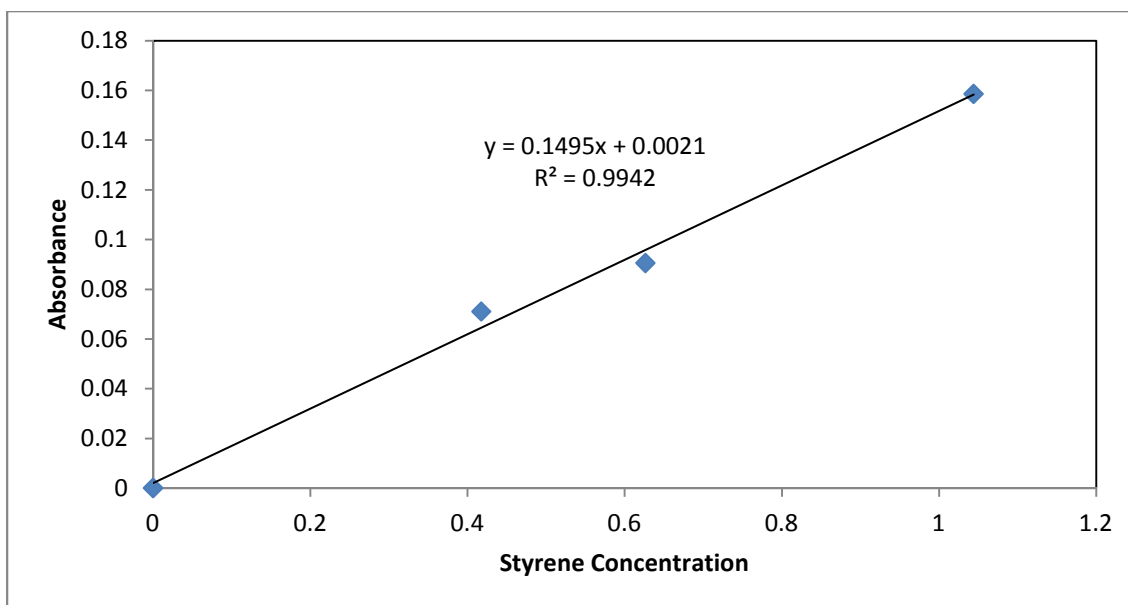


Figure C.1: UV-Vis absorbance against styrene concentration (from Table C.1).

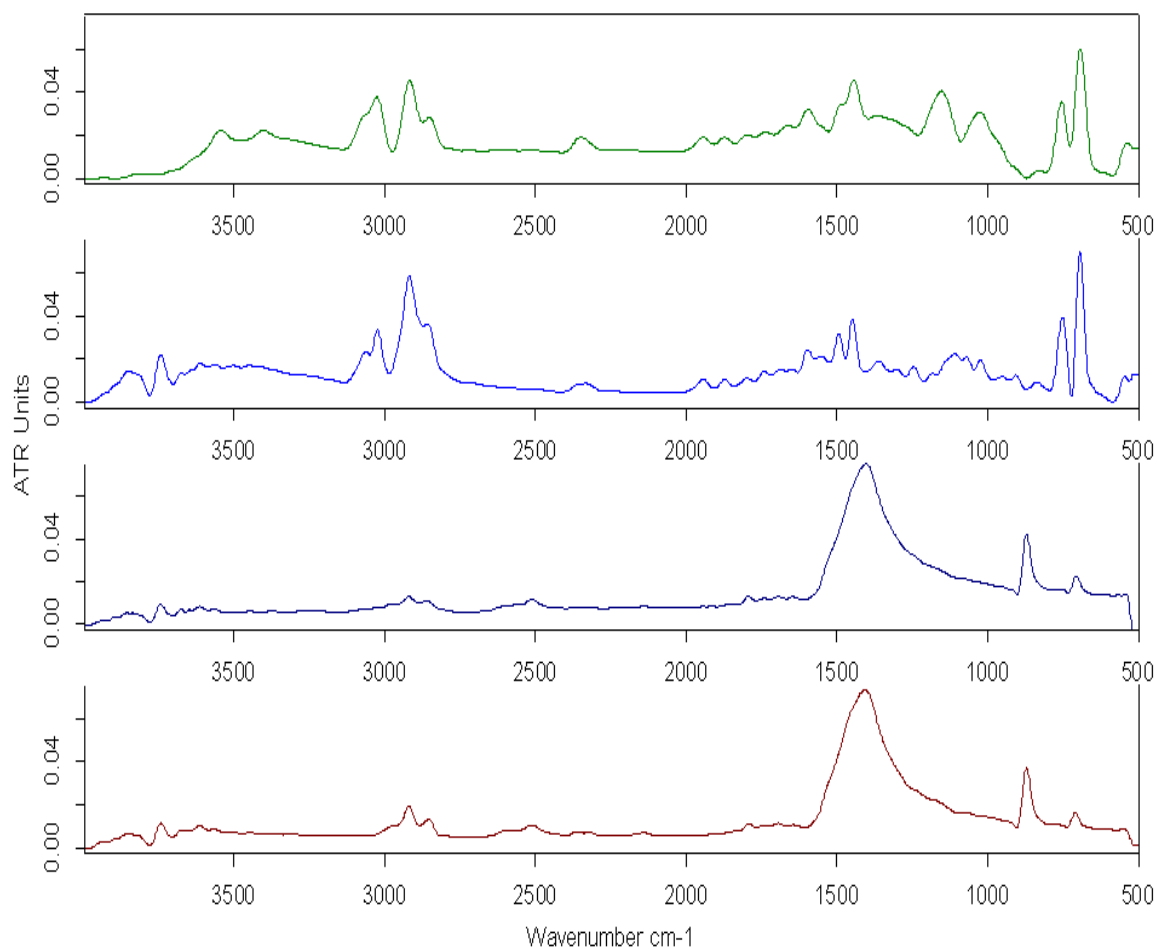
C.3 Styrene Adsolubilization Data

s/n	XF caco3 (g)	V1 Vsty (mL)	Vwater (mL)	Vol. TX-100 (mL)	c2 (μM)	UV-Vis KABS	Equil conc (μM)	(c2 - Equil conc) adsolubilized styrene (μM)	μmol adsol	adsol (2) (μmol/g)
1	3.0181	0	39	1	0	0	0	0.0000	0.0000	0
2	3.0216	3	36	1	208.8338	0.0118	65	143.9508	5.7580	2
3	3.044	6	33	1	417.6675	0.0349	219	198.2695	7.9308	3
4	3.0045	9	30	1	626.5013	0.0601	388	238.5414	9.5417	3
5	3.025	12	27	1	835.335	0.0801	522	313.5959	12.5438	4
6	3.0382	15	24	1	1044.169	0.0972	636	408.0483	16.3219	5
7	3.0316	18	21	1	1253.003	0.1111	729	523.9055	20.9562	7
8	3.0455	21	18	1	1461.836	0.127	835	626.3847	25.0554	8
9	3.0125	24	15	1	1670.67	0.1382	910	760.3021	30.4121	10
10	3.0298	27	12	1	1879.504	0.1489	982	897.5640	35.9026	12
11	3.0384	30	9	1	2088.338	0.1593	1052	1036.8325	41.4733	14
12	3.0105	33	6	1	2297.171	0.1702	1124	1172.7565	46.9103	16
13	3.0281	36	3	1	2506.005	0.1826	1207	1298.6471	51.9459	17
14	3.04	39	0	1	2714.839	0.1805	1193	1521.5277	60.8611	20

APPENDIX D

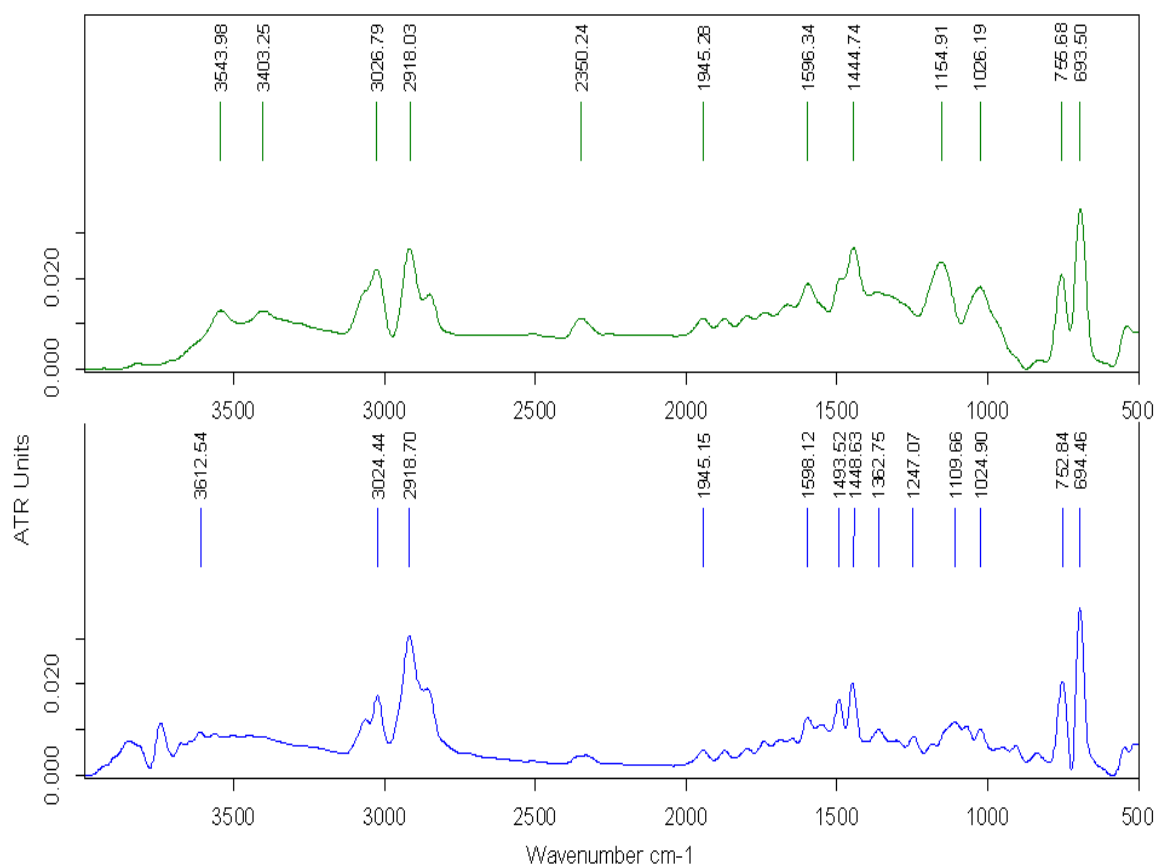
D.1 Some Results from FTIR-ATR Analyses

FTIR-ATR spectra of polystyrene standard (MW 400,000), polymer extract from Coarse CC, treated Coarse CC before extraction, and treated Coarse CC after extraction



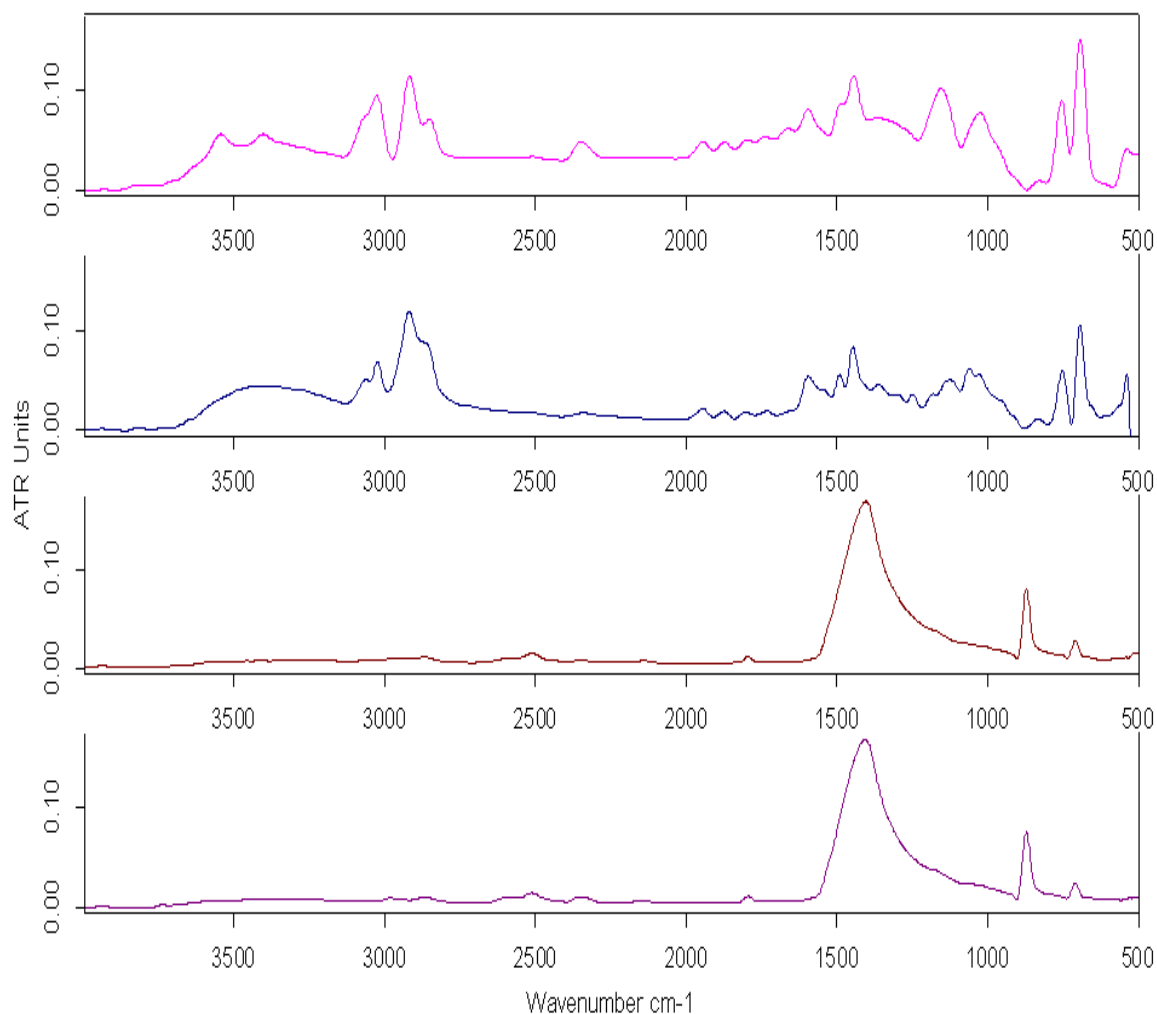
C:\Documents and Settings\Tensor 27.D51GX51\Desktop\Gbenga\Polymer Extract 10-10-2012\PolystyreneStandard\Polystyrene Std MW 400000.	21/12/2011
C:\Documents and Settings\Tensor 27.D51GX51\Desktop\Gbenga\Polymer Extract 10-25-2012-Coarse\Poly6 Coarse Extract (a)2.0	poly6 Co 05/01/2012
C:\Documents and Settings\Tensor 27.D51GX51\Desktop\Gbenga\Polymer Extract 10-25-2012-Coarse\Poly6 Coarse BeforeExtraction.0	poly 05/01/2012
C:\Documents and Settings\Tensor 27.D51GX51\Desktop\Gbenga\Polymer Extract 10-25-2012-Coarse\Poly6 Coarse AfterExtraction.0	poly6 05/01/2012

FTIR-ATR spectra (with peaks) of polystyrene standard (MW 400,000) and polymer extract from Coarse CC



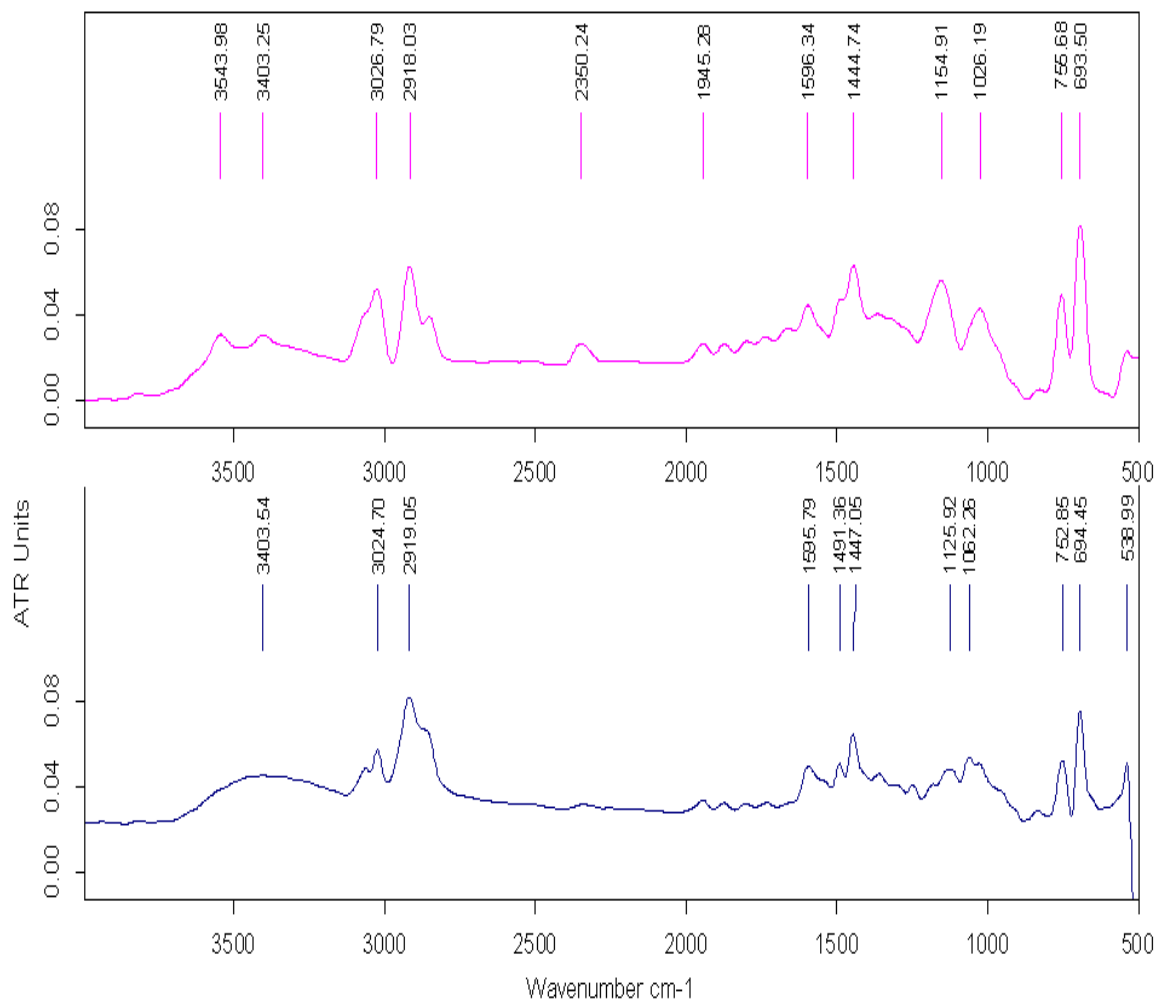
C:\Documents and Settings\Tensor 27.D51GXX51\Desktop\Gbenga\Polymer Extract 10-10-2012\PolystyreneStandard\Polystyrene Std MW 400000.	21/12/2011
C:\Documents and Settings\Tensor 27.D51GXX51\Desktop\Gbenga\Polymer Extract 10-25-2012-Coarse\Poly6 Coarse Extract (a)2.0	poly6 Co 05/01/2012

FTIR-ATR spectra of polystyrene standard (MW 400,000), polymer extract from Fine CC, treated Fine CC before extraction, and treated Fine CC after extraction



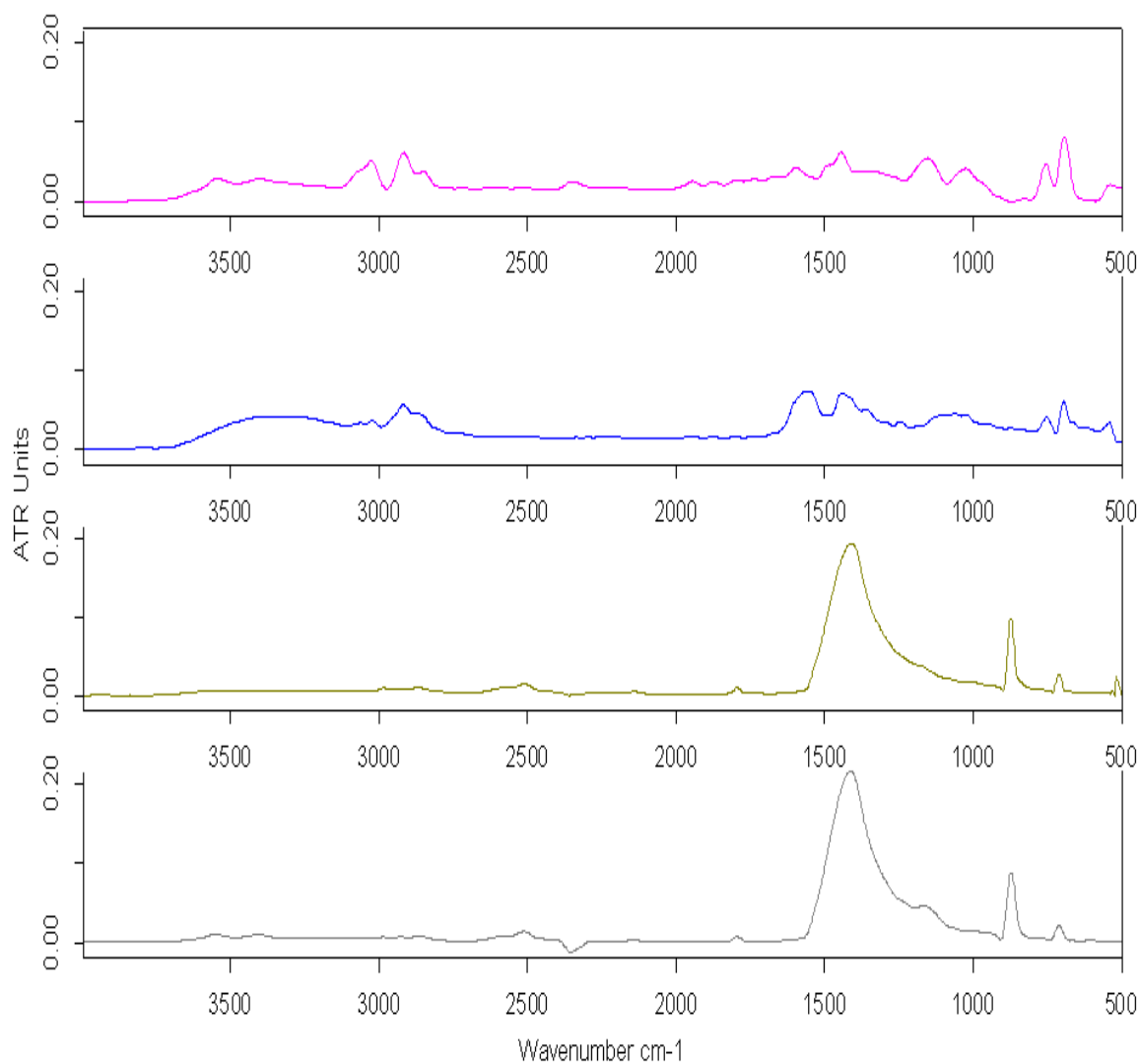
C:\Documents and Settings\Tensor 27.D51GX51\Desktop\Gbenga\Polymer Extract 10-10-2012\PolystyreneStandard\Polystyrene Std MW 400000.	21/12/2011
C:\Documents and Settings\Tensor 27.D51GX51\Desktop\Gbenga\Polymer Extract 10-11-2012\Poly5FINE Ext-a.0	poly5 Fine Ext-a 22/12/2011
C:\Documents and Settings\Tensor 27.D51GX51\Desktop\Gbenga\Polymer Extract 10-11-2012\Fine Poly5 b4 Ext-a.0	poly5 Fine b4 Ext-a 22/12/2011
C:\Documents and Settings\Tensor 27.D51GX51\Desktop\Gbenga\Polymer Extract 10-11-2012\Fine Poly5 After Ext-a.0	poly5 Fine After Ext 22/12/2011

FTIR-ATR spectra (with peaks) of polystyrene standard (MW 400,000) and polymer extract from Fine CC



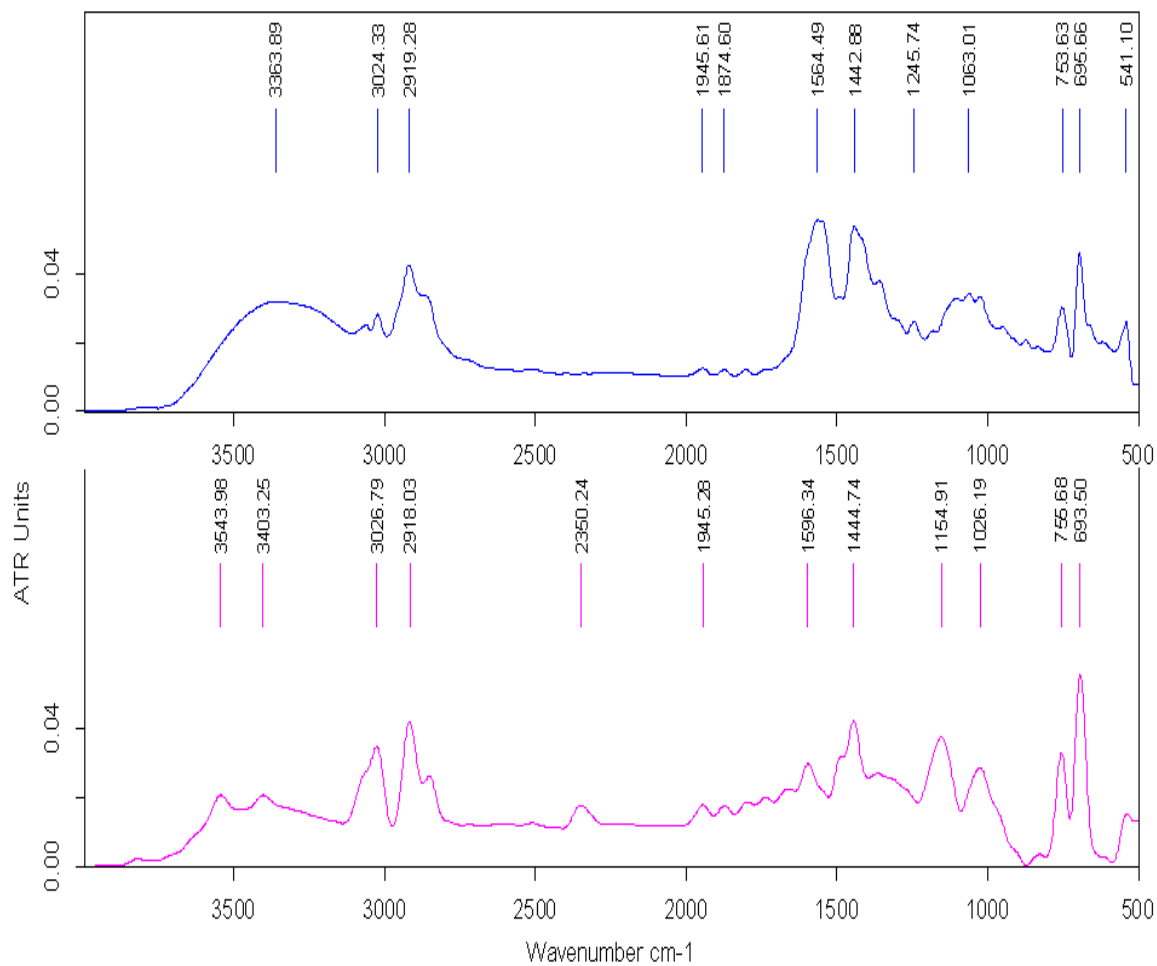
C:\Documents and Settings\Tensor 27.D51GX51\Desktop\Gbenga\Polymer Extract 10-10-2012\PolystyreneStandard\Polystyrene Std MW 400000.	21/12/2011
C:\Documents and Settings\Tensor 27.D51GX51\Desktop\Gbenga\Polymer Extract 10-11-2012\Poly5FINE Ext-a.0	poly5 Fine Ext-a
Pil	22/12/2011

FTIR-ATR spectra of polystyrene standard (MW 400,000), polymer extract from Extrafine CC, treated Extrafine CC before extraction, and treated Extrafine CC after extraction



C:\Documents and Settings\Tensor 27.D51GX51\Desktop\Gbenga\Polymer Extract 10-10-2012\PolystyreneStandard\Polystyrene Std MW 400000	21/12/2011
C:\Documents and Settings\Tensor 27.D51GX51\Desktop\Gbenga\Polymer Extract 10-11-2012\XFine Poly6 After Ext-2a.0	poly6 ExtraFine A 27/12/2011
C:\Documents and Settings\Tensor 27.D51GX51\Desktop\Gbenga\Polymer Extract 10-10-2012\Poly5 XFCCbeforeExtract.0	XFCCbpoly5 BEF 21/12/2011
C:\Documents and Settings\Tensor 27.D51GX51\Desktop\Gbenga\Polymer Extract 10-10-2012\Poly5 XFCCafterExtract.0	XFCCbpoly5 AFTE 21/12/2011

FTIR-ATR spectra (with peaks) of polymer extract from Extrafine CC and polystyrene standard (MW 400,000)



C:\Documents and Settings\Tensor 27.D51GX51\Desktop\Gbenga\Polymer Extract 10-11-2012\Fine Poly6 After Ext-2a.0	poly6 ExtraFine A	27/12/2011
C:\Documents and Settings\Tensor 27.D51GX51\Desktop\Gbenga\Polymer Extract 10-10-2012\PolystyreneStandard\Polystyrene Std MW 400000		21/12/2011

VITA

Olugbenga Samuel Ojo was born in Ogotun-Ekiti, Ekiti State, Nigeria. He attended Awori College Ojo, Lagos, Nigeria, finishing as the best graduating student in 2000. He obtained his undergraduate degree (B.Sc. Chemical Engineering) in November, 2008 from the prestigious Obafemi Awolowo University, Ile-Ife, Nigeria. He obtained his Masters of Science in Chemical Engineering from the University of Mississippi, USA in December, 2012. He looks forward to becoming a certified Project Management Professional (PMP). He enjoys playing chess, tennis, soccer, and reading at his leisure time. He is an active member of Project Management Institute, PMI, National Society of Black Engineers, NSBE, Engineers Without Borders, EWB, and the American Institute of Chemical Engineers, AIChE. He was the 2011 Ole Miss Graduate Student Council (GSC) Senator representing Chemical Engineering department, and the 2011 Special Projects Chair, NSBE, Ole Miss Chapter. He is a 2012 NSBE Major Scholar. He looks forward to applying his academic, research, and project management skills in the oil and gas industry as a Project Engineer.